



HAL
open science

Tetrafluoroterephthalonitrile as an anion- π donor: theoretical evaluation and application to anion recognition

Olfa Zayene, Romain Plais, Laurie Rolhion, Flavien Bourdreux, Grégory Pieters, Anne Gaucher, Gilles Clavier, Anabelle Cœuret, Jean-yves Salpin, Damien Prim

► **To cite this version:**

Olfa Zayene, Romain Plais, Laurie Rolhion, Flavien Bourdreux, Grégory Pieters, et al.. Tetrafluoroterephthalonitrile as an anion- π donor: theoretical evaluation and application to anion recognition. *ChemistrySelect*, 2024, 9 (2), pp.e202302763. 10.1002/slct.202302763 . hal-04396536

HAL Id: hal-04396536

<https://hal.science/hal-04396536>

Submitted on 26 Jan 2024

HAL is a multi-disciplinary open access archive for the deposit and dissemination of scientific research documents, whether they are published or not. The documents may come from teaching and research institutions in France or abroad, or from public or private research centers.

L'archive ouverte pluridisciplinaire **HAL**, est destinée au dépôt et à la diffusion de documents scientifiques de niveau recherche, publiés ou non, émanant des établissements d'enseignement et de recherche français ou étrangers, des laboratoires publics ou privés.

Tetrafluoroterephthalonitrile as an anion- π donor: theoretical evaluation and application to anion recognition

Olfa Zayene,^a Romain Plais,^a Laurie Rolhion,^a Flavien Bourdreux,^a Grégory Pieters,^b Anne Gaucher,^a Gilles Clavier,^c Anabelle Cœuret,^d Jean-Yves Salpin,^d and Damien Prim,^{*,a}

^a *Université Paris-Saclay, UVSQ, CNRS, Institut Lavoisier de Versailles, 78035 Versailles, France*

^b *Université Paris-Saclay, CEA, INRAE, Département Médicaments et Technologies pour la Santé (DMTS), SCBM, 91190 Gif-sur-Yvette, France*

^c *Université Paris-Saclay, ENS Paris-Saclay, CNRS, PPSM, 91190 Gif-sur-Yvette, France*

^d *Université Paris-Saclay, Univ Evry, CY Cergy Paris Université, CNRS, LAMBE, 91025, Evry-Courcouronnes, France*

Abstract

The ability of perfluorinated terephthalonitrile to act as an anion- π donor fragment in anion receptors is evaluated. New receptors combining an urea and a perfluorinated terephthalonitrile motif into a single architecture have been designed and synthesized. Their molecular recognition properties towards Cl^- , Br^- and I^- , have been studied in solution by means of ^1H and ^{19}F NMR as well as photophysical experiments. A complementary electrospray ionization-tandem mass spectrometry study confirmed the ranking of recognition properties between the receptors. A further theoretical evaluation of binding properties confirmed the association constant trend and suggests a main contribution of the urea motif weakly complemented by a η^2 -type anion- π interaction.

Introduction

Anion recognition has become a significant field of interest in supramolecular chemistry^[1-3]. Anion recognition is based on the association between a molecular receptor (a host) and an anion (a guest) through non-covalent interactions. Among these, hydrogen bonding has dominated this field of investigation so far.^[4,5] More recently, the anion- π interaction also emerged as a promising stakeholder for supramolecular chemistry.^[6-8] Moreover, the combination of several different weak interactions within a single receptor has aroused the growing curiosity of supramolecular chemists over the past twenty years.^[9] The exploration of binding properties of receptors combining both H-bond donor and anion- π donor fragments is an emerging trend depending on the nature of the two fragments involved and the topology of the receptor.^[10] As an example, within the same family of receptors combining urea and tetrazine derivatives, cooperative or *anti*-cooperative effects on chloride binding events have recently been observed.^[10-13] Furthermore, the symmetric architecture and 1,4-bis-substitution pattern of *s*-tetrazine derivatives tend to form receptor-anion complexes with a preferential η^6 coordination mode.^[12] Therefore, moving from tetrazine derivatives to new anion- π -acidic arenes^[10] will allow gaining insights into the relationship between fragments and rationalizing binding events for a better understanding of the associated recognition phenomena and fine structure-properties relationships.

The typical profile of a potential anion- π donor includes a π -deficient ring with a high positive quadrupole moment (Q_{zz}), a high molecular polarizability ($\alpha||$) or a balance between these two parameters. Other advantages are the commercial availability of the precursor, the possibility of multiple functionalizations using step-economical approaches, the potential desymmetrization of receptors and the generation of other coordination modes.

In this context, owing to the presence of several strong electron withdrawing fluorine atoms and nitrile groups, perfluorinated terephthalonitrile emerged as a potential candidate. This electron-poor aromatic motif has extensively been used in the design of twisted donor-acceptor fluorophores able to generate Thermally Activated Delayed Fluorescence (TADF)^[15-18].

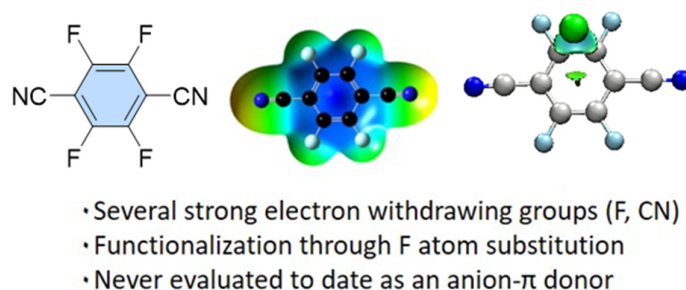


Figure 1 Fluorinated terephthalonitrile (left), Electrostatic potential (ESP) map of **1** (center, in deep blue, π -deficient central fragment) and NCIplot of the corresponding Cl^- complex (right).

Nevertheless, to the best of our knowledge, the ability of perfluorinated terephthalonitrile to be used as anion- π donor has not yet been studied.

The ability of an aromatic ring to interact with anions and the strength of this interaction is related to the combination of a permanent quadrupole moment (Q_{zz}) and molecular polarizability (α_{\parallel}). For example, the well-known anion- π receptor *s*-tetrazine displays an averaged Q_{zz} of +2.5 B^[19] and a high α_{\parallel} of 47.4 a.u. (MP2/6-311+G(d,p)). To anticipate the ability of **1** to generate anion- π interactions, we optimized its geometry at the MP2 level and computed Q_{zz} and α_{\parallel} . Molecule **1** displays a Q_{zz} of +14.64 B (MP2/6-311G(d,p))^[20] and an α_{\parallel} of 101.04 a.u. (MP2/6-311+G(d,p)), confirming the potentially strong anion- π interaction properties of **1**.

The electrostatic potential map (ESP) and NCIPLOT (Figure 1), computed at the same level, illustrates nicely the electron-deficient aromatic system. ESP map also highlights different electron-deficient regions over the aromatic ring, both at the center and the peripheral of the ring, thus highlighting potential binding sites with anions. Further, the NCIPLOT of the corresponding Cl⁻ complex (Figure 1), highlights a privileged location of the anion leading to a η^2 coordination mode.

Based on these preliminary computational results, we describe in this communication our approach toward anion receptors **2** and **3** involving an unprecedented combination of a fluorinated terephthalonitrile unit as a π -acidic ring and a urea motif as hydrogen bond donor (Figure 2). Urea fragments are substituted by aromatics bearing electron-withdrawing substituents. After the synthesis and characterizations of the target receptors **2** and **3**, their molecular recognition properties have been studied in solution by a combination of NMR, UV-Visible and fluorescence spectroscopies. Theoretical investigations and tandem mass spectrometry including studying receptor interactions with Cl, Br, and I anions, also complemented the recognition properties in solution.

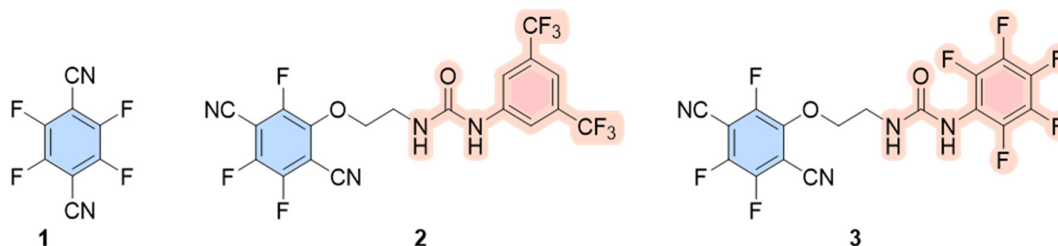


Figure 2 Molecules studied in this article.

Results and discussion

Synthesis

2 and **3** were both readily synthesized by using nucleophilic aromatic substitution (S_NAr) as the key step to selectively install the urea motif^[17]. Starting from ureas intermediates **4** and **5**^[11,12] and 1,2,4,5-tetrafluoro-terephthalonitrile **1**, the reaction in acetonitrile at room temperature and

in presence of potassium carbonate as an adequate base, proceeded smoothly to obtain **2** and **3** in 35% and 12% yields, respectively (Figure 3). The two receptors were fully characterized by diverse analytical techniques (see the Supporting Information for details).

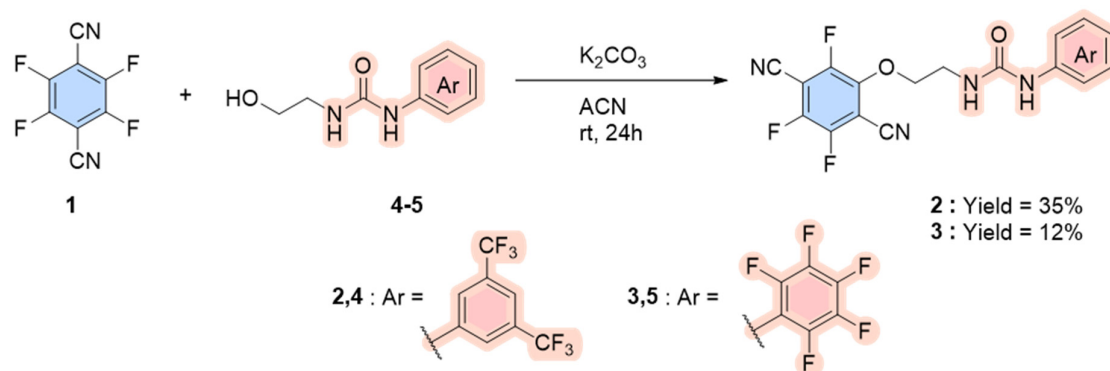


Figure 3 Synthesis route of anion receptors **2** and **3**

Photophysical experiments: investigating the anion- π donor role of terephthalonitrile moiety

The affinity of **2** and **3** towards halide anions (Cl^- , Br^- , I^- as their NBu_4X salts) was evaluated thanks to their photophysical properties. UV-visible and steady state fluorescence spectroscopies were carried out in acetonitrile in order to investigate the role of the anion- π donor in the anion recognition.

The absorption spectra of **2** and **3**, recorded in acetonitrile, and TD-DFT calculations have been performed at the PBE0/6-311G(d,p) level) to attribute the bands corresponding to the trifluoroterephthalonitrile fragments (Figures SI S23 and S24). For **2**, its corresponding bands ($\pi-\pi^*$ transitions) are visible at 322 nm and 239 nm. For **3**, those transitions are located between 323 nm and 250 nm (Figures 4 and 5).

During the titration of **2** with chloride anion, both a hypochromic and bathochromic shift are observed for the band at around 320 nm, attributed to the $\pi-\pi^*$ transition of the trifluoroterephthalonitrile. Similar observations can be made for the titration of **2** with bromide (Figure SI S28). With iodide, a more intense hypochromic and bathochromic shift of the band at 320 nm is observed. Besides, a new absorption band at 370 nm appears during the titration (Figure SI S31). This band was already observed in our previous studies and is attributed to iodide excess in solution.^[11–13]

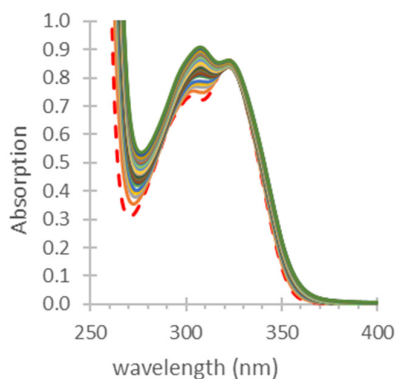


Figure 4 Absorption spectra of **2** recorded during the titration with TBACl from 0 to 70 equivalents in ACN ($[2] = 2.10^{-4}M$). Zoom on the 250-400 nm area.

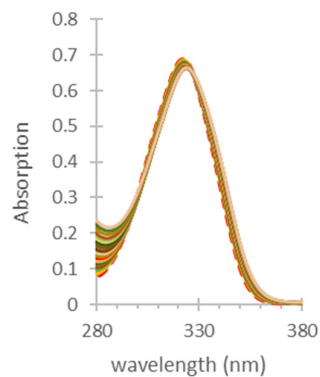


Figure 5 Absorption spectra of **3** recorded during the titration with TBACl from 0 to 70 equivalents in ACN ($[3] = 2.10^{-4}M$). Zoom on the 280-380 nm area.

UV-visible titrations of **2** and **3** with chloride, bromide and iodide showed similar results (SI Figures S34, S37, S40).

Fluorescence spectra of compounds **2** and **3** were recorded in acetonitrile. An emission band is visible with a maximum at nearly 376 nm for **2** and 375 nm for **3**, attributed to the fluorescence of the trifluoroterephthalonitrile moiety.

During the fluorescence titration of **2** and **3** with chloride anion, a very clear quenching of fluorescence is observed thereby proving the complexation (Figures 6 and 7). Nevertheless, despite the anion excess, a total quenching is not reached. Similar quenching is observed for **2** and **3** with bromide and iodide anions (SI, Figures S29, S32, S38, S41).

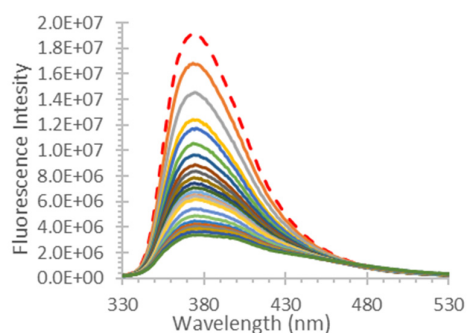


Figure 6 Fluorescence spectra of **2** recorded during the titration with TBACl from 0 to 70 equivalents in ACN ($[2] = 2.10^{-4}M$, $\lambda_{exc} = 325$ nm).

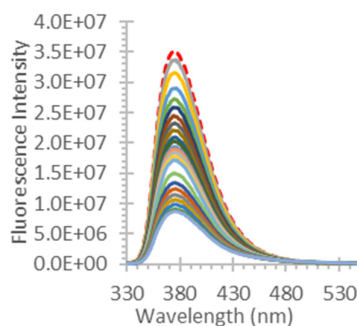


Figure 7 Fluorescence spectra of **3** recorded during the titration with TBACl from 0 to 70 equivalents in ACN ($[3] = 2.10^{-4}M$, $\lambda_{exc} = 325$ nm).

From these fluorescence and UV-visible titrations, association constants were calculated with a global spectral analysis using SPECFIT software and a single wavelength nonlinear least square model. Both methods and both titrations give similar trends and fits to a 1 to 1 complex model.

A stronger complexation on chloride anion is visible with fluorescence (1263 L/mol for **2**-Cl and 529 L/mol for **3**-Cl, Table 1, Entries 1 and 4). For bromide complexes, weaker association constants are determined (275 L/mol for **2**-Br and 125 L/mol for **3**-Br, Table 1, Entries 2 and 5). Finally, the weakest complexes of the series are characterized with iodide anion (49 L/mol for **2**-I and 37 L/mol for **3**-I, Table 1, Entries 3 and 6).

Besides, the same trend is observed with association constants determined from absorption spectroscopy. Therefore, **2** shows a better affinity to halide anions than **3**.

Table 1 Association constants determined from photophysical experiments

Entry	$K_{A, \text{abs, SPECFIT}}^{\text{a}}(\%)^{\text{b}}$	$K_{A, \text{fluo SPECFIT}}^{\text{a}}(\%)^{\text{b}}$
1 2 -Cl	1111 (1%)	1263 (1%)
2 2 -Br	327 (0.3%)	275 (1%)
3 2 -I	494 (6%)	49 (2%)
4 3 -Cl	389 (0.5%)	529 (1%)
5 3 -Br	99 (0.8%)	125 (3%)
6 3 -I	7 (3%)	37 (1%)

^a: K_A in L/mol ^b: Relative error of Fit

NMR experiments: Fundamental state binding studies

The affinity of **2** and **3** towards halide anions (Cl^- , Br^- and I^-) was also assessed experimentally by proton and fluorine NMR titrations in acetonitrile at 298 K using NBu_4X salts ($\text{X}=\text{anion}$, SI, Figures S9 to S20).

Figure a shows the ^1H NMR titration spectra of **2** with chloride anion. Two broad singlets at 7.77 and 5.70 ppm are attributed to urea protons H_a and H_b , respectively. Two singlets, attributed to aromatic hydrogen atoms, are visible at 8.00 and 7.55 ppm. Finally, two signals at 4.47 and 3.60 ppm are attributed to protons from the aliphatic linker. ^{19}F spectrum has also been given significant attention (Figure b and SI Figure S10). Four signals are visible on the spectrum: one at -62.38 ppm attributed to CF_3 (which is poorly affected by the chloride anion and will therefore not be further discussed) and three signals at -123.68 ppm, -132.20 ppm and -134.62 ppm, attributed to the three fluorine atoms of the terephthalonitrile moiety, noted F_a , F_b and F_c in the following discussion.

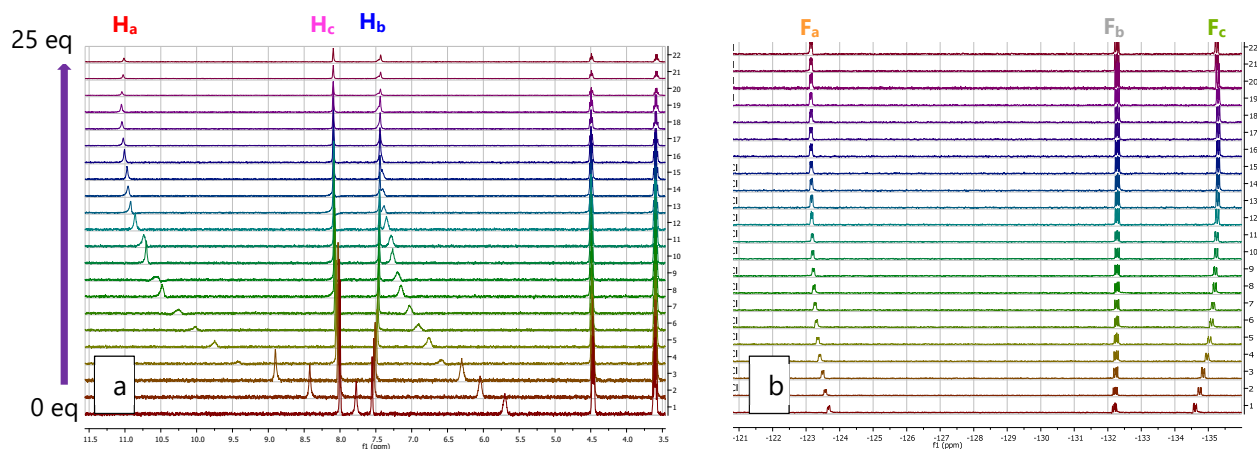
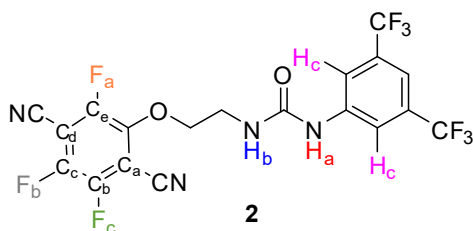


Figure 8 (a) ^1H and (b) ^{19}F NMR titrations of **2** with chloride anion in ACN ($[\mathbf{2}] = 3.5 \cdot 10^{-3}\text{M}$)

During the addition of up to 25 equivalents of chloride anion, substantial modifications of NMR spectra are observed. Signals attributed to urea protons H_a and H_b undergo important downfield shifts up to 11.04 ppm for H_a ($\delta\Delta_{\text{H}_a,\text{Cl}} = 3.27$ ppm) and 7.46 ppm for H_b ($\delta\Delta_{\text{H}_b,\text{Cl}} = 1.76$ ppm). The presence of the withdrawing aromatic ring close to H_a explains the difference between $\delta\Delta_{\text{H}_a,\text{Cl}}$ and $\delta\Delta_{\text{H}_b,\text{Cl}}$. In addition, H_c undergoes a minor downfield shift ($\delta\Delta_{\text{H}_c,\text{Cl}}$). Fluorine atom signals of the terephthalonitrile group are also greatly affected by the addition of chloride anion (Figure b and SI Figure S10). While F_a signal undergoes a downfield shift ($\delta\Delta_{\text{F}_a,\text{Cl}} = 0.52$ ppm), F_b and F_c signals are upshifted ($\delta\Delta_{\text{F}_b,\text{Cl}} = -0.09$ ppm and $\delta\Delta_{\text{F}_c,\text{Cl}} = -0.65$ ppm).

Titration were next extended to bromide and iodide anions. Less important downfield shifts are observed for H_a and H_b signals. In the same way, less important shifts are observed for F_a , F_b and F_c . (SI, Figures S11 to S14).

Receptor **3** was next subjected to titration process using the halide anions (SI, Figures S15 to S20). In addition, receptor **6**^[12] in which the terephthalonitrile moiety is replaced by a methyl ether group as an inert group *vis-a-vis* of anions, was tested to underline the role of terephthalonitrile in anion recognition. The binding constants of the corresponding complexes are determined by a single proton method^[21] and a global analysis of the protons implied in H-bond interaction with SPECFIT software.

Table 2 Association constants determined by NMR experiments

Entry	$K_{A,SPECIFIT}^a(\%)^b$
2 -Cl	2000 (0.02%)
6 -Cl	1757 (0.1%)
2 -Br	205 (0.1%)
2 -I	23 (0.04%)
3 -Cl	493 (0.04%)
3 -Br	139 (0.02%)
3 -I	12 (0.04%)

^a: K_A in L/mol ^b: Relative error of Fit

In agreement with the $\delta H_{a,b,c}$ observed during the titration, **2** and **3** seem to display the following order of affinity: **2**-Cl > **2**-Br > **2**-I and **3**-Cl > **3**-Br > **3**-I, respectively. A significant drop of **6** binding constant is also observed, confirming the contribution of the terephthalonitrile in the binding event.

Theoretical investigation: anion recognition of 2 and 3

Based on these aforementioned experimental results, we also investigated theoretically the interaction of receptors **2** and **3** with anions.^[11,12] To this end, we optimized geometries of **2** and **3** (level: APFD/aug-cc-pVDZ) with and without halide anions (Cl⁻, Br⁻, I⁻). Receptor **2** adopts an overall linear topology in which the trifluoroterephthalonitrile fragment is almost orthogonal to the urea moiety (Table 3, Entry 1). The relative positions of the urea and terephthalonitrile moieties are very similar within receptor **3** (SI, Table S1). A notable difference between both receptors refers to the spatial arrangement of the bis-(trifluoromethyl)phenyl or pentafluorophenyl aromatic group relative to urea. Indeed, receptor **3** displays a deformation and a loss of coplanarity between the pentafluorophenyl moiety and the urea unit, as already reported for tetrazine analogues.^[11] Adding the chloride anion (Table 3, entry 2 for receptor **2** and SI, Table S1 for receptor **3**) leads to a folding of receptors **2** and **3** around the anion. As a general trend, the urea and the terephthalonitrile are spatially the closest to the anion, maximizing a potential interaction.

In deep contrast with the parent symmetrically substituted *s*-tetrazine complexes, the theoretical analysis of **2** and **3** anion complexes geometries (Figure 2) highlighted the possible existence of two conformational isomers **A** and **B**, both isomers differing from each other by the terephthalonitrile “face” interacting with the anion and arising from the rotation of the

terephthalonitrile along the C-O bond (Figure). Therefore, we optimized both geometries of complexes **2** and **3** with halide anions. Optimizations were done at the APFD/aug-cc-pVDZ level for receptors alone and complexes. In each anion-receptor combination, isomers **A** appear to be the most stable by nearly 0.9 to 1.1 kcal/mol. As a consequence, isomers **A** are most likely contributing to geometrical descriptors of the corresponding complexes. We checked for several systems that this energy order is unchanged at the APFD/aug-cc-pVTZ level. Thus, the following section will consider isomer **A** for each receptor-anion combination (Table 3 for receptor **2**, Table S1 for receptor **3**).

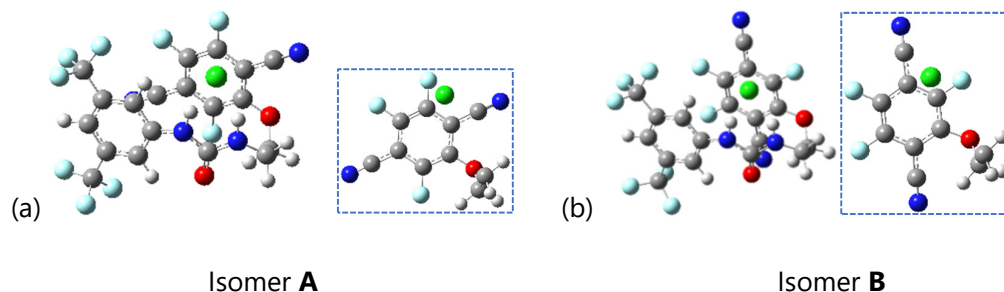
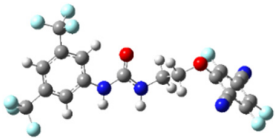
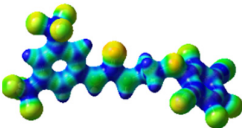
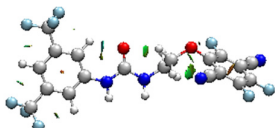
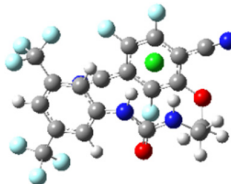
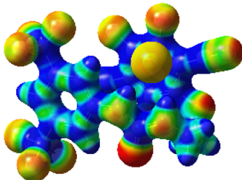
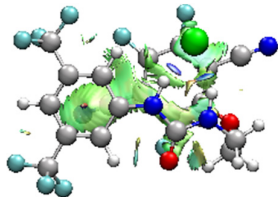
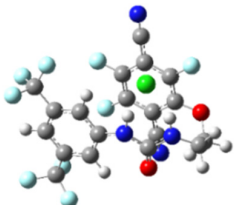
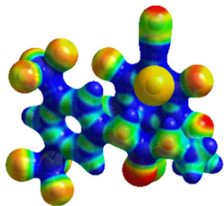
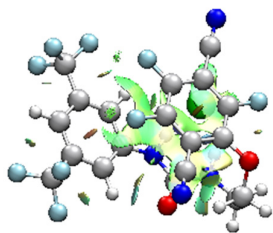
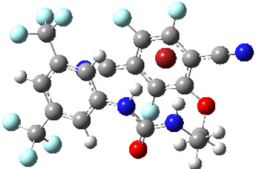
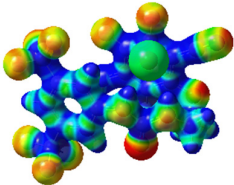
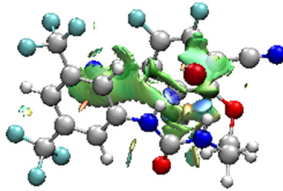
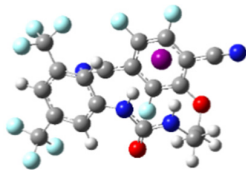
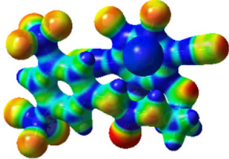
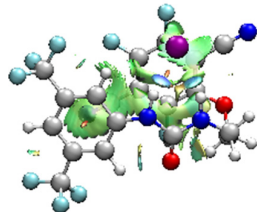


Figure 9 (a) Isomer A and (b) isomer B obtained by theoretical calculations with **2-Cl** (insert: simplified views of chloride position over the terephthalonitrile motif)

We examined the hydrogen bond between the urea motif and the anion in receptor **2**. The urea motif establishes two hydrogen bonds with the anions as evidenced by the presence of interaction surfaces in NCIPLOTS.^[11,12] As a result, N_a-H_a and N_b-H_b lengths increase from 1.009 Å in receptor **2** to 1.03-1.04 Å for complexes **2-X**, while complexing with different anions, thus highlighting the formation of intermolecular hydrogen bonds (SI, Table S2).

Table 3 Optimized geometries, ESP maps and NCIPLOT of receptor **2** and corresponding complexes (level: APFD/aug-cc-pVDZ)

Entry		Optimized geometries	ESP	NCIplot
1	2			
2	2-Cl⁻A			
3	2-Cl⁻B			
4	2-Br⁻A			
5	2-I⁻A			

Moving from chloride to iodide anion shows a modulation of intermolecular hydrogen bond lengths. Indeed, $\text{H}_a \cdots \text{X}$ (from 2.02 to 2.43 Å) and $\text{H}_b \cdots \text{X}$ (from 2.19 to 2.58 Å) lengths increase

with the increasing anion polarizability (SI, Table S2). $H_c \cdots X$ lengths also increase from 3.17 to 3.39 Å with anion polarizability, showing a potential additional interaction between the hydrogen atom of the aromatic ring and the anion. Similar modifications of characteristic bond lengths can be observed when examining receptor **3** complexes (SI, Table S3). The anion- π interaction was examined as well. To characterize the anion- π interaction formed, geometrical descriptors such as distances between the terephthalonitrile centroid and the anion as well as between each terephthalonitrile carbon atom and the anion were measured (SI, Table S2 and S3). As expected, distances between the terephthalonitrile centroid and the anion increase from 3.14 to 3.52 Å for complex **2** with the increasing anion polarizability, confirming a better affinity for Cl^- by comparison to Br^- and I^- . (SI, Table S2).

Interestingly, distances between the anion and each terephthalonitrile carbon atom are markedly different indicating a particular location of the anion with respect to the centroid of the aromatic cycle. Indeed, in complexes **2**-Cl, through space C_a -Cl (3.36 Å) and C_b -Cl (3.26 Å) distances are shorter than those with C_c , C_d or C_e (3.91 Å, 4.58 Å and 4.65 Å, respectively). Similar observations can be made for distances within **2**-Br and **2**-I. Our data confirm a privileged interaction of the anion with the C_a - C_b fragment of the terephthalonitrile and the existence of an η^2 anion- π interaction. Such a behavior has already been observed by Albrecht group with pentafluorophenyl groups, and by Hay group with different tetracyanoarenes.^[22,23]

As the spatial arrangement between the terephthalonitrile and urea moieties, and thus their relative conformations, are likely to impact the through space distances, we examined the same geometrical descriptors for isomer **2**-Cl-B. In this case, a privileged location of the anion is also observed between the C_d - C_e fragment and the anions (SI, Table S2).

A similar analysis of through space distances has been performed for receptor **3**. A similar trend can be observed, in which the distances from the centroid increase with the anion polarizability from 3.34 Å to 3.56 Å (SI, Table S3). Similarly, to receptor **2**, privileged C-anion bond distances can be observed in complexes **3** confirming a particular location of the anion with respect to the terephthalonitrile fragment.

We also performed a second order perturbation theory energy analysis of “donor-acceptor” interactions in the NBO framework in order to further characterize the contribution of each receptor fragment and their respective strengths. As foreseen, this analysis follows the same trend as the experimental results. The computed interaction energies predicted the establishment of both interactions, with a more important contribution of urea moiety (hydrogen bonding). For complex **2**-Cl-A (SI section 2.4), the overall $E[LP_{Cl}-\sigma^*_{N-H_a}]$ and $E[LP_{Cl}-\sigma^*_{N-H_b}]$ interaction energies between the chloride anion and NH_a/NH_b are 37.6 kcal/mol and 20.2 kcal/mol, respectively. The anion- π interaction is mostly generated by the C_b - F_c bond (0.26 kcal/mol), CN group carried by C_a atom (0.45 kcal/mol) and C_a - C_b bond (0.36 kcal/mol). The

computed interaction energies also point to a decrease of the H bond strength when going from Cl⁻ to I⁻.

Gas-phase complexation energies have been computed at different levels of calculations and are gathered in Table 4.

Table 4 Computed complexation energies and BSSE

Complex	APFD/Aug-cc-pVDZ		APFD/Aug-cc-pVTZ //Aug-cc-pVDZ	APFD/Aug-cc-pVTZ	
	Complexation energy ^a	BSSE	Complexation energy ^a	Complexation energy ^a	BSSE
2 -Cl-A	-63.5	0.7	-62.6	nd	nd
2 -Br-A	-59.1	0.6	-57.0	nd	nd
2 -I-A	-52.8	0.5	-50.0	nd	nd
3 -Cl-A	-57.0	0.7	-53.5	-55.8	0.3
3 -Br-A	-52.9	0.6	-51.7	-51.7	0.2
3 -I-A	-46.8	0.5	-45.8	-45.8	0.2

^a Values given in kcal/mol, including ZPE corrections

The predicted complexation energies of the complexes studied follow the same trend as the association constants determined experimentally from both photophysical and NMR experiments (Tables 1 and 2) and indicate a slightly higher affinity of receptor **2** in the gas phase whatever the halide. The associated BSSE (Basis Set Superposition Error) values are low (in the order of 0.6 at the APFD/aug-cc-pVDZ level). APFD/aug-cc-pVTZ single point calculations suggest that increasing the level of calculation has practically no effect on the computed complexation energies. For complexes involving receptor **3**, we also computed complexation energies and BSSE at the APFD/Aug-cc-pVTZ level of optimization (Table 4). BSSE are slightly reduced when employing triple-zeta basis sets. Our observations also evidence that increasing the level of geometry optimization has no noticeable effect onto the computed complexation energies and the relative order.

Mass spectrometry experiments

Mass spectrometry experiments were also carried out in order to determine whether the computed adducts could be observed experimentally in the gas phase. To this end, we used the same type of solutions as those studied for tetrazine receptors, by introducing in the electrospray ionization source of a quadrupole ion trap (Bruker AmaZon Speed ETD), a 10⁻⁴ M or 10⁻⁵ M equimolar mixture of receptor/NBu₄X (X= Cl, Br, I; in a 90/10 ACN/H₂O solvent composition), and by adopting similar experimental conditions (see Supporting Information). A typical electrospray spectrum is given in Figure 10, and turned out to be remarkably simple. Mass to charge ratios mentioned in the present section all imply the lightest halogen isotope (namely ³⁵Cl and ⁷⁹Br). This spectrum shows that the 1:1 **2**-X and **3**-X complexes studied

theoretically could be readily generated in the gas phase by electrospray, and systematically corresponded to the most intense ion (presently [(**3**)+Cl]⁻; *m/z* 485). A complex with a 1:2 stoichiometry, [(**receptor**)₂+X]⁻, was also systematically detected (presently *m/z* 935), albeit in low abundance. Other stoichiometries could not be observed. The deprotonated receptor and its associated dimer were systematically detected (here [(**3**)-H]⁻ and [(**3**)₂-H]⁻ at *m/z* 449 and 899, respectively). Two additional interesting ions were also detected. The first one, at *m/z* 197, corresponds to the [C₈F₃N₂O]⁻ terephthalonitrile moiety. This anion in turn interacts with the neutral receptor to form the adduct detected at *m/z* 647 in Figure 10a. With receptor **2**, this species is shifted to *m/z* 693 and was systematically less intense, suggesting a higher affinity of receptor **3** towards [C₈F₃N₂O]⁻. In order to have additional information about the structure of the 1:1 adducts, [(**receptor**)+X]⁻ ions were isolated and submitted to collision induced dissociation (CID) experiments. Representative CID spectra are presented in Figure 10b and 10c for [(**3**)+Cl]⁻ and [(**3**)+I]⁻ ions. First, we can notice that these ions dissociate along a reduced number of fragmentation pathways, compared to the adducts involving the *s*-tetrazine motif.^[11-13] Three main dissociation channels are indeed observed, which can be summarized below (Scheme 1).

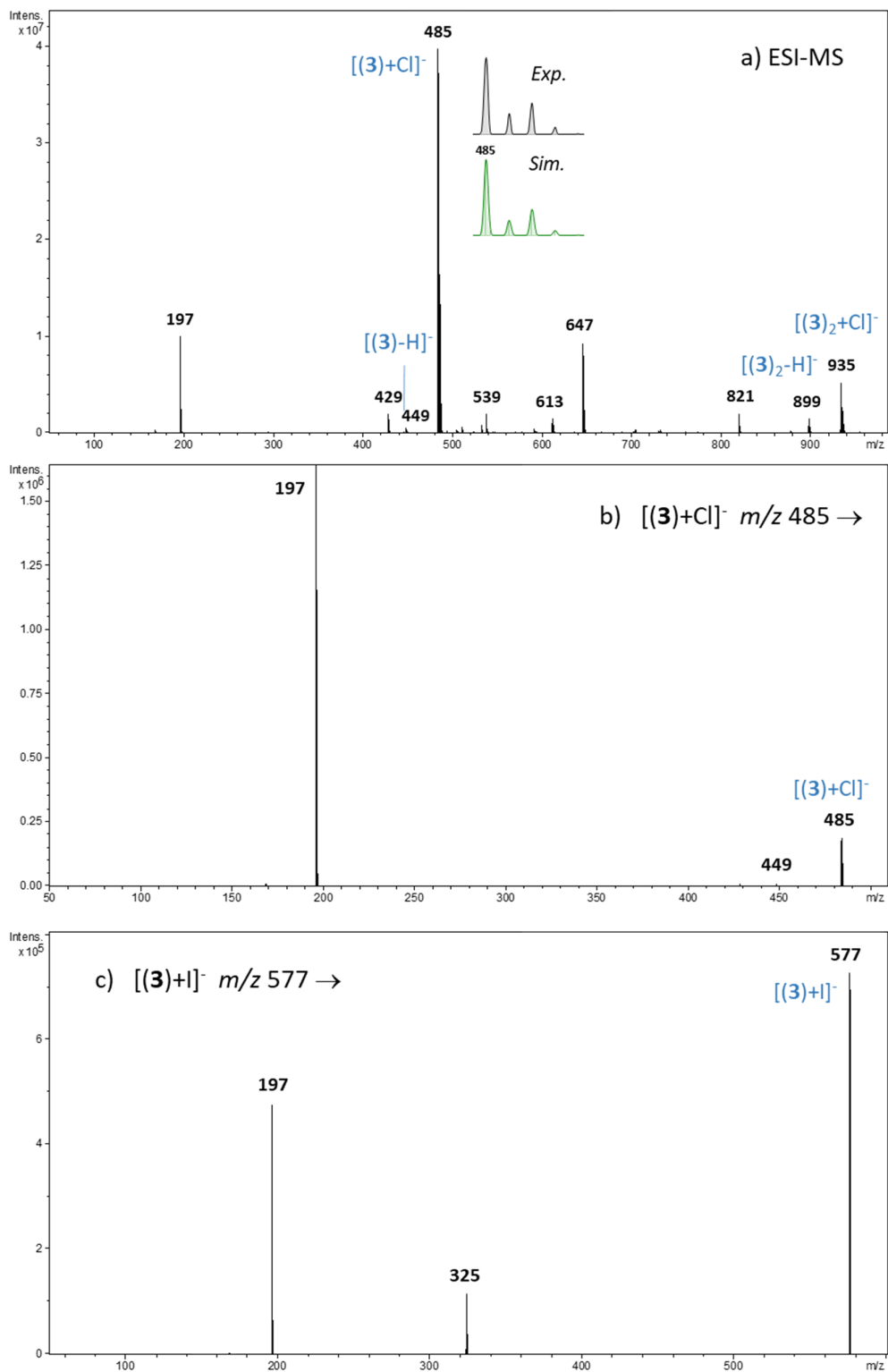
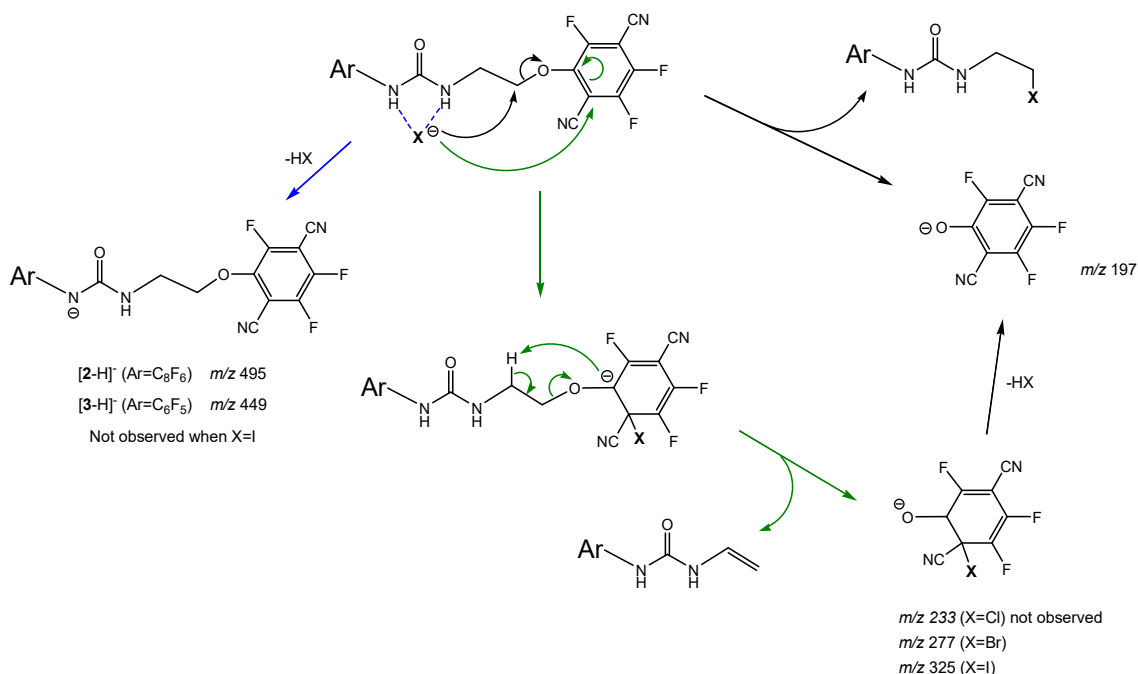


Figure 10 (a) Negative-ion electrospray mass spectrum of an equimolar mixture of **3**/ NBu_4Cl (10^{-5}M) in a 90/10 ACN/water solution, MS/MS spectrum of the (b) $[(\mathbf{3}) + \text{Cl}]^-$ ion (m/z 485) and (c) $[(\mathbf{3}) + \text{I}]^-$ ion (m/z 577).



Scheme 1 Proposed mechanisms for the common dissociation processes observed with receptors **2-3** in interaction with the halides.

The first channel is associated with deprotonation of the receptor and elimination of HX, leading to the deprotonated receptor. This process is very likely associated with removal of the H_a urea proton as the resulting anion in that case is stabilized through mesomeric effect. Deprotonation was found to be much less pronounced than with tetrazine receptors, including when the basic Cl⁻ ion is considered. The most intense product ion systematically corresponded to the anion detected at m/z 197, which includes the terephthalonitrile moiety. To account for its formation, we may assume a nucleophilic substitution at one of the methylene groups of the spacer, the terephthalonitrile moiety acting as the leaving group. The third series of product ions (m/z 277 and 325) is observed regardless of nature of the electron withdrawing group. Their formation could be explained by an aromatic nucleophilic attack of the terephthalonitrile moiety onto C_b carbon atom, which is consistent with the η^2 anion- π interaction involved in the calculated structures. The extent of the fragmentation increases in the following order: Cl⁻ (not observed) < Br⁻ < I⁻, that is with the increasing order of the halide nucleophilicity. Note that MS³ experiments confirmed that in turn these two ions expelled HX upon collision. The two latter processes may be promoted by the folding of the receptor around the anion, as evidenced by the DFT calculations. Overall, the different product ions suggest the interaction of the halides with both the urea and the terephthalonitrile units. In addition, a fourth but non informative process can correspond to the loss of the intact receptor leading to the halide X⁻. It could be observed here with the iodide, by modifying the low mass cutoff of the ion trap to

allow the detection of m/z 127 (SI Figure S43). On the other hand, similar experiments could not be achieved for Cl^- and Br^- .

We also recorded the MS/MS spectra of the 1:2 complexes. A MS/MS spectrum of the $[(2)_2+I]^-$ is given as an example in the supporting information (SI Figure S44). No matter the adduct upon investigation, these ions all dissociate according to elimination of an intact molecule of receptor. This behavior is characteristic of dimeric systems involving weak intermolecular interactions. One can then use this particular reactivity to establish the relative affinity of the two anionic receptors through the unimolecular dissociation of heterodimers, similarly to the kinetic method of measurement of gas-phase basicities or acidities.^[24,25]

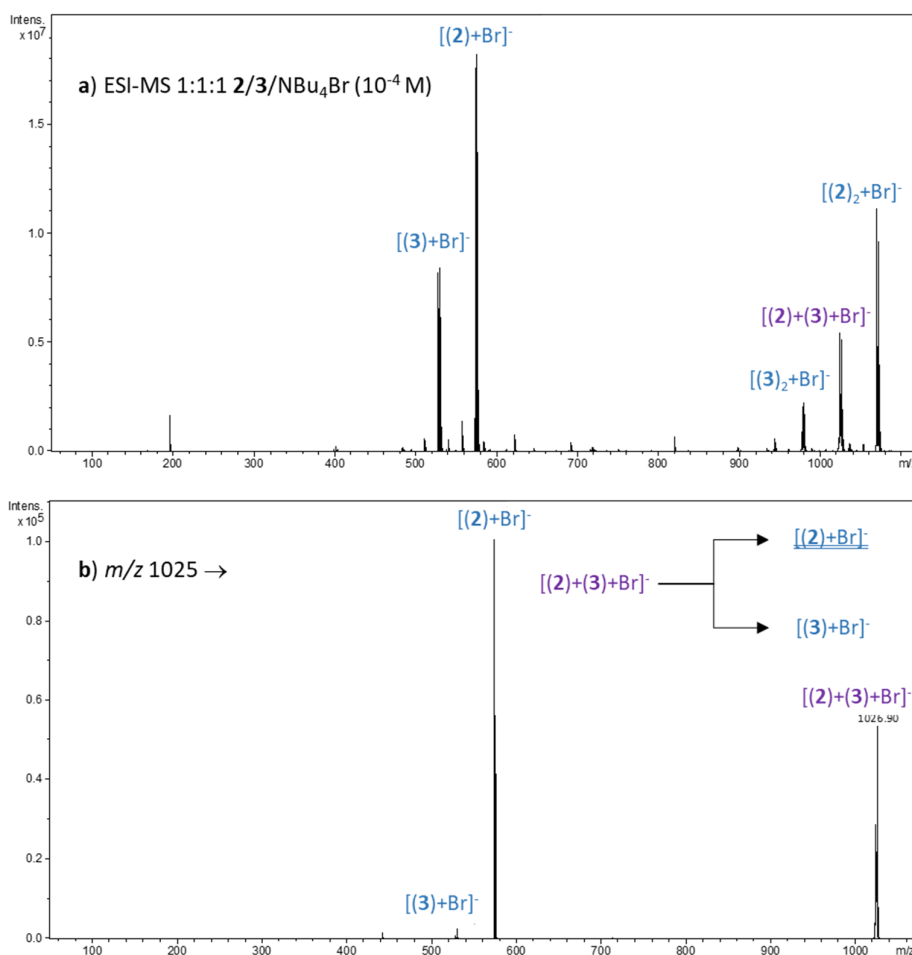


Figure 11 (a) Negative-ion electrospray mass spectrum of an equimolar mixture of **2/3**/ NBu_4Br (10^{-4}M) in a 90/10 ACN/water solution, (b) MS/MS spectrum of the $[(2)+(3)+\text{Br}]^-$ heterodimer (m/z 1025)

The kinetic method of measurement of proton affinity is based on the competitive dissociation of heterodimers $[\text{AHB}]^+$. In the case that weak interactions are involved within the dimer, this ion dissociates to generate two monomers $[\text{AH}]^+$ and $[\text{BH}]^+$, the most intense ion corresponding to the molecule having the highest proton affinity. One could therefore

transpose this approach to measure relative halide affinities^[26–28] provided heterodimers could be presently generated. To this end, we studied equimolar 1:1:1 mixtures of **2/3**/NBu₄X by electrospray to generate these heterodimers. The electrospray spectrum obtained with NBu₄Br is displayed in Figure 11. One can see that both homo- and heterodimers can be easily generated from these ternary mixtures. By isolating the heterodimer, one can record its dissociation spectrum (Figure 11b). The dominant dissociation channel corresponds to the formation of the [(**2**)+Br]⁻ monomer, clearly indicating that receptor **2** has a higher affinity for Br⁻ than receptor **3** in the gas phase. The same result is obtained with Cl⁻ and I⁻. These results are in agreement not only with relative affinity constants in solution deduced from NMR or photophysical experiments (*vide supra*), but also with the complexation energies computed in the gas phase (Table 4). The important difference in relative intensities of the monomers (Figure 11b) is consistent with the difference in computed complexation energies of 6.2 kcal/mol (APFD/aug-cc-pVDZ level), the kinetic method being sensitive to small energy variations.

Conclusion

In this paper, we examined the ability of perfluorinated terephthalonitrile to act as an anion- π receptor. Our rational approach is based first on the theoretical evaluation of electron acceptor properties of tetrafluoro-terephthalonitrile (quadrupole moment and polarizability) and the examination of the electrostatic potential map, which illustrates the electron deficiency of the aromatic system and highlights potential binding sites with anions. Second, we designed and synthesized new anion receptors comprising both a urea motif and a fluorinated terephthalonitrile fragment. The molecular recognition properties were studied in solution by a combination of NMR, UV-Visible and fluorescence spectroscopies. The association constants were determined and pointed to a better affinity of receptor **2** than receptor **3**, whatever the anion studied, both in NMR and photophysics. In all cases, the order of affinity is as follows: Cl⁻ > Br⁻ > I⁻. In addition, we studied these interactions in the gas phase, both theoretically and experimentally by tandem mass spectrometry. The gas-phase affinity trend (based on geometrical parameters and mass spectrometry experiments) agrees with the association constants determined experimentally from photophysical and NMR experiments. Our study confirmed the presence of a strong H-bond interaction with anions and a weaker interaction of the anion with one C-C bond of the terephthalonitrile.

Although perfluorinated terephthalonitrile appeared to be a slightly less efficient anion- π receptor than former *s*-tetrazine derivatives synthesized, our study sets a contribution and a synergistic role of terephthalonitrile in the binding event.

Keywords: terephthalonitrile • π -anion interaction • halide • recognition • affinity

Acknowledgements

We are grateful to the CNRS and the University of Versailles Saint Quentin. We thank the French Ministère de l'Enseignement Supérieur et de la Recherche for funding (O.Z. and R.P.). This work has been supported as part of France 2030 programme "ANR-11-IDEX-0003", awarded by the Graduate School Chemistry of the Université Paris-Saclay (L.R.). JYS would like to thank the ANR CHARMMMAT (ANR-LABX-0039) for the financial support allowing the acquisition of the 3D ion trap instrument. Theoretical calculations were performed using HPC resources from the "Mésocentre" computing center of CentraleSupélec and École Normale Supérieure Paris-Saclay supported by CNRS and Région Île-de-France (<http://mesocentre.centralesupelec.fr/>).

- [1] X. Wu, A. M. Gilchrist, P. A. Gale, *Chem.* **2020**, *6*, 1296–1309.
- [2] J. Zhao, D. Yang, X.-J. Yang, B. Wu, *Coord. Chem. Rev.* **2019**, *378*, 415–444.
- [3] S. Kubik, C. Reyheller, S. Stüwe, *J. Incl. Phenom. Macrocycl. Chem.* **2005**, *52*, 137–187.
- [4] A. L. Da Róz, M. Ferrieira, F. de Lima Leite, O. N. Oliveira, *Nanostructures*, **2016**.
- [5] J.-M. Lehn, *Supramolecular Chemistry: Concepts and Perspectives*, **1995**.
- [6] P. Gamez, *Inorg. Chem. Front.* **2014**, *1*, 35–43.
- [7] A. Frontera, P. Gamez, M. Mascal, T. J. Mooibroek, J. Reedijk, *Angew. Chem. Int. Ed.* **2011**, *50*, 9564–9583.
- [8] B. L. Schottel, H. T. Chifotides, K. R. Dunbar, *Chem. Soc. Rev.* **2008**, *37*, 68–83.
- [9] A. S. Mahadevi, G. N. Sastry, *Chem. Rev.* **2016**, *116*, 2775–2825.
- [10] R. Plais, G. Clavier, J.-Y. Salpin, A. Gaucher, D. Prim, *Eur. J. Org. Chem.* **2023**, *26*, e202201281.
- [11] R. Plais, G. Gouarin, A. Bournier, O. Zayene, V. Mussard, F. Bourdreux, J. Marrot, A. Brosseau, A. Gaucher, G. Clavier, J.-Y. Salpin, D. Prim, *ChemPhysChem* **2022**, e202200524.
- [12] The distances between the four nitrogen atoms of tetrazine and the anions in the recent receptors are very similar, which seems to (i) indicate that the anion is close to the tetrazine centroid and (ii) imply an π - π coordination mode. All spherical anions displayed similar behavior within the same set of receptors. See. Plais, G. Gouarin, A. Gaucher, V. Haldys, A. Brosseau, G. Clavier, J.-Y. Salpin, D. Prim, *ChemPhysChem* **2020**, *21*, 1249–1257.
- [13] R. Plais, H. Boufroura, G. Gouarin, A. Gaucher, V. Haldys, A. Brosseau, G. Clavier, J.-Y. Salpin, D. Prim, *RSC Adv.* **2021**, *11*, 9476–9487.
- [14] R. Plais. Interactions π -anion et liaisons hydrogène : un outil au service de la reconnaissance moléculaire et de la catalyse. PhD thesis, Université Paris-Saclay, **2021**.
- [15] S. Feuillastre, M. Pauton, L. Gao, A. Desmarchelier, A. J. Riives, D. Prim, D. Tondelier, B. Geffroy, G. Muller, G. Clavier, G. Pieters, *J. Am. Chem. Soc.* **2016**, *138*, 3990–3993.
- [16] L. Frédéric, A. Desmarchelier, L. Favereau, G. Pieters, *Adv. Funct. Mater.* **2021**, *31*, 2010281.
- [17] L. Frédéric, A. Desmarchelier, R. Plais, L. Lavnevich, G. Muller, C. Villafuerte, G. Clavier, E. Quesnel, B. Racine, S. Meunier-Della-Gatta, J.-P. Dognon, P. Thuéry, J. Crassous, L. Favereau, G. Pieters, *Adv. Funct. Mater.* **2020**, *30*, 2004838.
- [18] L. Poulard, S. Kasemthaveechok, M. Coehlo, R. A. Kumar, L. Frédéric, P. Sumsalee, T. d'Anfray, S. Wu, J. Wang, T. Matulaitis, J. Crassous, E. Zysman-Colman, L. Favereau, G. Pieters, *Chem. Commun.* **2022**, *58*, 6554–6557.

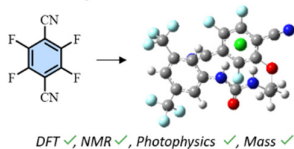
- [19] M. Savastano, C. García-Gallarín, M. D. López De La Torre, C. Bazzicalupi, A. Bianchi, M. Melguizo, *Coord. Chem. Rev.* **2019**, 397, 112–137.
- [20] V. Gorteau, G. Bollot, J. Mareda, S. Matile, *Org. Biomol. Chem.* **2007**, 5, 3000.
- [21] G. Tardajos, G. González-Gaitano, *J. Chem. Educ.* **2004**, 81, 270.
- [22] M. Albrecht, C. Wessel, M. de Groot, K. Rissanen, A. Lüchow, *J. Am. Chem. Soc.* **2008**, 130, 4600–4601.
- [23] O. B. Berryman, V. S. Bryantsev, D. P. Stay, D. W. Johnson, B. P. Hay, *J. Am. Chem. Soc.* **2007**, 129, 48–58.
- [24] R. Graham Cooks, J. S. Patrick, T. Kotiaho, S. A. McLuckey, *Mass Spectrom. Rev.* **1994**, 13, 287–339.
- [25] G. Bouchoux, *Mass Spectrom. Rev.* **2007**, 26, 775–835.
- [26] C.-C. Liou, J. S. Brodbelt, *J. Am. Soc. Mass Spectrom.* **1993**, 4, 242–248.
- [27] R. Augusti, D. V. Augusti, H. Chen, R. G. Cooks, *Eur J Mass Spectrom.* **2004**, 10, 847–855.
- [28] S. A. Chacko, P. G. Wenthold, *Int. J. Mass Spectrom.* **2007**, 267, 277–283.
- [29] H. E. Gottlieb, V. Kotlyar, A. Nudelman, *J. Org. Chem.* **1997**, 62, 7512–7515.
- [30] J. Contreras-García, E. R. Johnson, S. Keinan, R. Chaudret, J.-P. Piquemal, D. N. Beratan, W. Yang, *J. Chem. Theory Comput.* **2011**, 7, 625–632.
- [31] H. S. Rzepa, Script for creating an NCI surface as a JVXL compressed file from a (Gaussian) cube of total electron density, can be found under <https://www.ch.ic.ac.uk/rzepa/cub2nci/>, **2013**.
- [32] E. F. Pettersen, T. D. Goddard, C. C. Huang, G. S. Couch, D. M. Greenblatt, E. C. Meng, T. E. Ferrin, *J. Comput. Chem.* **2004**, 25, 1605–1612.
- [33] B. Valeur, M. N. Berberan-Santos, *Molecular Fluorescence: Principles and Applications, Second Edition*, **2012**.
- [34] H. Gampp, M. Maeder, C. J. Meyer, A. D. Zuberbühler, *Talanta* **1985**, 32, 95–101.
- [35] H. Gampp, M. Maeder, C. J. Meyer, A. D. Zuberbühler, *Talanta* **1985**, 32, 257–264.
- [36] C. Würth, M. Grabolle, J. Pauli, M. Spieles, U. Resch-Genger, *Nat Protoc* **2013**, 8, 1535–1550.
- [37] A. M. Brouwer, *Pure Appl. Chem.* **2011**, 83, 2213–2228.

TOC

Perfluorinated terephthalonitrile in combination with urea motif represents key fragments of new anion receptors. Their molecular recognition properties towards Cl^- , Br^- and I^- , have been evaluated. Combined experimental and theoretical data confirmed a privileged location site of the anions in agreement with a η^2 -type anion- π interaction.

TOC graphic

Tetrafluoroterephthalonitrile-based anion receptors



SUPPORTING INFORMATION

Tetrafluoroterephthalonitrile as an anion- π donor: theoretical evaluation and application to anion recognition

Olfa Zayene,^a Romain Plais,^a Laurie Rolhion,^a Flavien Bourdreux,^a Grégory Pieters,^b Anne Gaucher,^a Gilles Clavier,^c Anabelle Cœuret,^d Jean-Yves Salpin,^d and Damien Prim,^{*,a}

^a *Université Paris-Saclay, UVSQ, CNRS, Institut Lavoisier de Versailles, 78035 Versailles, France*

^b *Université Paris-Saclay, CEA, INRAE, Département Médicaments et Technologies pour la Santé (DMTS), SCBM, 91190 Gif-sur-Yvette, France*

^c *Université Paris-Saclay, ENS Paris-Saclay, CNRS, PPSM, 91190 Gif-sur-Yvette, France*

^d *Université Paris-Saclay, Univ Evry, CY Cergy Paris Université, CNRS, LAMBE, 91025, Evry-Courcouronnes, France*

Table of content

1.	General procedures, Material and Instrumentation.....	4
1.1	General experimental procedures and Materials	4
1.2	Instrumentation	4
1.3	Molecular modelling and software	5
2.	Computational data.....	6
2.1	Coordinates and thermodynamic data of 2	6
2.2	Coordinates and thermodynamic data of 3	16
	16
2.3.	Distances calculation.....	27
2.4.	NBO analysis.....	29
2.5.	BSSE and complexation energy calculation.....	37
3	Synthetic procedures.....	38
a.	Preparation of 4 , 5 and 6	38
b.	Preparation of 2 and 3	38
4	NMR titrations	44
4.1	Practical analysis procedure.....	44
4.2	Titration of 2 with NBu ₄ Cl.....	44
4.3	Titration of 2 with NBu ₄ Br	47
4.4	Titration of 2 with NBu ₄ I.....	50
4.5	Titration of 3 with NBu ₄ Cl.....	53
4.6	Titration of 3 with NBu ₄ Br	56
4.7	Titration of 3 with NBu ₄ I.....	59
5.	Photophysical analysis and procedures	62
5.1.	General practical analysis procedure	62
5.2.	Determination of quantum yields of 2 and 3	62
5.3.	Time dependent DFT analysis of compounds 2 and 3	64
5.4.	Titration of 2 with Nbu ₄ Cl.....	65
5.5.	Titration of 2 with NBu ₄ Br	69
5.6.	Titration of 2 with NBu ₄ I.....	73
5.7.	Titration of 3 with NBu ₄ Cl.....	77
5.8.	Titration of 3 with NBu ₄ Br	81
5.9.	Titration of 3 with NBu ₄ I.....	85
6.	Mass spectrometry experiments.....	89
7.	Bibliography.....	90

Figure S1 ¹ H NMR spectrum of 2 (200MHz)	39
Figure S2 ¹³ C NMR spectrum of 2 (75 MHz)	39
Figure S3 ¹⁹ F NMR spectrum of 2 (282 MHz).....	40
Figure S4 Mass spectrum of 2 (TOF MS ES+).....	40
Figure S5 ¹ H NMR spectrum of 3 (200 MHz)	42
Figure S6 ¹³ C NMR spectrum of 3 (75 MHz)	42
Figure S7 ¹⁹ F NMR spectrum of 3 (282 MHz).....	43
Figure S8 Mass spectrum of 3 (TOF MS ES+).....	43
Figure S9 ¹ H NMR titration of 2 with TBACl	44
Figure S10 ¹⁹ F NMR titration of 2 with TBACl.....	46
Figure S11 ¹ H NMR titration of 2 with TBABr	47
Figure S12 ¹⁹ F NMR titration of 2 with TBABr	49
Figure S13 ¹ H NMR titration of 2 with TBAI	50
Figure S14 ¹⁹ F NMR titration of 2 with TBAI.....	52
Figure S15 ¹ H NMR titration of 3 with TBACl	53
Figure S16 ¹⁹ F NMR titration of 3 with TBACl.....	55
Figure S17 ¹ H NMR titration of 3 with TBABr	56
Figure S18 ¹⁹ F NMR titration of 3 with TBABr	58
Figure S19 ¹ H NMR titration of 3 with TBAI	59
Figure S20 ¹⁹ F NMR titration of 3 with TBAI.....	61
Figure S21 Emission curves of 2 and Quinine in Quinine conditions	63
Figure S22 Emission curves of 3 and Quinine in Quinine conditions	63
Figure S23 Experimental (orange) and calculated (blue) absorption spectra of 2 (from 200 to 50 nm)	64
Figure S24 Experimental (orange) and calculated (blue) absorption spectra of 3	64
Figure S25 UV-visible titration of 2 with TBACl	65
Figure S26 Fluorescence titration of 2 with TBACl	67
Figure S27 Mathematical fit of fluorescence titration of 2 with TBACl.....	67
Figure S28 UV-visible titration of 2 with TBABr.....	69
Figure S29 Fluorescence titration of 2 with TBABr	71
Figure S30 Mathematical fit of fluorescence titration of 2 with TBABr	71
Figure S31 UV-visible titration of 2 with TBAI	73
Figure S32 Fluorescence titration of 2 with TBAI	75
Figure S33 Mathematical fit of fluorescence titration of 2 with TBAI.....	75
Figure S34 UV-visible titration of 3 with TBACl	77
Figure S35 Fluorescence titration of 3 with TBACl.....	79
Figure S36 Mathematical fit of fluorescence titration of 3 with TBACl.....	79
Figure S37 UV-visible titration of 3 with TBABr.....	81
Figure S38 Fluorescence titration of 3 with TBABr	83
Figure S39 Mathematical fit of fluorescence titration of 3 with TBABr	83
Figure S40 UV-visible titration of 3 with TBAI	85
Figure S41 Fluorescence titration of 3 with TBAI	87
Figure S42 Mathematical fit of fluorescence of 3 with TBAI	87
Figure S43 MS CID spectrum of the [(3) + I] ⁻ ion (<i>m/z</i> 577) after reduction of the low mass cutoff at <i>m/z</i> 100.....	89
Figure S44 CID spectrum of the [(2) ₂ + I] ⁻ dimeric ion (<i>m/z</i> 1119). The only product ion observed is associated with the elimination of the intact receptor.....	89

1. General procedures, Material and Instrumentation

1.1 General experimental procedures and Materials

Unless otherwise noted, all starting materials were obtained from commercial suppliers and used without purification. N,N-Dimethylformamide (100mL, Anhydrous, 99.8%) was purchased at Sigma-Aldrich. Dichloromethane was distilled over Sodium and under argon. For NMR titrations, deuterated acetonitrile (99.80% D) was purchased in 0.75mL pre-coated bulbs from Eurisotop®. For photophysical analysis, acetonitrile RS –SPECTROSOL – For optical spectroscopy was purchased from Carlo Erba®.

Reaction progress was carried out using pre-coated TLC sheets ALUGRAM® Xtra SIL G/UV₂₅₄ (0.20mm) from Macherey-Nagel® and visualized under 254 and 365 nm UV lamp from Fisher Bioblock Scientific®. Flash chromatography were proceeded using Silica 60M (0.04-0.063mm) for column chromatography silica gel from Macherey-Nagel®.

1.2 Instrumentation

¹H NMR spectra were recorded with Bruker AV-I 300MHz spectrometer at 298K, referenced to TMS signal and were calibrated using residual proton in Acetone d6 ($\delta=2.05$ ppm), according to the literature.^[1] ¹⁹F NMR spectra were recorded with Bruker AV-I 300MHz spectrometer at 282MHz and 298K and were not calibrated. ¹³C NMR spectra were recorded with a Bruker AV-I 300MHz spectrometer at 75MHz and 298 K and were calibrated using Acetone d6 ($\delta = 30.60$ ppm).^[1] ¹H NMR spectroscopic data are reported as follow: chemical shift δ [parts per million] (multiplicity, coupling constants in Hertz, integration). Multiplicities are reported as follow: s = singlet, d = doublet, t = triplet, q = quadruplet, quint = quintuplet, sext = sextuplet, hept = heptuplet, dd = doublet of doublet, td = triplet of doublet, tt = triplet of triplet, ddd = doublet of doublet of doublet, m = multiplet. ¹³C NMR spectroscopic data are reported in terms of chemical shifts δ [ppm] and when it is necessary multiplicity and coupling constant in Hertz.

To check the structure of the product obtained during the synthesis, high resolution mass spectra (HRMS) were obtained with a Waters Xevo QTOF instrument fitted with an electrospray ionization source (ESI+), using Leucine Enkephaline solution as internal calibrant.

Studies of the gas-phase interactions of **2** and **3** with the various anions, were performed onto a 3D ion trap instrument (Bruker Amazon Speed ETD). Complexes were generated in the gas phase by electrospray ionization. To this end, equimolar mixtures of **2**/NBu₄X and **3**/NBu₄X were prepared. Starting from 5 10⁻² M stock solutions of **2** and **3** and NBu₄X solubilized in acetonitrile (ACN) and purified water, respectively, 10⁻⁴ M or 10⁻⁵ M mixtures of **2**/ NBu₄X and **3**/NBu₄X (90/10 ACN/H₂O) were introduced in the electrospray source by a syringe pump (4-5 μ L/min). Typical experimental conditions were as followed: Capillary voltage: - 4500 V; End plate offset : -500 V; Dry gas: 10 L/min / Dry gas temperature: 200 °C, Nebulizer gas : 7.3 PSI ; Cap exit and Trap drive values automatically adjusted through the target mass parameter : 550 and 1025 to study the monomers and dimers, respectively.

All spectra were recorded in the "Maximum Resolution mode"

MS analysis : ICC mode : "on" (80000 ions) and acquisition time : auto.

MSⁿ analysis : ICC mode off / accumulation time 1 to 5 ms to reach c.a. 20000 ions for the selected precursor / Isolation window 4 to 8 Da / Fragmentation delay 40 ms/ amplitude of fragmentation : 0.20-1.0 depending on the ions / Low mass cutoff : Auto (except where indicated)

UV-Visible spectra were recorded at 25°C on a Cary 400 (Agilent) double-beam spectrometer using a 10 mm path quartz cell.

Corrected emission spectra were measured on a Fluoromax-3 (Horiba) or a Fluorolog-3 (Horiba) spectrofluorometer. An angle configuration of 90° was used. Optical density of the samples was checked to be less than 0.1 to avoid reabsorption artifacts.

1.3 Molecular modelling and software

All calculations were carried out using Gaussian 16® program:

Gaussian 16, Revision B.01, M. J. Frisch, G. W. Trucks, H. B. Schlegel, G. E. Scuseria, M. A. Robb, J. R. Cheeseman, G. Scalmani, V. Barone, G. A. Petersson, H. Nakatsuji, X. Li, M. Caricato, A. V. Marenich, J. Bloino, B. G. Janesko, R. Gomperts, B. Mennucci, H. P. Hratchian, J. V. Ortiz, A. F. Izmaylov, J. L. Sonnenberg, D. Williams-Young, F. Ding, F. Lipparini, F. Egidi, J. Goings, B. Peng, A. Petrone, T. Henderson, D. Ranasinghe, V. G. Zakrzewski, J. Gao, N. Rega, G. Zheng, W. Liang, M. Hada, M. Ehara, K. Toyota, R. Fukuda, J. Hasegawa, M. Ishida, T. Nakajima, Y. Honda, O. Kitao, H. Nakai, T. Vreven, K. Throssell, J. A. Montgomery, Jr., J. E. Peralta, F. Ogliaro, M. J. Bearpark, J. J. Heyd, E. N. Brothers, K. N. Kudin, V. N. Staroverov, T. A. Keith, R. Kobayashi, J. Normand, K. Raghavachari, A. P. Rendell, J. C. Burant, S. S. Iyengar, J. Tomasi, M. Cossi, J. M. Millam, M. Klene, C. Adamo, R. Cammi, J. W. Ochterski, R. L. Martin, K. Morokuma, O. Farkas, J. B. Foresman, and D. J. Fox, Gaussian, Inc., Wallingford CT, 2016.

Computed structures were preoptimized with a MM2 forcefield using Chem3D®. Then, optimizations were calculated at APFD/aug-cc-pVDZ calculation level using Gaussian 16® software without any solvent correction. For several systems, APFD/aug-cc-pVTZ calculations were performed to evaluate the effect of a more extended basis set onto both the geometry and computed energies. Basis sets for bromide and iodide were downloaded on basisetexchange.org. Stationary points were verified by a harmonic vibrational frequencies calculation. None of the predicated geometry has any imaginary frequency implying that the optimized geometry of each of the molecules under study lay at a minimum local point on the potential energy surface.

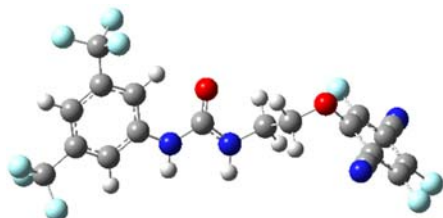
Effect of solvent (acetonitrile) on geometries was evaluated by proceeding optimization calculations at APFD/ aug-cc-pVDZ by adding the Polarizable Continuum Model (PCM) using the integral equation formalism variant (IEFPCM). Once again, stationary points were checked by a harmonic vibrational frequencies' calculation. None of the predicated geometry has any imaginary frequency implying that the optimized geometry of each of the molecules under study lay at a minimum local point on the potential energy surface.

Theoretical UV-Visible spectra were calculated on optimized geometries structures by an energy calculation using time dependant DFT calculation at TD PBE0/6-311+g(d,p)//apfd/6-31+g(d,p) level and solving on 24 first singlet states. A standard solvation model (IEFPCM) for acetonitrile was used. Electrostatic Potentials Surfaces (ESP) were thus calculated using Gaussview® software from optimized structures using a fine grid for Total Density and a medium grid of ESP. NCIplots were generated from total densities using the script developed by Rzepa available on the website application of the Imperial College London.^[2,3]

Distances were measured using Gaussview software on structures optimized without any solvent correction. Distances between trifluoroterephthalonitrile centroid (defined using the six atoms of the terephthalonitrile rings) and anions were measured using UCSF Chimera software.^[4]

2. Computational data

2.1 Coordinates and thermodynamic data of **2**



2 (in vacuum)
APFD/aug-cc-pVDZ
Charge: 0
Spin Multiplicity: Singlet
Imaginary frequencies: 0
Electronic Energy: -1996.222576 Hartree
Zero-point correction= 0.268821 (Hartree/Particle)
Thermal correction to Energy= 0.299848
Thermal correction to Enthalpy= 0.300792
Thermal correction to Gibbs Free Energy= 0.197283
Sum of electronic and zero-point Energies= -1995.953755
Sum of electronic and thermal Energies= -1995.922728
Sum of electronic and thermal Enthalpies= -1995.921784
Sum of electronic and thermal Free Energies= -1996.025293

Atomic Number	Coordinates (Angstrom)			Atomic Number	Coordinates (Angstrom)		
	X	Y	Z		X	Y	Z
6	-5.836563	0.078888	0.072583	6	5.163982	0.850448	-0.697852
6	-5.391043	-1.201789	-0.253486	6	6.383956	0.255845	-1.04382
6	-4.044786	-1.464186	-0.463046	6	6.970192	-0.649599	-0.150639
6	-3.098089	-0.43441	-0.346085	6	6.348535	-0.946116	1.05492
6	-3.52815	0.856627	-0.020723	6	5.133462	-0.339613	1.393663
6	-4.888045	1.087683	0.183639	6	4.521398	-0.641101	2.646688
6	-5.302952	2.493073	0.540261	9	4.596535	1.700149	-1.55093
6	-6.401841	-2.303699	-0.432877	6	7.012853	0.55327	-2.288544
9	-4.930376	3.375826	-0.413658	9	8.125455	-1.232351	-0.455064
9	-4.725765	2.90021	1.69413	9	6.922734	-1.806681	1.891702
9	-6.636819	2.613361	0.697437	7	4.005881	-0.889936	3.657283
9	-5.852085	-3.531254	-0.296529	7	7.521601	0.791426	-3.304646
9	-6.964323	-2.261477	-1.66417	1	-6.892517	0.278079	0.238265
9	-7.409311	-2.21319	0.460055	1	-3.728596	-2.477672	-0.712988
7	-1.759515	-0.776561	-0.554342	1	-2.806772	1.663398	0.066489
6	-0.660094	0.065528	-0.536843	1	-1.600496	-1.73875	-0.816323
8	-0.722746	1.276598	-0.383074	1	0.581139	-1.590635	-0.59429
7	0.534751	-0.592501	-0.739459	1	2.551478	-0.428127	-1.179772
6	1.769631	0.159189	-0.68012	1	1.637009	1.09363	-1.236236
6	2.163457	0.474268	0.761773	1	1.412178	1.118567	1.227602
8	3.386893	1.23502	0.818465	1	2.26269	-0.445613	1.35768
6	4.52031	0.573337	0.508482				



2 (in acetonitrile)
 APFD/aug-cc-pVDZ, scrf=(iefpcm, solvent=acetonitrile)
 Charge: 0

Spin Multiplicity: Singlet

Imaginary frequencies: 0

Electronic Energy: -1996.247500 Hartree

Zero-point correction= 0.268378 (Hartree/Particle)

Thermal correction to Energy= 0.299339

Thermal correction to Enthalpy= 0.300283

Thermal correction to Gibbs Free Energy= 0.198284

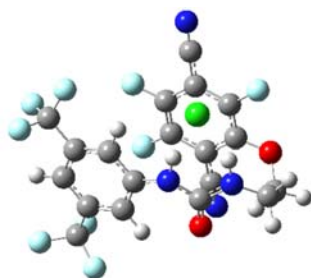
Sum of electronic and zero-point Energies= -1995.979123

Sum of electronic and thermal Energies= -1995.948162

Sum of electronic and thermal Enthalpies= -1995.947217

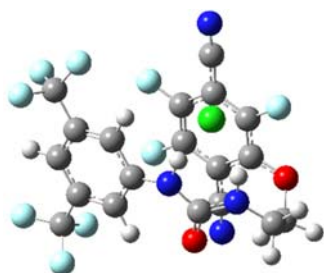
Sum of electronic and thermal Free Energies= -1996.049216

Atomic Number	Coordinates (Angstrom)			Atomic Number	Coordinates (Angstrom)		
	X	Y	Z		X	Y	Z
6	-5.762502	0.473628	0.189168	6	4.543271	-0.061271	-0.307445
6	-5.548482	-0.884344	0.430408	6	5.769278	-0.283278	-0.953309
6	-4.323362	-1.483739	0.17646	6	6.99534	-0.121106	-0.31219
6	-3.256049	-0.722313	-0.332038	6	7.015771	0.275854	1.032251
6	-3.453825	0.642222	-0.578627	6	5.825835	0.511452	1.691394
6	-4.699108	1.211771	-0.314218	6	4.588407	0.362736	1.039134
6	-4.851874	2.685139	-0.579112	6	3.427254	0.716955	1.788346
6	-6.696491	-1.72041	0.926284	9	5.753704	-0.672872	-2.227992
9	-4.507481	3.007114	-1.850146	6	8.214056	-0.372368	-1.008118
9	-4.051863	3.425401	0.22951	9	8.176548	0.427406	1.668767
9	-6.113163	3.124491	-0.389719	9	5.851022	0.904056	2.965148
9	-6.290802	-2.858026	1.530326	7	2.513831	1.038822	2.429713
9	-7.518611	-2.09196	-0.089102	7	9.207644	-0.576029	-1.573059
9	-7.465939	-1.050842	1.81461	1	-6.726085	0.934718	0.391342
7	-2.053419	-1.38489	-0.552631	1	-4.188461	-2.546881	0.37484
6	-0.880162	-0.863352	-1.070032	1	-2.639044	1.241791	-0.971554
8	-0.757948	0.300929	-1.451712	1	-2.052323	-2.367227	-0.313067
7	0.136711	-1.772214	-1.138273	1	0.035601	-2.679474	-0.7065
6	1.447369	-1.370884	-1.592229	1	1.989719	-2.260907	-1.929568
6	2.216205	-0.670696	-0.480538	1	1.33643	-0.688957	-2.443262
8	3.459164	-0.238708	-1.064727	1	1.653763	0.197479	-0.119448
				1	2.420971	-1.357017	0.352314



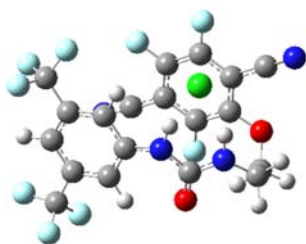
2-Cl-B (in vacuum)
 APFD/aug-cc-pVDZ
 Charge: -1
 Spin Multiplicity: Singlet
 Imaginary frequencies: 0
 Electronic Energy: -2456.0496562 Hartree
 Zero-point correction= 0.270080 (Hartree/Particle)
 Thermal correction to Energy= 0.302037
 Thermal correction to Enthalpy= 0.302981
 Thermal correction to Gibbs Free Energy= 0.201754
 Sum of electronic and zero-point Energies= -2456.226482
 Sum of electronic and thermal Energies= -2456.194525
 Sum of electronic and thermal Enthalpies= -2456.193581
 Sum of electronic and thermal Free Energies= -2456.294808

Atomic Number	Coordinates (Angstrom)			Atomic Number	Coordinates (Angstrom)		
	X	Y	Z		X	Y	Z
6	3.321840	0.112817	0.148177	6	-0.503039	-0.161606	-1.701517
6	2.544622	1.217863	0.505195	6	-1.532519	-1.078969	-1.451100
6	1.285690	1.070837	1.063203	6	-2.990346	0.760775	-0.907525
6	0.752317	-0.218540	1.273159	6	-1.974777	1.679438	-1.180883
6	1.526106	-1.337520	0.931607	9	-4.191407	1.205754	-0.554166
6	2.790960	-1.149837	0.374862	9	0.687935	-0.595680	-2.118034
7	-0.527097	-0.280804	1.782671	9	0.272580	2.053247	-1.834118
6	-1.381784	-1.363750	1.699496	6	-2.217997	3.084682	-1.135600
8	-1.030262	-2.520195	1.448210	6	-1.303935	-2.454593	-1.747679
7	-2.683286	-1.000128	1.886256	7	-2.408671	4.227873	-1.203689
6	-3.749313	-1.928274	1.618968	7	-1.139021	-3.562437	-2.057276
6	-3.749387	-2.464960	0.188584	1	1.121040	-2.333976	1.082331
8	-3.863404	-1.413611	-0.793603	1	4.305276	0.240763	-0.297152
6	-2.794312	-0.619136	-1.010858	1	0.681721	1.942483	1.318139
1	-1.005962	0.632958	1.948268	6	3.573958	-2.379929	0.009943
1	-2.878323	0.007136	2.002635	6	3.113770	2.586588	0.260357
1	-3.684385	-2.802735	2.287529	9	3.812963	-3.167028	1.090792
1	-4.692450	-1.408160	1.827192	9	4.782519	-2.092093	-0.530932
1	-4.635786	-3.087456	0.017771	9	2.919749	-3.153593	-0.886029
1	-2.851818	-3.065128	0.009205	9	2.246803	3.579605	0.526874
17	-2.368284	2.109657	2.132863	9	4.219095	2.812473	1.023685
6	-0.717548	1.199130	-1.565914	9	3.515488	2.741624	-1.027186



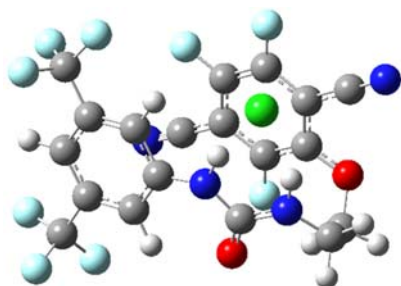
2-Cl-B (in acetonitrile)
 APFD/aug-cc-pVDZ, scrf=(iefpcm, solvent=acetonitrile)
 Charge: -1
 Spin Multiplicity: Singlet
 Imaginary frequencies: 0
 Electronic Energy: -2456.566320 Hartree
 Zero-point correction= 0.269758 (Hartree/Particle)
 Thermal correction to Energy= 0.300146
 Thermal correction to Enthalpy= 0.301090
 Thermal correction to Gibbs Free Energy= 0.206505
 Sum of electronic and zero-point Energies= -2456.296561
 Sum of electronic and thermal Energies= -2456.266173
 Sum of electronic and thermal Enthalpies= -2456.265229
 Sum of electronic and thermal Free Energies= -2456.359815

Atomic Number	Coordinates (Angstrom)			Atomic Number	Coordinates (Angstrom)		
	X	Y	Z		X	Y	Z
6	3.260610	-0.102165	0.213408	6	-0.468479	-0.561188	-1.772979
6	2.603426	1.098378	0.493044	6	-1.653765	-1.223474	-1.422127
6	1.326026	1.120493	1.028157	6	-2.711675	0.907557	-1.086568
6	0.649728	-0.086299	1.292698	6	-1.535744	1.571420	-1.439482
6	1.301662	-1.299041	1.035393	9	-3.791249	1.621127	-0.778587
6	2.587892	-1.283157	0.496466	9	0.604475	-1.267730	-2.127374
7	-0.646779	0.018792	1.764738	9	0.726497	1.432229	-2.129894
6	-1.609187	-0.974292	1.751642	6	-1.480931	2.994946	-1.475036
8	-1.366396	-2.177348	1.608927	6	-1.672526	-2.644608	-1.527238
7	-2.869281	-0.475218	1.873435	7	-1.422951	4.152687	-1.537744
6	-4.036144	-1.306470	1.691179	7	-1.673838	-3.798515	-1.660466
6	-4.092107	-1.981670	0.323710	1	0.791657	-2.236297	1.232938
8	-3.999168	-1.022911	-0.757483	1	4.259379	-0.109420	-0.216523
6	-2.800578	-0.488203	-1.048615	1	0.824081	2.068442	1.219521
1	-1.013368	0.978352	1.872431	6	3.240067	-2.611796	0.231035
1	-2.973565	0.540967	1.928606	6	3.316120	2.385850	0.186367
1	-4.075591	-2.103100	2.449578	9	3.514406	-3.275958	1.383649
1	-4.913135	-0.665337	1.832320	9	4.405818	-2.500112	-0.440213
1	-5.064777	-2.462588	0.180047	9	2.442689	-3.431029	-0.496617
1	-3.304610	-2.734305	0.230549	9	2.528522	3.471550	0.326678
17	-2.221217	2.693269	2.080839	9	4.389780	2.571883	0.996883
6	-0.404495	0.819547	-1.781289	9	3.793024	2.404774	-1.082702



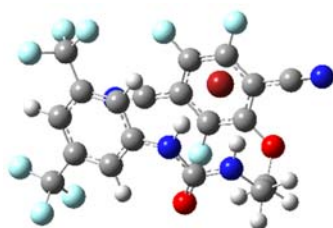
2-Cl-A (in vacuum)
 APFD/aug-cc-pVDZ
 Charge: -1
 Spin Multiplicity: Singlet
 Imaginary frequencies: 0
 Electronic Energy: -2456.498258 Hartree
 Zero-point correction= 0.270266 (Hartree/Particle)
 Thermal correction to Energy= 0.302169
 Thermal correction to Enthalpy= 0.303113
 Thermal correction to Gibbs Free Energy= 0.202976
 Sum of electronic and zero-point Energies= -2456.227992
 Sum of electronic and thermal Energies= -2456.196090
 Sum of electronic and thermal Enthalpies= -2456.195146
 Sum of electronic and thermal Free Energies= -2456.295282

Atomic Number	Coordinates (Angstrom)			Atomic Number	Coordinates (Angstrom)		
	X	Y	Z		X	Y	Z
6	3.429973	0.235042	-0.193108	6	-0.637192	0.196794	1.704382
6	2.556536	1.255696	-0.575768	6	-3.244857	0.692155	0.836465
6	1.290778	0.982018	-1.067460	9	-0.184021	2.513054	1.532726
6	0.853581	-0.354341	-1.187956	1	1.393052	-2.420411	-0.899809
6	1.724912	-1.389569	-0.818886	1	4.412947	0.461832	0.211378
6	2.991095	-1.075001	-0.327821	1	0.613411	1.789013	-1.348896
7	-0.431545	-0.544405	-1.648115	6	3.890605	-2.217604	0.051268
6	-1.200560	-1.680541	-1.483555	6	3.012389	2.676062	-0.397376
8	-0.765890	-2.783849	-1.141057	9	4.271795	-2.939488	-1.038374
7	-2.524971	-1.433835	-1.708395	9	5.030176	-1.812368	0.657581
6	-3.518338	-2.404117	-1.330778	9	3.287466	-3.091056	0.888265
6	-3.500332	-2.746366	0.157870	9	2.144527	3.579269	-0.892731
8	-3.787732	-1.602976	0.993111	9	4.207078	2.900089	-1.010633
6	-2.853391	-0.634409	1.098364	9	3.202246	2.984751	0.909863
1	-0.974001	0.314748	-1.890550	6	-4.585758	0.947505	0.420828
1	-2.792668	-0.460834	-1.919894	6	0.673101	-0.043441	2.212129
1	-3.365819	-3.348678	-1.878116	7	-5.697889	1.129434	0.139841
1	-4.497939	-1.998707	-1.612516	7	1.729321	-0.225583	2.659582
1	-4.306970	-3.451464	0.391975	6	-2.344560	1.751145	0.992063
1	-2.537950	-3.189938	0.431663	6	-1.551608	-0.851226	1.563050
17	-2.422712	1.670933	-2.259073	9	-2.732462	3.001172	0.776076
6	-1.044900	1.501736	1.401000	9	-1.171501	-2.083793	1.918776



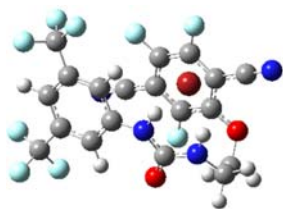
2-Cl-A (in acetonitrile)
 APFD/aug-cc-pVDZ, scrf=(iefpcm, solvent=acetonitrile)
 Charge: -1
 Spin Multiplicity: Singlet
 Imaginary frequencies: 0
 Electronic Energy: -2456.567546 Hartree
 Zero-point correction= 0.269827 (Hartree/Particle)
 Thermal correction to Energy= 0.302057
 Thermal correction to Enthalpy= 0.303001
 Thermal correction to Gibbs Free Energy= 0.201272
 Sum of electronic and zero-point Energies= -2456.297719
 Sum of electronic and thermal Energies= -2456.265489
 Sum of electronic and thermal Enthalpies= -2456.264545
 Sum of electronic and thermal Free Energies= -2456.366274

Atomic Number	Coordinates (Angstrom)			Atomic Number	Coordinates (Angstrom)		
	X	Y	Z		X	Y	Z
6	3.393919	0.243334	-0.239874	6	-0.572944	0.006954	1.801698
6	2.510890	1.281627	-0.543883	6	-3.104658	0.728273	0.896417
6	1.231414	1.032787	-1.013445	9	0.069733	2.283964	1.712148
6	0.787684	-0.292351	-1.188717	1	1.339281	-2.370377	-1.034000
6	1.667588	-1.344373	-0.903619	1	4.391425	0.448298	0.141326
6	2.947694	-1.057121	-0.431353	1	0.554737	1.857745	-1.233445
7	-0.515733	-0.463036	-1.620720	6	3.852826	-2.220679	-0.135479
6	-1.289169	-1.598346	-1.462246	6	2.969677	2.693374	-0.307594
8	-0.846925	-2.698155	-1.116522	9	4.221340	-2.871610	-1.269916
7	-2.611300	-1.364674	-1.694321	9	4.991927	-1.854628	0.489198
6	-3.614619	-2.341135	-1.335790	9	3.250417	-3.144827	0.650826
6	-3.625343	-2.682367	0.151731	9	2.060383	3.614942	-0.684991
8	-3.842907	-1.509254	0.975674	9	4.115284	2.969739	-0.979616
6	-2.834970	-0.633775	1.133826	9	3.237313	2.918480	1.003745
1	-1.037183	0.394523	-1.864978	6	-4.404373	1.106115	0.449303
1	-2.890058	-0.407567	-1.920411	6	0.714115	-0.354317	2.295467
1	-3.455828	-3.281345	-1.884453	6	-2.127704	1.707954	1.098120
1	-4.586152	-1.935914	-1.639326	6	-1.562540	-0.963217	1.618504
1	-4.474988	-3.333151	0.381519	9	-2.406412	2.989954	0.880899
1	-2.698023	-3.181553	0.444085	9	-1.280252	-2.227015	1.944792
17	-2.501571	1.811980	-2.414454	7	-5.475600	1.404913	0.114950
6	-0.864066	1.349326	1.533200	7	1.761492	-0.636976	2.708780



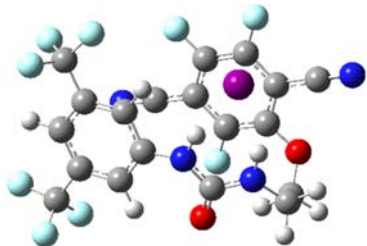
2-Br-A (in vacuum)
 APFD/aug-cc-pVDZ
 Charge: -1
 Spin Multiplicity: Singlet
 Imaginary frequencies: 0
 Electronic Energy: -2413.272852 Hartree
 Zero-point correction= 0.269974 (Hartree/Particle)
 Thermal correction to Energy= 0.302114
 Thermal correction to Enthalpy= 0.303058
 Thermal correction to Gibbs Free Energy= 0.201732
 Sum of electronic and zero-point Energies= -2413.002877
 Sum of electronic and thermal Energies= -2412.970737
 Sum of electronic and thermal Enthalpies= -2412.969793
 Sum of electronic and thermal Free Energies= -2413.071119

Atomic Number	Coordinates (Angstrom)			Atomic Number	Coordinates (Angstrom)		
	X	Y	Z		X	Y	Z
6	3.221727	-0.921422	-0.461402	6	-0.381150	-0.167621	1.868975
6	3.568117	0.396438	-0.197072	6	-3.069563	0.209804	1.214404
6	2.603015	1.380676	-0.422173	9	-0.119065	2.181618	1.974466
6	1.337048	1.063462	-0.886555	1	0.587582	1.840209	-1.044614
6	0.996206	-0.281750	-1.140558	1	4.551097	0.654484	0.188269
6	1.958657	-1.279220	-0.930679	1	1.700773	-2.317771	-1.115512
7	-0.293612	-0.522978	-1.567328	6	2.962355	2.804670	-0.104729
6	-0.972736	-1.723771	-1.485435	6	4.221384	-2.024045	-0.253014
7	-2.321989	-1.558844	-1.616325	9	4.092705	3.193068	-0.756583
8	-0.442030	-2.819114	-1.284128	9	3.217126	2.977633	1.216339
6	-3.220964	-2.639703	-1.307951	9	1.998014	3.683158	-0.438338
6	-3.098845	-3.141364	0.129464	9	3.729573	-3.025999	0.509425
8	-3.424449	-2.123284	1.101031	9	4.593562	-2.593482	-1.432269
6	-2.560758	-1.101613	1.279508	9	5.359632	-1.597771	0.340810
6	-0.906326	1.125964	1.759398	6	-4.452019	0.400506	0.916540
1	-0.897210	0.313354	-1.699621	6	0.972254	-0.357920	2.274527
1	-2.677976	-0.597906	-1.714217	6	-2.245800	1.313435	1.460425
1	-4.240601	-2.282241	-1.497236	6	-1.219567	-1.263499	1.643785
1	-3.029997	-3.502724	-1.966374	9	-0.724300	-2.493619	1.821869
1	-2.094130	-3.536702	0.307842	9	-2.744034	2.542743	1.438684
1	-3.839102	-3.928441	0.316682	7	-5.592331	0.519952	0.731200
35	-2.543687	1.737047	-1.881543	7	2.064123	-0.504422	2.642337



2-Br-A (in acetonitrile)
 APFD/6-31+G(d,p) for H, C, N, O, F atoms and APFD/aug-cc-pvtz for Br atom
 scrf=(iefpcm, solvent=acetonitrile)
 Charge: -1
 Spin Multiplicity: Singlet
 Imaginary frequencies: 0
 Electronic Energy: -2413.340912 Hartree
 Zero-point correction= 0.269687 (Hartree/Particle)
 Thermal correction to Energy= 0.302026
 Thermal correction to Enthalpy= 0.302971
 Thermal correction to Gibbs Free Energy= 0.201136
 Sum of electronic and zero-point Energies= -2413.071225
 Sum of electronic and thermal Energies= -2413.038886
 Sum of electronic and thermal Enthalpies= -2413.037941
 Sum of electronic and thermal Free Energies= -2413.139776

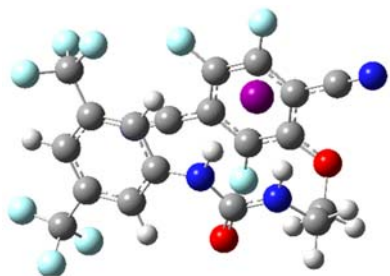
Atomic Number	Coordinates (Angstrom)			Atomic Number	Coordinates (Angstrom)		
	X	Y	Z		X	Y	Z
6	3.192424	-0.857242	-0.587796	6	-0.287092	-0.383362	1.940675
6	3.528073	0.445519	-0.246020	6	-2.931695	0.187888	1.284432
6	2.536709	1.422155	-0.363747	9	0.134053	1.939568	2.119614
6	1.258951	1.110309	-0.798699	1	0.496019	1.884716	-0.874372
6	0.929902	-0.218667	-1.128048	1	4.524583	0.697423	0.108716
6	1.916824	-1.206926	-1.029722	1	1.676654	-2.234907	-1.281294
7	-0.376160	-0.459584	-1.519780	6	2.878918	2.830376	0.035144
6	-1.041745	-1.669760	-1.453422	6	4.215073	-1.955390	-0.493645
7	-2.391286	-1.532757	-1.583128	9	3.940513	3.307424	-0.662043
8	-0.487273	-2.756072	-1.264989	9	3.222045	2.908107	1.345869
6	-3.285053	-2.632776	-1.299308	9	1.862484	3.695668	-0.155375
6	-3.178909	-3.145997	0.133795	9	3.767022	-3.003157	0.239676
8	-3.451776	-2.103927	1.104328	9	4.527632	-2.456615	-1.717012
6	-2.520532	-1.159311	1.321814	9	5.373094	-1.548995	0.067657
6	-0.719380	0.946035	1.870386	6	-4.289154	0.486212	0.967036
1	-0.975373	0.371114	-1.633573	6	1.058715	-0.671918	2.310126
1	-2.768189	-0.588739	-1.678702	6	-2.038773	1.227608	1.562729
1	-4.303571	-2.284648	-1.503576	6	-1.193309	-1.417351	1.688810
1	-3.078570	-3.482668	-1.966419	9	-0.774615	-2.677157	1.834306
1	-2.196065	-3.586724	0.318715	9	-2.451360	2.491526	1.543807
1	-3.953185	-3.896524	0.321590	7	-5.404514	0.713828	0.737049
35	-2.639093	1.865375	-1.947825	7	2.153509	-0.895622	2.624761



2-I-A (in vacuum)
 APFD/aug-cc-pVDZ
 Charge: -1
 Spin Multiplicity: Singlet
 Imaginary frequencies: 0
 Electronic Energy: -2292.170653 Hartree
 Zero-point correction= 0.269773 (Hartree/Particle)
 Thermal correction to Energy= 0.302092
 Thermal correction to Enthalpy= 0.303036
 Thermal correction to Gibbs Free Energy= 0.200326
 Sum of electronic and zero-point Energies= -2291.900879
 Sum of electronic and thermal Energies= -2291.868561
 Sum of electronic and thermal Enthalpies= -2291.867617
 Sum of electronic and thermal Free Energies= -2291.970327

Atomic Number	Coordinates (Angstrom)			Atomic Number	Coordinates (Angstrom)		
	X	Y	Z		X	Y	Z
6	3.449353	-0.676544	-0.627281	6	-2.075564	0.738015	1.871477
6	3.692631	0.621608	-0.201071	6	-0.814448	-1.726392	1.617687
6	2.633212	1.530576	-0.243580	9	-0.004093	1.728427	2.390607
6	1.374648	1.158200	-0.686817	1	0.552526	1.875454	-0.703162
6	1.140370	-0.167807	-1.105621	1	2.021826	-2.112651	-1.394533
6	2.196925	-1.087878	-1.081171	1	4.670125	0.919056	0.169652
7	-0.147620	-0.475649	-1.500596	6	2.885085	2.928848	0.246211
6	-0.713552	-1.735765	-1.540907	6	4.552489	-1.697289	-0.618616
7	-2.077285	-1.690001	-1.589575	9	1.821184	3.740802	0.104538
8	-0.076103	-2.790333	-1.500651	9	3.919716	3.512540	-0.418297
6	-2.856572	-2.884743	-1.394251	9	3.227973	2.947438	1.558570
6	-2.610826	-3.556832	-0.044952	9	4.896283	-2.074524	-1.880438
8	-2.966556	-2.709676	1.069398	9	4.198655	-2.829561	0.029250
6	-2.185563	-1.646036	1.350307	9	5.684418	-1.243952	-0.033406
6	-0.706725	0.642683	2.064086	6	-2.812867	-0.394519	1.508287
1	-0.817145	0.313137	-1.517374	6	-0.063267	-0.596365	1.955064
1	-2.533623	-0.770282	-1.573346	9	-2.682429	1.901772	2.065358
1	-3.912805	-2.605016	-1.490281	9	-0.201668	-2.915133	1.592172
1	-2.625190	-3.630798	-2.171798	6	-4.225927	-0.304004	1.329950
1	-1.568122	-3.878984	0.033399	6	1.325182	-0.709779	2.258108
1	-3.270403	-4.425751	0.065793	7	-5.383572	-0.277803	1.239847
53	-2.733871	1.801753	-1.536610	7	2.447243	-0.799851	2.543946

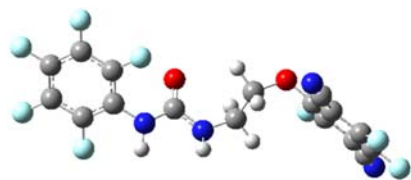
2-I-A (in acetonitrile)
 APFD/aug-cc-pVDZ
 scrf=(iefpcm, solvent=acetonitrile)



Charge: -1
 Spin Multiplicity: Singlet
 Imaginary frequencies: 0
 Electronic Energy: -2292.237791 Hartree
 Zero-point correction= 0.269480 (Hartree/Particle)
 Thermal correction to Energy= 0.302000
 Thermal correction to Enthalpy= 0.302944
 Thermal correction to Gibbs Free Energy= 0.199709
 Sum of electronic and zero-point Energies= -2291.968311
 Sum of electronic and thermal Energies= -2291.935792
 Sum of electronic and thermal Enthalpies= -2291.934847
 Sum of electronic and thermal Free Energies= -2292.038082

Atomic Number	Coordinates (Angstrom)			Atomic Number	Coordinates (Angstrom)		
	X	Y	Z		X	Y	Z
6	3.404119	-0.540384	-0.756514	6	-1.857477	0.573712	1.965666
6	3.614346	0.730102	-0.238665	6	-0.723332	-1.938869	1.606996
6	2.51707	1.590723	-0.166464	9	0.260446	1.441754	2.513901
6	1.25719	1.196938	-0.587358	1	0.41066	1.879703	-0.514154
6	1.058206	-0.099437	-1.098519	1	2.010736	-1.97102	-1.58524
6	2.150792	-0.969236	-1.192536	1	4.59645	1.043224	0.10738
7	-0.235678	-0.434695	-1.467655	6	2.726146	2.957632	0.423049
6	-0.760408	-1.711737	-1.54111	6	4.545853	-1.511994	-0.871775
7	-2.122749	-1.724069	-1.584154	9	1.613041	3.718237	0.400723
8	-0.078816	-2.739572	-1.534949	9	3.690507	3.647366	-0.236024
6	-2.864616	-2.95509	-1.423737	9	3.129214	2.8868	1.71688
6	-2.609896	-3.644958	-0.086683	9	4.864111	-1.760945	-2.168829
8	-2.932035	-2.785207	1.035414	9	4.246723	-2.712398	-0.319457
6	-2.093149	-1.785547	1.35506	9	5.672235	-1.072364	-0.272623
6	-0.496221	0.406375	2.150476	6	-2.649268	-0.506917	1.562951
1	-0.918042	0.332845	-1.445257	6	0.08052	-0.857031	1.978124
1	-2.61801	-0.836359	-1.535558	9	-2.407036	1.764611	2.183928
1	-3.926879	-2.709551	-1.52859	9	-0.159841	-3.146783	1.526492
1	-2.603439	-3.670801	-2.216894	6	-4.050465	-0.324546	1.373757
1	-1.57531	-3.988998	-0.015278	6	1.471565	-1.040612	2.228048
1	-3.2842	-4.499454	0.027919	7	-5.197179	-0.195178	1.243238
53	-2.827261	1.944638	-1.5086	7	2.602641	-1.182972	2.446891

2.2 Coordinates and thermodynamic data of **3**



3 (in vacuum)
 APFD/aug-cc-pVDZ
 Charge: 0
 Spin Multiplicity: Singlet
 Imaginary frequencies: 0
 Electronic Energy: -1818.382583 Hartree
 Zero-point correction= 0.219208 (Hartree/Particle)
 Thermal correction to Energy= 0.247184
 Thermal correction to Enthalpy= 0.248129
 Thermal correction to Gibbs Free Energy= 0.156429
 Sum of electronic and zero-point Energies= -1818.163375
 Sum of electronic and thermal Energies= -1818.135399
 Sum of electronic and thermal Enthalpies= -1818.134455
 Sum of electronic and thermal Free Energies= -1818.226154

Atomic Number	Coordinates (Angstrom)			Atomic Number	Coordinates (Angstrom)		
	X	Y	Z		X	Y	Z
6	-6.539032	0.148987	-0.299892	6	3.727037	2.651697	0.434494
6	-6.213196	-0.969055	0.464257	9	3.588355	-1.653236	-1.700499
6	-4.902432	-1.139499	0.894682	6	6.04968	-2.389418	-0.65313
6	-3.901902	-0.212096	0.602543	9	7.295625	-0.499178	0.978725
6	-4.256748	0.915905	-0.141772	9	6.173478	1.898593	1.503047
6	-5.557629	1.090247	-0.604841	7	3.24897	3.685611	0.661239
7	-2.597797	-0.396457	1.07266	7	6.524681	-3.426438	-0.869942
6	-1.53627	-0.44677	0.157039	1	-2.516577	-0.998116	1.882428
8	-1.683693	-0.324274	-1.044928	1	-0.234801	-0.413574	1.740531
7	-0.321088	-0.656135	0.763573	1	1.679869	-1.137894	0.523705
6	0.876645	-0.655271	-0.048859	1	0.68945	-1.255173	-0.946287
6	1.272179	0.762813	-0.456203	1	0.492556	1.20892	-1.080468
8	2.452941	0.761996	-1.284492	1	1.430801	1.401438	0.425909
6	3.61518	0.458461	-0.672208	9	-3.352912	1.863182	-0.393351
6	4.218707	-0.773752	-0.925166	9	-5.87581	2.171569	-1.317779
6	5.462742	-1.118469	-0.382021	9	-7.789576	0.324005	-0.728447
6	6.115817	-0.196847	0.44586	9	-7.147876	-1.872714	0.765328
6	5.535615	1.03502	0.716873	9	-4.585832	-2.227386	1.619194
6	4.295658	1.371889	0.16182				

3 (in acetonitrile)

APFD/aug-cc-pVDZ, scrf=(iefpcm, solvent=acetonitrile)

Charge: 0

Spin Multiplicity: Singlet

Imaginary frequencies: 0

Electronic Energy: -1818.406212 Hartree

Zero-point correction= 0.218640 (Hartree/Particle)

Thermal correction to Energy= 0.246743

Thermal correction to Enthalpy= 0.247687

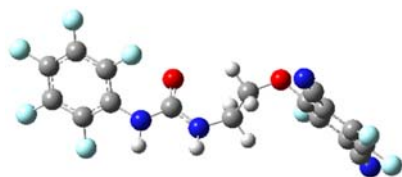
Thermal correction to Gibbs Free Energy= 0.155665

Sum of electronic and zero-point Energies= -1818.187571

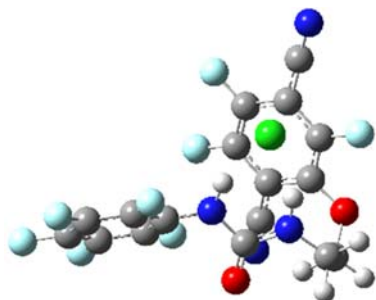
Sum of electronic and thermal Energies= -1818.159469

Sum of electronic and thermal Enthalpies= -1818.158524

Sum of electronic and thermal Free Energies= -1818.250547

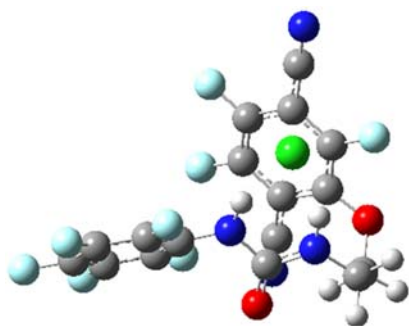


Atomic Number	Coordinates (Angstrom)			Atomic Number	Coordinates (Angstrom)		
	X	Y	Z		X	Y	Z
6	-6.576729	0.133114	-0.288019	6	4.379285	1.36981	0.160881
6	-6.225254	-0.992116	0.451242	6	3.870512	2.676955	0.419462
6	-4.909851	-1.151252	0.871195	9	3.521645	-1.63666	-1.665374
6	-3.924821	-0.200737	0.594654	6	5.975374	-2.448701	-0.666553
6	-4.308856	0.933227	-0.126716	9	7.324788	-0.602526	0.926887
6	-5.613755	1.094813	-0.58005	9	6.305918	1.844263	1.451866
7	-2.618968	-0.368361	1.055425	7	3.454088	3.741407	0.624135
6	-1.551549	-0.392864	0.156812	7	6.412049	-3.49987	-0.895079
8	-1.703519	-0.238698	-1.05169	1	-2.514408	-0.879039	1.923097
7	-0.343502	-0.605062	0.747732	1	-0.263287	-0.537387	1.752588
6	0.864641	-0.611043	-0.045296	1	1.637467	-1.150746	0.515088
6	1.313324	0.814473	-0.357916	1	0.675071	-1.150957	-0.979716
8	2.474326	0.825544	-1.221844	1	0.541735	1.34376	-0.924507
6	3.643034	0.476811	-0.645479	1	1.526388	1.372363	0.565012
6	4.195677	-0.776051	-0.904358	9	-3.426545	1.908077	-0.366225
6	5.437966	-1.158817	-0.385662	9	-5.954306	2.187681	-1.271412
6	6.144013	-0.258916	0.420338	9	-7.834862	0.294507	-0.707727
6	5.617504	0.995375	0.691907	9	-7.144221	-1.920401	0.736165
				9	-4.578882	-2.252057	1.563881



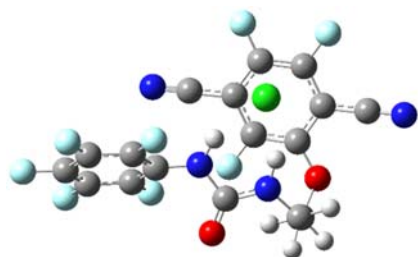
3-Cl-B (in vacuum)
 APFD/aug-cc-pVDZ
 Charge: -1
 Spin Multiplicity: Singlet
 Imaginary frequencies: 0
 Electronic Energy : -2278.644059 Hartree
 Zero-point correction= 0.219713 (Hartree/Particle)
 Thermal correction to Energy= 0.248998
 Thermal correction to Enthalpy= 0.249942
 Thermal correction to Gibbs Free Energy= 0.157648
 Sum of electronic and zero-point Energies= -2278.424347
 Sum of electronic and thermal Energies= -2278.395062
 Sum of electronic and thermal Enthalpies= -2278.394118
 Sum of electronic and thermal Free Energies= -2278.486411

Atomic Number	Coordinates (Angstrom)			Atomic Number	Coordinates (Angstrom)		
	X	Y	Z		X	Y	Z
6	4.520648	0.002255	0.348868	9	3.937429	-2.109064	1.229025
6	4.141574	1.160807	-0.321717	1	0.144164	1.416717	-1.032926
6	2.841603	1.288163	-0.798461	1	-1.591817	0.885299	-1.978822
6	1.876185	0.289258	-0.610929	1	-1.688197	-1.425883	-3.784843
6	2.278649	-0.853308	0.096349	1	-3.057798	-0.415500	-3.247463
6	3.584437	-1.006059	0.553659	1	-3.303432	-2.816822	-2.556096
7	0.586709	0.471643	-1.071470	1	-1.757224	-2.707738	-1.670223
6	-0.063543	-0.483021	-1.841305	17	-1.378229	2.811557	-1.124358
8	0.423483	-1.576150	-2.129437	6	-1.769443	-1.523544	0.893101
7	-1.305729	-0.077720	-2.223907	6	-2.673793	1.095734	1.348209
6	-2.185994	-0.986631	-2.904730	9	-1.066221	1.292469	3.079087
6	-2.630893	-2.141210	-2.014331	6	-3.199962	2.386648	1.653863
8	-3.419195	-1.689697	-0.889307	6	-1.395769	-2.894598	0.785419
6	-2.783516	-0.985648	0.071468	6	-1.185520	-0.729050	1.887585
6	-1.626767	0.564217	2.109467	6	-3.229315	0.310350	0.337091
9	1.399610	-1.808068	0.402994	9	-0.228122	-1.232520	2.671115
9	2.516169	2.397420	-1.473018	9	-4.211066	0.811255	-0.409478
9	5.040194	2.135245	-0.529711	7	-3.681680	3.387066	1.993339
9	5.775857	-0.136035	0.804169	7	-1.144478	-4.027883	0.731342



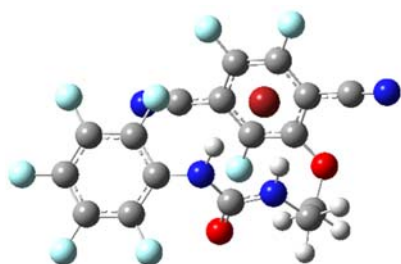
3-Cl-B (in acetonitrile)
 APFD/aug-cc-pVDZ, scrf=(irfpcm, solvent=acetonitrile)
 Charge: -1
 Spin Multiplicity: Singlet
 Imaginary frequencies: 0
 Electronic Energy : -2278.717471 Hartree
 Zero-point correction= 0.219875 (Hartree/Particle)
 Thermal correction to Energy= 0.249316
 Thermal correction to Enthalpy= 0.250260
 Thermal correction to Gibbs Free Energy= 0.157587
 Sum of electronic and zero-point Energies= -2278.497596
 Sum of electronic and thermal Energies= -2278.468155
 Sum of electronic and thermal Enthalpies= -2278.467211
 Sum of electronic and thermal Free Energies= -2278.559884

Atomic Number	Coordinates (Angstrom)			Atomic Number	Coordinates (Angstrom)		
	X	Y	Z		X	Y	Z
6	4.425809	-0.141440	0.226475	9	3.816232	-2.343905	0.819699
6	4.054498	1.104579	-0.268646	1	0.101726	1.555732	-0.865238
6	2.745546	1.316425	-0.683218	1	-1.685223	1.236642	-1.869057
6	1.764561	0.321260	-0.603234	1	-1.963954	-0.827885	-3.910734
6	2.160434	-0.913484	-0.075369	1	-3.246287	0.184504	-3.211469
6	3.473748	-1.150806	0.318409	1	-3.665106	-2.225538	-2.767906
7	0.460354	0.596165	-0.989491	1	-2.064004	-2.379825	-1.998718
6	-0.233151	-0.207747	-1.884005	17	-1.280190	3.219025	-0.934990
8	0.201827	-1.279831	-2.308630	6	-1.815149	-1.673862	0.716206
7	-1.450003	0.300631	-2.211102	6	-2.344371	0.907166	1.657714
6	-2.404841	-0.473258	-2.966989	9	-0.682275	0.597180	3.316940
6	-2.894425	-1.694401	-2.200380	6	-2.647062	2.201473	2.172179
8	-3.548948	-1.324390	-0.961499	6	-1.575116	-3.024967	0.333020
6	-2.783804	-0.888309	0.056225	6	-1.109366	-1.157088	1.811597
6	-1.360574	0.122178	2.271763	6	-3.037887	0.389063	0.563941
9	1.271071	-1.893817	0.112288	9	-0.212465	-1.912399	2.444209
9	2.418992	2.517907	-1.183966	9	-3.969536	1.135215	-0.025999
9	4.961762	2.083537	-0.365718	7	-2.909808	3.233727	2.633950
9	5.684904	-0.363067	0.619929	7	-1.393145	-4.136213	0.047847



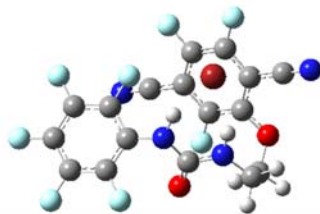
3-Cl-A (in vacuum)
 APFD/aug-cc-pVDZ
 Charge: -1
 Spin Multiplicity: Singlet
 Imaginary frequencies: 0
 Electronic Energy : -2278.647438 Hartree
 Zero-point correction= 0.220060 (Hartree/Particle)
 Thermal correction to Energy= 0.249310
 Thermal correction to Enthalpy= 0.250254
 Thermal correction to Gibbs Free Energy= 0.158199
 Sum of electronic and zero-point Energies= -2278.427379
 Sum of electronic and thermal Energies= -2278.398128
 Sum of electronic and thermal Enthalpies= -2278.397184
 Sum of electronic and thermal Free Energies= -2278.489240

Atomic Number	Coordinates (Angstrom)			Atomic Number	Coordinates (Angstrom)		
	X	Y	Z		X	Y	Z
6	-4.806449	-0.183543	-0.200941	9	-4.465077	1.290115	-2.012770
6	-4.290657	-0.858867	0.900125	1	-0.284890	-0.519141	1.326549
6	-2.964609	-0.663150	1.268604	1	1.452104	0.443732	1.763144
6	-2.107514	0.183505	0.553497	1	1.482415	3.383756	2.084198
6	-2.645955	0.828242	-0.569247	1	2.868952	2.268385	2.206754
6	-3.979470	0.662745	-0.931282	1	3.044441	3.915105	0.298480
7	-0.782005	0.305148	0.930935	1	1.559276	3.211396	-0.405248
6	-0.165779	1.538008	1.113547	17	1.373547	-1.647683	1.989287
8	-0.709419	2.619045	0.894806	6	1.714987	0.469660	-1.298240
7	1.119374	1.399140	1.545454	6	1.343368	-0.858918	-1.512860
6	1.993618	2.536536	1.601138	6	3.454674	-1.569119	-0.598701
6	2.435851	3.006308	0.219537	6	3.796490	-0.237625	-0.341978
8	3.326841	2.073385	-0.438327	9	0.879001	1.436923	-1.684486
6	2.916128	0.810866	-0.673450	9	1.899731	-3.154638	-1.372016
6	2.230613	-1.882146	-1.162822	9	4.298843	-2.547899	-0.275323
9	-1.879287	1.576314	-1.360211	6	5.038879	0.063877	0.289295
9	-2.503489	-1.300503	2.352468	6	0.063388	-1.165333	-2.059887
9	-5.082717	-1.671753	1.616642	7	-0.980692	-1.413348	-2.504311
9	-6.088646	-0.355038	-0.560441	7	6.057237	0.311912	0.791299



3-Br-A (in vacuum)
 APFD/aug-cc-pVDZ
 Charge: -1
 Spin Multiplicity: Singlet
 Imaginary frequencies: 0
 Electronic Energy : -2235.422306 Hartree
 Zero-point correction= 0.219732 (Hartree/Particle)
 Thermal correction to Energy= 0.249165
 Thermal correction to Enthalpy= 0.250109
 Thermal correction to Gibbs Free Energy= 0.157392
 Sum of electronic and zero-point Energies= -2235.202574
 Sum of electronic and thermal Energies= -2235.173141
 Sum of electronic and thermal Enthalpies= -2235.172197
 Sum of electronic and thermal Free Energies= -2235.264914

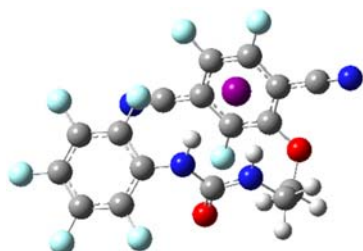
Atomic Number	Coordinates (Angstrom)			Atomic Number	Coordinates (Angstrom)		
	X	Y	Z		X	Y	Z
6	4.292187	0.962352	0.306843	1	-2.942569	3.607948	-1.947999
6	4.536623	-0.393997	0.117832	9	1.218043	-1.727914	0.634062
6	3.490281	-1.301005	0.248690	9	3.714009	-2.609145	0.080003
6	2.212760	-0.835677	0.535071	9	5.775333	-0.824075	-0.166923
6	1.929060	0.525547	0.708128	9	5.309713	1.834493	0.229655
6	3.012870	1.411528	0.621308	9	2.863076	2.707277	0.907281
7	0.638965	0.934522	0.992328	35	-1.826322	-0.446808	2.566952
6	0.023777	1.964598	0.291451	6	-0.658617	-1.215355	-1.729569
7	-1.280961	2.127551	0.645554	6	-3.144040	-0.494727	-0.689610
8	0.590964	2.634477	-0.570678	9	-0.865769	-3.317647	-0.662807
6	-2.107801	3.097648	-0.021019	6	-4.419762	-0.132625	-0.163885
6	-2.307220	2.829412	-1.508818	6	0.601886	-1.581813	-2.285396
8	-3.040453	1.609682	-1.759370	6	-2.613294	-1.761089	-0.423973
6	-2.440911	0.434350	-1.479904	6	-1.214211	0.034246	-2.017475
6	-1.371777	-2.113397	-0.926146	9	-3.304487	-2.641564	0.289945
1	0.016015	0.306329	1.538799	9	-0.559034	0.845382	-2.855820
1	-1.685339	1.458573	1.318544	7	-5.476866	0.165344	0.214243
1	-3.078617	3.108469	0.490274	7	1.628074	-1.875238	-2.743831
1	-1.662861	4.102945	0.063675				
1	-1.341019	2.814107	-2.022404				



3-Br-A (in acetonitrile)
 APFD/aug-cc-pvDZ
 scrf=(iefpcm, solvent=acetonitrile)
 Charge: -1

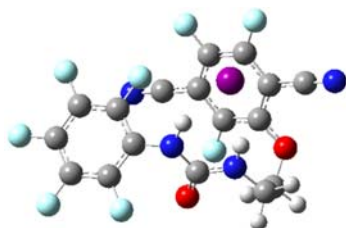
Spin Multiplicity: Singlet
 Imaginary frequencies: 0
 Electronic Energy : -2235.493536 Hartree
 Zero-point correction= 0.219693 (Hartree/Particle)
 Thermal correction to Energy= 0.249338
 Thermal correction to Enthalpy= 0.250282
 Thermal correction to Gibbs Free Energy= 0.156907
 Sum of electronic and zero-point Energies= -2235.273844
 Sum of electronic and thermal Energies= -2235.244198
 Sum of electronic and thermal Enthalpies= -2235.243254
 Sum of electronic and thermal Free Energies= -2235.336629

Atomic Number	Coordinates (Angstrom)			Atomic Number	Coordinates (Angstrom)		
	X	Y	Z		X	Y	Z
6	4.260698	0.946748	0.277926	1	-1.413521	2.664981	-2.296296
6	4.484084	-0.421876	0.166397	1	-3.023765	3.431484	-2.233778
6	3.423096	-1.304101	0.340344	9	1.140926	-1.674727	0.739316
6	2.152651	-0.803957	0.593610	9	3.623074	-2.622642	0.240986
6	1.891144	0.566399	0.689417	9	5.712306	-0.885527	-0.088713
6	2.985897	1.429178	0.557626	9	5.286025	1.798266	0.152405
7	0.602100	1.018185	0.938920	9	2.844182	2.744179	0.753202
6	-0.006432	1.970657	0.130916	35	-1.894623	-0.195053	2.752694
7	-1.310611	2.182420	0.446453	6	-0.607137	-1.305460	-1.765475
8	0.581492	2.548230	-0.784692	6	-3.063931	-0.589802	-0.677279
6	-2.123785	3.116172	-0.297963	9	-0.723120	-3.358613	-0.591362
6	-2.357466	2.711879	-1.747384	6	-4.312821	-0.225899	-0.094988
8	-3.066845	1.452473	-1.850841	6	0.662532	-1.657319	-2.308192
6	-2.420836	0.315314	-1.544047	6	-2.497879	-1.830984	-0.371453
6	-1.269769	-2.183811	-0.900056	6	-1.201111	-0.086378	-2.101797
1	-0.013558	0.445182	1.532168	9	-3.134437	-2.677499	0.433905
1	-1.727332	1.609591	1.183774	9	-0.584496	0.692465	-2.994743
1	-3.081479	3.205957	0.227037	7	-5.337318	0.067972	0.366528
1	-1.651669	4.110025	-0.310180	7	1.707568	-1.935673	-2.730949



3-I-A (in vacuum)
 APFD/aug-cc-pVDZ
 Charge: -1
 Spin Multiplicity: Singlet
 Imaginary frequencies: 0
 Electronic Energy : -2114.320565 Hartree
 Zero-point correction= 0.219587 (Hartree/Particle)
 Thermal correction to Energy= 0.249188
 Thermal correction to Enthalpy= 0.250132
 Thermal correction to Gibbs Free Energy= 0.156255
 Sum of electronic and zero-point Energies= -2114.100979
 Sum of electronic and thermal Energies= -2114.071378
 Sum of electronic and thermal Enthalpies= -2114.070433
 Sum of electronic and thermal Free Energies= -2114.164311

Atomic Number	Coordinates (Angstrom)			Atomic Number	Coordinates (Angstrom)		
	X	Y	Z		X	Y	Z
6	-4.439945	0.722994	-0.613562	1	0.961653	3.430042	1.397060
6	-4.647775	-0.538237	-0.064276	1	2.543299	4.239723	1.191805
6	-3.565930	-1.394306	0.112736	9	-1.260653	-1.797203	-0.030374
6	-2.290582	-0.964927	-0.233563	9	-3.754480	-2.612355	0.631393
6	-2.045977	0.306035	-0.768466	9	-5.884986	-0.931807	0.272213
6	-3.160654	1.128774	-0.982235	9	-5.489004	1.531806	-0.828162
7	-0.754838	0.685474	-1.095648	9	-3.035631	2.301830	-1.607074
6	-0.212958	1.887902	-0.658565	6	0.406391	-0.546646	2.220827
7	1.108184	2.011804	-0.964142	6	2.952522	-0.039923	1.200384
8	-0.855272	2.733730	-0.038989	9	0.755951	-2.855947	1.840470
6	1.856038	3.170933	-0.554371	53	1.986456	-1.099174	-2.288124
6	1.959558	3.341569	0.957257	6	-0.887006	-0.796040	2.765766
8	2.705674	2.276659	1.586864	6	4.264355	0.214797	0.700548
6	2.160348	1.044312	1.625421	6	2.479343	-1.353783	1.285445
6	1.207127	-1.604375	1.772368	6	0.904461	0.758121	2.169099
1	-0.094528	-0.037390	-1.431164	9	3.253898	-2.370092	0.924701
1	1.577657	1.229853	-1.439285	9	0.162696	1.743478	2.686520
1	2.858906	3.083649	-0.990818	7	5.347147	0.441864	0.346789
1	1.388321	4.089073	-0.946923	7	-1.941454	-0.992348	3.211691



3-I-A (in acetonitrile)
 APFD/aug-cc-pVDZ
 scrf=(iefpcm, solvent=acetonitrile)

Charge: -1
 Spin Multiplicity: Singlet
 Imaginary frequencies: 0
 Electronic Energy : -2114.390646 Hartree
 Zero-point correction= 0.219679 (Hartree/Particle)
 Thermal correction to Energy= 0.249448
 Thermal correction to Enthalpy= 0.250392
 Thermal correction to Gibbs Free Energy= 0.155767
 Sum of electronic and zero-point Energies= -2114.170967
 Sum of electronic and thermal Energies= -2114.141199
 Sum of electronic and thermal Enthalpies= -2114.140254
 Sum of electronic and thermal Free Energies= -2114.234879

Atomic Number	Coordinates (Angstrom)			Atomic Number	Coordinates (Angstrom)		
	X	Y	Z		X	Y	Z
6	-4.359721	0.149530	-1.020153	1	0.973493	3.735448	-0.634060
6	-4.563876	-0.590740	0.140082	1	2.579974	4.280334	-1.187153
6	-3.474570	-1.167589	0.784039	9	-1.159166	-1.519839	0.925871
6	-2.197392	-0.970609	0.275743	9	-3.655325	-1.884343	1.898134
6	-1.957141	-0.212552	-0.873895	9	-5.799536	-0.760701	0.621773
6	-3.075475	0.315591	-1.529229	9	-5.408849	0.672475	-1.666218
7	-0.659798	-0.032221	-1.339459	9	-2.941988	0.952649	-2.696634
6	-0.147322	1.237876	-1.577106	6	0.222589	0.913457	2.214212
7	1.179771	1.238933	-1.868140	6	2.788802	0.669951	1.170861
8	-0.834181	2.257481	-1.513326	9	0.465898	-1.216683	3.219484
6	1.895595	2.466791	-2.132243	53	2.136320	-2.251903	-1.370579
6	1.970661	3.406292	-0.936049	6	-1.100778	1.033601	2.728781
8	2.665878	2.803537	0.183154	6	4.101996	0.529821	0.635057
6	2.053592	1.838560	0.888403	6	2.257515	-0.348875	1.967748
6	0.975912	-0.236976	2.475590	6	0.778790	1.947974	1.457269
1	0.011141	-0.796798	-1.203171	9	2.979891	-1.432296	2.241949
1	1.681121	0.352009	-1.865811	9	0.071017	3.070247	1.305467
1	2.904648	2.190627	-2.457973	7	5.177593	0.425845	0.209389
1	1.416639	3.022076	-2.952650	7	-2.187289	1.117845	3.129605

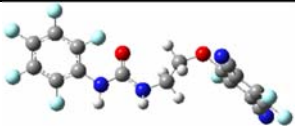
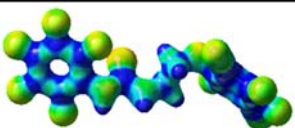
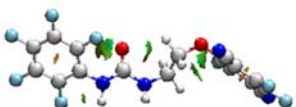
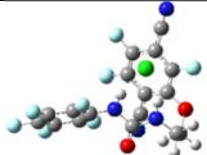
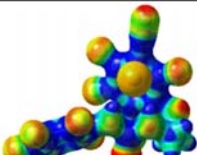
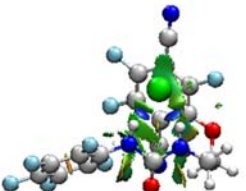
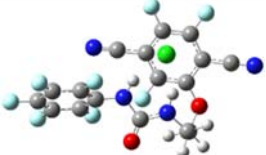
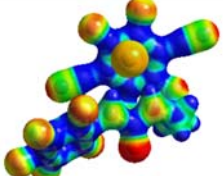
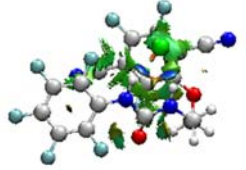
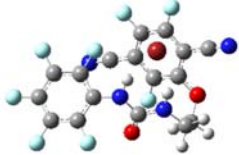
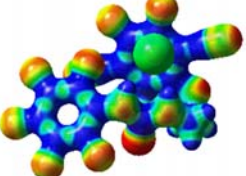


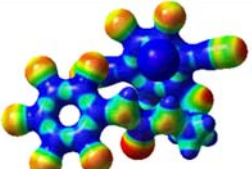
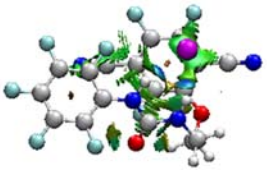
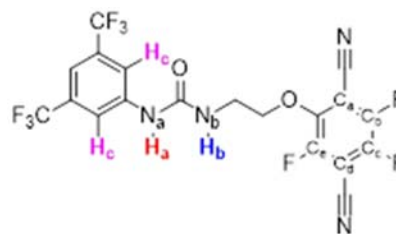
Entry	Optimized geometries	ESP	NCIplot	
1	3			
2	3 Cl-B			
3	3-Cl-A			
4	3-Br-A			
5	3-I-A			

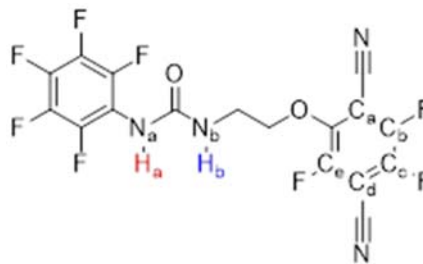
Table S1 Summary of computational data of 3 and 3-X at the APFD/aug-cc-pVDZ level.

2.3. Distances calculation



Distance (Å)	2	(2-Cl)A	(2-Cl)B	(2-Br)A	(2-I)A
N_a-H_a	1.009	1.044	1.044	1.0039	1.035
N_b-H_b	1.009	1.031	1.032	1.029	1.027
C-H_c	1.087	1.090	1.090	1.090	1.091
H_a-X	--	2.018	2.017	2.184	2.428
H_b-X	--	2.19	2.167	2.344	2.580
H_c-X	--	3.171	3.161	3.242	3.391
X-centroid	--	3.141	3.165	3.267	3.515
C_a-X	--	3.350	4.869	3.492	3.755
C_b-X	--	3.253	4.831	3.381	3.633
C_c-X	--	3.914	4.151	4.038	4.291
C_d-X	--	4.590	3.364	4.730	5.007
C_e-X	--	4.661	3.383	4.815	5.107

Table S2 Bond distances of **2** and **2-X** in Angstrom calculated at APFD/aug-cc-pVDZ level.

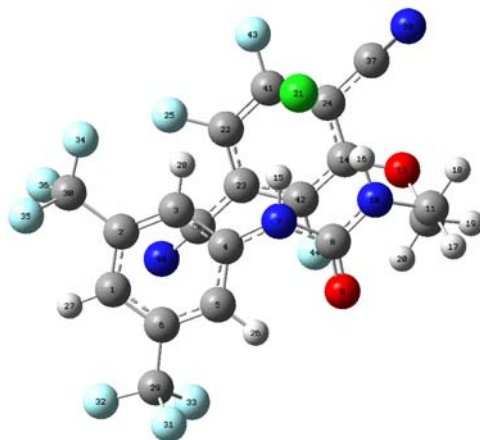


Distance (Å)	3	(3-Cl)-A	(3-Cl)B	(3-Br)A	(3-I)A
N_a-H_a	1.011	1.039	1.044	1.040	1.035
N_b-H_b	1.010	1.034	1.034	1.031	1.028
H_a-X	--	2.113	2.067	2.24	2.488
H_b-X	--	2.105	2.118	2.282	2.512
X-centroid	--	3.337	3.196	3.320	3.560
C_a-X	--	3.646	4.797	3.513	3.771
C_b-X	--	3.321	4.652	3.360	3.616
C_c-X	--	3.274	3.945	3.896	4.165
C_d-X	--	3.590	3.276	4.518	4.809
C_e-X	--	3.925	3.437	4.650	4.948

Table S3 Bond distances of **3** and **3-X** in Angstrom calculated at APFD/aug-cc-pVDZ level.

2.4. NBO analysis

NBO analysis 2-Cl-A, APFD/aug-cc-pVDZ level (*H-bond interaction/ anion- π interaction*)

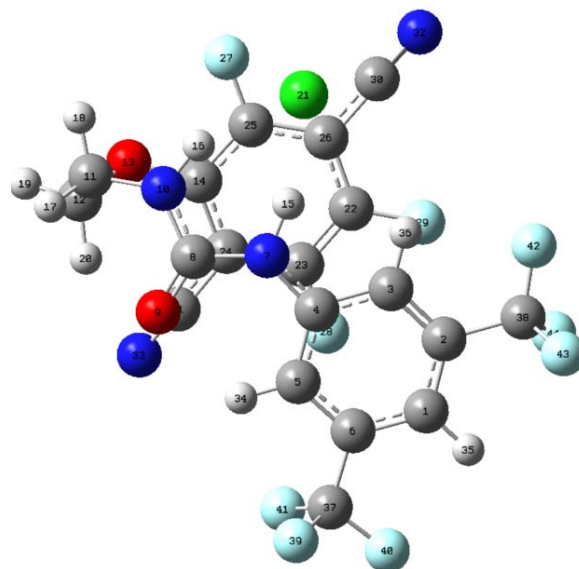


Second Order Perturbation Theory Analysis of Fock Matrix in NBO Basis

Threshold for printing: 0.50 kcal/mol
(Intermolecular threshold: 0.05 kcal/mol)

Donor NBO (i)	Acceptor NBO (j)	E(2) kcal/mol	E(j)-E(i) a.u.	F(i,j) a.u.
=====				
from unit 2 to unit 1				
101. LP (1)Cl 21	/852. BD*(1)N 7 - H 15	3.01	1.12	0.053
101. LP (1)Cl 21	/857. BD*(1)N 10 - H 16	1.30	1.14	0.035
101. LP (1)Cl 21	/883. BD*(1)C 37 - N 39	0.06	1.66	0.009
102. LP (2)Cl 21	/844. BD*(1)C 3 - H 28	0.06	0.67	0.006
102. LP (2)Cl 21	/852. BD*(1)N 7 - H 15	0.06	0.62	0.006
102. LP (2)Cl 21	/876. BD*(2)C 24 - C 41	0.18	0.23	0.006
102. LP (2)Cl 21	/883. BD*(1)C 37 - N 39	0.05	1.16	0.007
102. LP (2)Cl 21	/885. BD*(3)C 37 - N 39	0.14	0.33	0.006
102. LP (2)Cl 21	/889. BD*(1)C 41 - F 43	0.26	0.50	0.010
103. LP (3)Cl 21	/844. BD*(1)C 3 - H 28	0.52	0.66	0.017
103. LP (3)Cl 21	/852. BD*(1)N 7 - H 15	2.69	0.61	0.037
103. LP (3)Cl 21	/857. BD*(1)N 10 - H 16	8.61	0.64	0.066
103. LP (3)Cl 21	/876. BD*(2)C 24 - C 41	0.18	0.22	0.006
103. LP (3)Cl 21	/885. BD*(3)C 37 - N 39	0.20	0.33	0.007
104. LP (4)Cl 21	/852. BD*(1)N 7 - H 15	34.91	0.71	0.141
104. LP (4)Cl 21	/853. BD*(1)C 8 - O 9	0.11	0.91	0.009
104. LP (4)Cl 21	/857. BD*(1)N 10 - H 16	11.58	0.74	0.084

NBO analysis 2-Cl-B, APFD/aug-cc-pVDZ level (*H-bond interaction*/*anion- π interaction*)

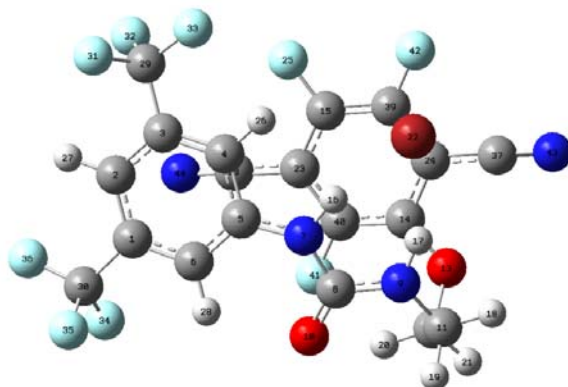


Second Order Perturbation Theory Analysis of Fock Matrix in NBO Basis

Threshold for printing: 0.50 kcal/mol
(Intermolecular threshold: 0.05 kcal/mol)

Donor NBO (i)	Acceptor NBO (j)	E(2) kcal/mol	E(j)-E(i) a.u.	F(i,j) a.u.
from unit 2 to unit 1				
101. LP (1)Cl 21	/852. BD*(1)N 7 - H 15	2.97	1.12	0.053
101. LP (1)Cl 21	/857. BD*(1)N 10 - H 16	1.55	1.14	0.038
101. LP (1)Cl 21	/879. BD*(1)C 30 - N 32	0.06	1.66	0.009
101. LP (1)Cl 21	/881. BD*(3)C 30 - N 32	0.05	0.83	0.006
102. LP (2)Cl 21	/857. BD*(1)N 10 - H 16	0.07	0.64	0.006
102. LP (2)Cl 21	/877. BD*(1)C 25 - F 27	0.10	0.50	0.006
102. LP (2)Cl 21	/880. BD*(2)C 30 - N 32	0.09	0.34	0.005
102. LP (2)Cl 21	/881. BD*(3)C 30 - N 32	0.52	0.34	0.012
103. LP (3)Cl 21	/844. BD*(1)C 3 - H 36	0.57	0.66	0.017
103. LP (3)Cl 21	/852. BD*(1)N 7 - H 15	3.47	0.61	0.042
103. LP (3)Cl 21	/857. BD*(1)N 10 - H 16	8.56	0.63	0.066
103. LP (3)Cl 21	/876. BD*(2)C 25 - C 26	0.17	0.22	0.006
103. LP (3)Cl 21	/881. BD*(3)C 30 - N 32	0.05	0.33	0.004
104. LP (4)Cl 21	/852. BD*(1)N 7 - H 15	34.23	0.71	0.140
104. LP (4)Cl 21	/853. BD*(1)C 8 - O 9	0.12	0.92	0.010
104. LP (4)Cl 21	/857. BD*(1)N 10 - H 16	13.01	0.73	0.089

NBO analysis 2-Br-A, APFD/aug-cc-pVDZ level (*H-bond interaction*/*anion- π interaction*)

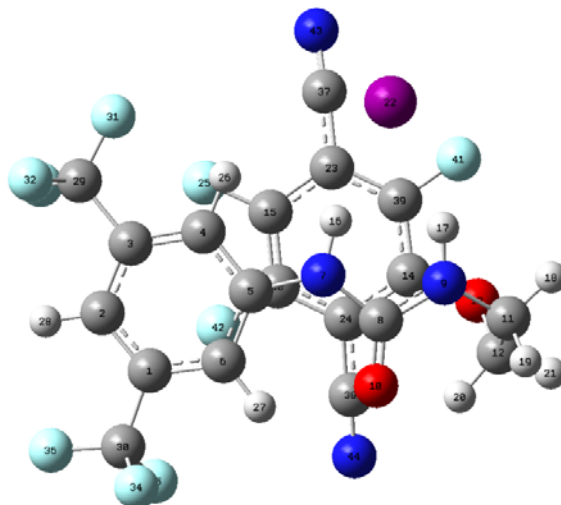


Second Order Perturbation Theory Analysis of Fock Matrix in NBO Basis

Threshold for printing: 0.50 kcal/mol
(Intermolecular threshold: 0.05 kcal/mol)

Donor NBO (i)	Acceptor NBO (j)	E(2) kcal/mol	E(j)-E(i) a.u.	F(i,j) a.u.
from unit 2 to unit 1				
105. LP (1)Br 22	/857. BD*(1)N 7 - H 16	2.38	1.11	0.047
105. LP (1)Br 22	/862. BD*(1)N 9 - H 17	1.05	1.14	0.031
105. LP (1)Br 22	/888. BD*(1)C 37 - N 43	0.06	1.67	0.009
106. LP (2)Br 22	/851. BD*(1)C 4 - H 26	0.10	0.65	0.007
106. LP (2)Br 22	/881. BD*(2)C 24 - C 39	0.21	0.21	0.007
106. LP (2)Br 22	/890. BD*(3)C 37 - N 43	0.14	0.32	0.006
106. LP (2)Br 22	/894. BD*(1)C 39 - F 42	0.28	0.48	0.010
107. LP (3)Br 22	/851. BD*(1)C 4 - H 26	0.67	0.65	0.019
107. LP (3)Br 22	/857. BD*(1)N 7 - H 16	2.74	0.59	0.036
107. LP (3)Br 22	/862. BD*(1)N 9 - H 17	6.84	0.61	0.058
107. LP (3)Br 22	/881. BD*(2)C 24 - C 39	0.15	0.20	0.006
107. LP (3)Br 22	/890. BD*(3)C 37 - N 43	0.22	0.31	0.007
108. LP (4)Br 22	/851. BD*(1)C 4 - H 26	0.08	0.72	0.007
108. LP (4)Br 22	/857. BD*(1)N 7 - H 16	29.95	0.66	0.126
108. LP (4)Br 22	/859. BD*(1)C 8 - O 10	0.10	0.87	0.009
108. LP (4)Br 22	/862. BD*(1)N 9 - H 17	11.33	0.69	0.080

NBO analysis 2-I-A, APFD/aug-cc-pVDZ level (*H-bond interaction*/*anion- π interaction*)

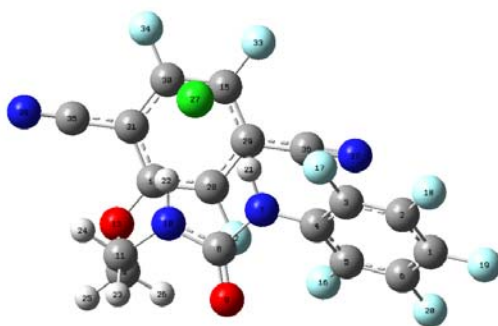


Second Order Perturbation Theory Analysis of Fock Matrix in NBO Basis

Threshold for printing: 0.50 kcal/mol
(Intermolecular threshold: 0.05 kcal/mol)

Donor NBO (i)	Acceptor NBO (j)	E(2) kcal/mol	E(j)-E(i) a.u.	F(i,j) a.u.
=====				
from unit 2 to unit 1				
105. LP (1) I 22	/854. BD*(1) N 7 - H 16	1.62	1.01	0.037
105. LP (1) I 22	/859. BD*(1) N 9 - H 17	0.91	1.03	0.028
105. LP (1) I 22	/885. BD*(1) C 37 - N 43	0.05	1.57	0.008
105. LP (1) I 22	/888. BD*(1) C 38 - N 44	0.09	4.85	0.019
105. LP (1) I 22	/890. BD*(3) C 38 - N 44	0.05	3.83	0.013
106. LP (2) I 22	/854. BD*(1) N 7 - H 16	0.15	0.57	0.008
106. LP (2) I 22	/859. BD*(1) N 9 - H 17	0.05	0.59	0.005
106. LP (2) I 22	/886. BD*(2) C 37 - N 43	0.12	0.38	0.006
106. LP (2) I 22	/887. BD*(3) C 37 - N 43	0.55	0.38	0.013
106. LP (2) I 22	/891. BD*(1) C 39 - F 41	0.07	0.47	0.005
107. LP (3) I 22	/848. BD*(1) C 4 - H 26	0.95	0.63	0.022
107. LP (3) I 22	/854. BD*(1) N 7 - H 16	2.51	0.56	0.034
107. LP (3) I 22	/859. BD*(1) N 9 - H 17	5.05	0.59	0.049
107. LP (3) I 22	/873. BD*(2) C 15 - C 40	0.13	0.24	0.005
107. LP (3) I 22	/876. BD*(2) C 23 - C 39	0.16	0.37	0.008
107. LP (3) I 22	/879. BD*(1) C 29 - F 31	0.07	0.49	0.005
107. LP (3) I 22	/882. BD*(1) C 30 - F 34	0.17	0.50	0.008
107. LP (3) I 22	/883. BD*(1) C 30 - F 35	0.11	0.47	0.006
107. LP (3) I 22	/884. BD*(1) C 30 - F 36	0.59	2.76	0.037
107. LP (3) I 22	/886. BD*(2) C 37 - N 43	0.21	0.38	0.008
107. LP (3) I 22	/888. BD*(1) C 38 - N 44	0.76	4.41	0.052
108. LP (4) I 22	/848. BD*(1) C 4 - H 26	0.15	0.68	0.009
108. LP (4) I 22	/854. BD*(1) N 7 - H 16	24.23	0.62	0.110
108. LP (4) I 22	/856. BD*(1) C 8 - O 10	0.11	0.84	0.009
108. LP (4) I 22	/859. BD*(1) N 9 - H 17	11.95	0.64	0.079

NBO analysis 3-Cl-A, APFD/aug-cc-pVDZ level (*H-bond interaction*/*anion- π interaction*)

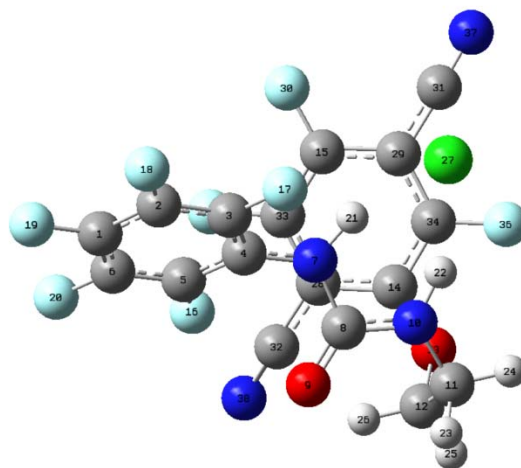


Second Order Perturbation Theory Analysis of Fock Matrix in NBO Basis

Threshold for printing: 0.50 kcal/mol
(Intermolecular threshold: 0.05 kcal/mol)

Donor NBO (i)	Acceptor NBO (j)	E(2) kcal/mol	E(j)-E(i) a.u.	F(i,j) a.u.
=====				
from unit 2 to unit 1				
107. LP (1)Cl 27	/762. BD*(1)N 7 - H 21	1.89	1.11	0.042
107. LP (1)Cl 27	/767. BD*(1)N 10 - H 22	2.01	1.13	0.043
108. LP (2)Cl 27	/762. BD*(1)N 7 - H 21	0.10	0.63	0.007
108. LP (2)Cl 27	/767. BD*(1)N 10 - H 22	0.12	0.65	0.008
108. LP (2)Cl 27	/780. BD*(2)C 15 - C 30	0.05	0.23	0.003
109. LP (3)Cl 27	/762. BD*(1)N 7 - H 21	6.05	0.61	0.055
109. LP (3)Cl 27	/767. BD*(1)N 10 - H 22	6.62	0.63	0.058
109. LP (3)Cl 27	/777. BD*(2)C 14 - C 31	0.05	0.22	0.003
109. LP (3)Cl 27	/780. BD*(2)C 15 - C 30	0.31	0.21	0.008
110. LP (4)Cl 27	/762. BD*(1)N 7 - H 21	20.25	0.71	0.108
110. LP (4)Cl 27	/763. BD*(1)C 8 - O 9	0.13	0.89	0.010
110. LP (4)Cl 27	/766. BD*(1)N 10 - C 11	0.05	0.71	0.006
110. LP (4)Cl 27	/767. BD*(1)N 10 - H 22	21.01	0.73	0.111

NBO analysis 3-Cl-B, APFD/aug-cc-pVDZ level (*H-bond interaction*/*anion- π interaction*)

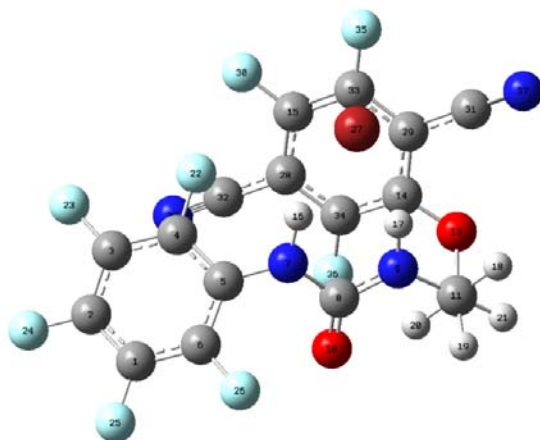


Second Order Perturbation Theory Analysis of Fock Matrix in NBO Basis

Threshold for printing: 0.50 kcal/mol
(Intermolecular threshold: 0.05 kcal/mol)

Donor NBO (i)	Acceptor NBO (j)	E(2) kcal/mol	E(j)-E(i) a.u.	F(i,j) a.u.
from unit 2 to unit 1				
107. LP (1)Cl 27	/762. BD*(1)N 7 - H 21	2.25	1.11	0.046
107. LP (1)Cl 27	/767. BD*(1)N 10 - H 22	1.95	1.13	0.043
107. LP (1)Cl 27	/787. BD*(1)C 31 - N 37	0.07	1.65	0.010
107. LP (1)Cl 27	/789. BD*(3)C 31 - N 37	0.08	0.82	0.007
108. LP (2)Cl 27	/762. BD*(1)N 7 - H 21	0.22	0.63	0.011
108. LP (2)Cl 27	/786. BD*(2)C 29 - C 34	0.26	0.23	0.008
108. LP (2)Cl 27	/787. BD*(1)C 31 - N 37	0.07	1.17	0.008
108. LP (2)Cl 27	/789. BD*(3)C 31 - N 37	0.72	0.34	0.014
109. LP (3)Cl 27	/762. BD*(1)N 7 - H 21	5.33	0.61	0.051
109. LP (3)Cl 27	/767. BD*(1)N 10 - H 22	8.06	0.63	0.064
109. LP (3)Cl 27	/786. BD*(2)C 29 - C 34	0.06	0.22	0.004
110. LP (4)Cl 27	/762. BD*(1)N 7 - H 21	25.28	0.71	0.120
110. LP (4)Cl 27	/763. BD*(1)C 8 - O 9	0.15	0.92	0.011
110. LP (4)Cl 27	/766. BD*(1)N 10 - C 11	0.06	0.71	0.006
110. LP (4)Cl 27	/767. BD*(1)N 10 - H 22	18.04	0.73	0.104

NBO analysis 3-Br-A, APFD/aug-cc-pVDZ level (*H-bond interaction*/*anion- π interaction*)

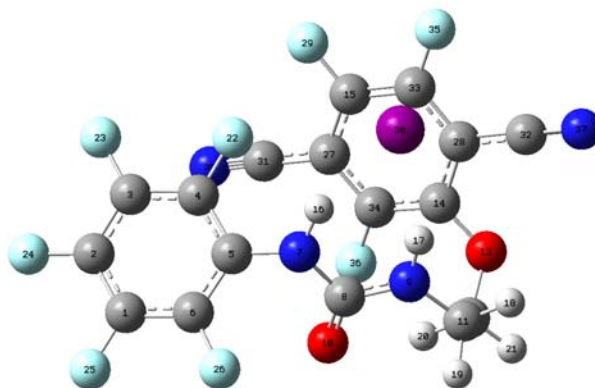


Second Order Perturbation Theory Analysis of Fock Matrix in NBO Basis

Threshold for printing: 0.50 kcal/mol
(Intermolecular threshold: 0.05 kcal/mol)

Donor NBO (i)	Acceptor NBO (j)	E(2) kcal/mol	E(j)-E(i) a.u.	F(i,j) a.u.
from unit 2 to unit 1				
111. LP (1)Br 27	/767. BD*(1)N 7 - H 16	1.71	1.11	0.040
111. LP (1)Br 27	/772. BD*(1)N 9 - H 17	1.41	1.13	0.036
111. LP (1)Br 27	/786. BD*(2)C 15 - C 33	0.05	0.72	0.006
112. LP (2)Br 27	/767. BD*(1)N 7 - H 16	0.09	0.60	0.007
112. LP (2)Br 27	/781. BD*(2)C 14 - C 29	0.19	0.21	0.006
112. LP (2)Br 27	/786. BD*(2)C 15 - C 33	0.86	0.21	0.013
112. LP (2)Br 27	/792. BD*(1)C 31 - N 37	0.06	1.15	0.007
112. LP (2)Br 27	/794. BD*(3)C 31 - N 37	0.06	0.32	0.004
112. LP (2)Br 27	/798. BD*(1)C 33 - F 35	0.24	0.48	0.010
113. LP (3)Br 27	/767. BD*(1)N 7 - H 16	4.60	0.59	0.047
113. LP (3)Br 27	/772. BD*(1)N 9 - H 17	6.30	0.61	0.056
113. LP (3)Br 27	/781. BD*(2)C 14 - C 29	0.18	0.20	0.006
113. LP (3)Br 27	/794. BD*(3)C 31 - N 37	0.15	0.30	0.006
114. LP (4)Br 27	/767. BD*(1)N 7 - H 16	21.87	0.66	0.108
114. LP (4)Br 27	/769. BD*(1)C 8 - O 10	0.13	0.86	0.010
114. LP (4)Br 27	/772. BD*(1)N 9 - H 17	16.31	0.68	0.095
114. LP (4)Br 27	/781. BD*(2)C 14 - C 29	0.08	0.27	0.005

NBO analysis 3-I-A, APFD/aug-cc-pVDZ level (*H-bond interaction/anion- π interaction*)



Second Order Perturbation Theory Analysis of Fock Matrix in NBO Basis

Threshold for printing: 0.50 kcal/mol
(Intermolecular threshold: 0.05 kcal/mol)

Donor NBO (i)	Acceptor NBO (j)	E(2) kcal/mol	E(j)-E(i) a.u.	F(i,j) a.u.
=====				
from unit 2 to unit 1				
114. LP (1) I 30	/767. BD*(1) N 7 - H 16	1.14	1.00	0.031
114. LP (1) I 30	/772. BD*(1) N 9 - H 17	1.05	1.02	0.030
115. LP (2) I 30	/781. BD*(2) C 14 - C 28	0.14	0.19	0.005
115. LP (2) I 30	/786. BD*(2) C 15 - C 33	0.63	0.19	0.011
115. LP (2) I 30	/795. BD*(1) C 32 - N 37	0.05	1.13	0.007
115. LP (2) I 30	/797. BD*(3) C 32 - N 37	0.07	0.30	0.004
115. LP (2) I 30	/798. BD*(1) C 33 - F 35	0.22	0.46	0.009
116. LP (3) I 30	/767. BD*(1) N 7 - H 16	3.81	0.57	0.042
116. LP (3) I 30	/772. BD*(1) N 9 - H 17	4.26	0.59	0.045
116. LP (3) I 30	/781. BD*(2) C 14 - C 28	0.13	0.19	0.005
116. LP (3) I 30	/797. BD*(3) C 32 - N 37	0.14	0.29	0.006
117. LP (4) I 30	/767. BD*(1) N 7 - H 16	17.74	0.62	0.094
117. LP (4) I 30	/769. BD*(1) C 8 - O 10	0.12	0.83	0.009
117. LP (4) I 30	/772. BD*(1) N 9 - H 17	15.50	0.64	0.090
117. LP (4) I 30	/781. BD*(2) C 14 - C 28	0.09	0.24	0.005
117. LP (4) I 30	/786. BD*(2) C 15 - C 33	0.06	0.23	0.004

2.5. BSSE and complexation energy calculation

pVDZ	E complex	E ligand	E ion	E complexation (Hartree)	E complexation (kcal/mol)
2-Cl-A	-2456.227992	-1995.953755	-460.173093	-0.101144	-63.5
2-Br-A	-2413.002877	-1995.953755	-416.954866	-0.094256	-59.1
2-I-A	-2291.900879	-1995.953755	-295.863027	-0.084097	-52.8
3-Cl-A	-2278.427379	-1818.163375	-460.173093	-0.090911	-57.0
3-Br-A	-2235.202574	-1818.163375	-416.954866	-0.084333	-52.9
3-I-A	-2114.100979	-1818.163375	-295.863027	-0.074577	-46.8

Table S4 Complexation Energy calculated at the APFD/aug-cc-pVDZ level of optimization.

pVTZ//pVDZ	E complex	E ligand	E ion	E complexation (Hartree)	E complexation (kcal/mol)
2-Cl-A	-2456.713717	-1996.429505	-460.184512	-0.0997	-62.6
2-Br-A	-2413.490819	-1996.429505	-416.970351	-0.090963	-57.0
2-I-A	-2292.376997	-1996.429505	-295.867872	-0.07962	-50.0
3-Cl-A	-2278.864551	-1818.594694	-460.184512	-0.085345	-53.5
3-Br-A	-2235.647392	-1818.594694	-416.970351	-0.082347	-51.7
3-I-A	-2114.535506	-1818.594694	-295.867872	-0.07294	-45.8

Table S5 Complexation Energy calculated at the APFD/aug-cc-pVTZ level from geometry optimisation at the APFD/aug-cc-pVDZ level.

pVTZ	E complex	E ligand	E ion	E complexation (Hartree)	E complexation (kcal/mol)
2-Cl-A		-1996.431164	-460.184512		
2-Br-A		-1996.431164	-416.970351		
2-I-A		-1996.431164	-295.867872		
3-Cl-A	-2278.868872	-1818.595459	-460.184512	-0.088901	-55.8
3-Br-A	-2235.648163	-1818.595459	-416.970351	-0.082353	-51.7
3-I-A	-2114.536276	-1818.595459	-295.867872	-0.072945	-45.8

Table S6 Complexation Energy calculated at the APFD/aug-cc-pVTZ level of optimization.

$$\Delta E_{int,vacuum} = \text{Energy of complexation vacuum} = E_{complex,vacuum} - E_{ligand,vacuum} - E_{ion,vacuum}$$

E = Electronic Energy + Zero-point correction

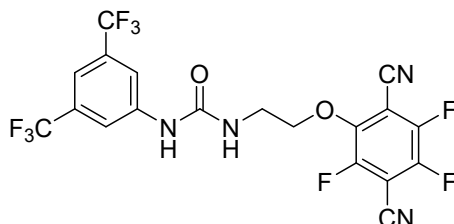
3 Synthetic procedures

a. Preparation of **4**, **5** and **6**

The synthesis procedures of **4**, **5** and **6** were reported in a previous publication.^[5,6]

b. Preparation of **2** and **3**

1-(3,5-bis(trifluoromethyl)phenyl)-3-(2-(2,5-dicyano-3,4,6-trifluorophenoxy)ethyl)urea



2,3,5,6-Tetrafluoroterephthalonitrile (100mg, 0.53mmol, 1eq), 1-(3,5-bis(trifluoromethyl)phenyl)-3-(2-hydroxyethyl)urea (158mg, 0.5mmol, 1eq) and dry K_2CO_3 (69mg, 0.5mmol, 1eq) were added to a dry flask with a magnetic stirrer. 2.5mL of dry acetonitrile were added under argon atmosphere. The mixture was stirred at room temperature. After no more evolution of the reaction followed by thin layer chromatography (15 hours), the mixture was diluted with methylene chloride and quenched with water at 0°C. Aqueous layers were extracted with DCM three times. Organic layers were collected, washed with brine and dried over $MgSO_4$. The crude product was purified by column chromatography on silica gel (Cyclohexane/EtOAc 70/30) affording 86 mg of the desired 1-(3,5-bis(trifluoromethyl)phenyl)-3-(2-(2,5-dicyano-3,4,6-trifluorophenoxy)ethyl)urea **37** as a white powder. Yield: 86mg, 35%.

1H NMR (200 MHz, Acetone d_6 , TMS): δ (ppm) 8.76 (s, 1H, -NH), 8.13 (s, 2H, H_{arom}), 7.54 (s, 1H, H_{arom}), 6.42 (s, 1H, -NH), 4.58 (td, 2H, $^3J_{H-H} = 6$ Hz, $^4J_{H-H} = 2$ Hz, -CH₂-) 3.71 (q, 2H, $^3J_{H-H} = 6$ Hz, -CH₂-).

^{19}F NMR (282 MHz, Acetone d_6 , $CFCl_3$): δ (ppm) -62.6 (s, 6F, -CF₃), -124.3 (dd, 1F, $^3J_{C-F} = 17$ Hz, $^3J_{C-F} = 8$ Hz, F_{arom}), -132.2 (dd, 1F, $^2J_{C-F} = 31$ Hz, $^3J_{C-F} = 20$ Hz, F_{arom}), -134.7 (dd, 1F, $^2J_{C-F} = 28$ Hz, $^3J_{C-F} = 6$ Hz, F_{arom}).

^{13}C NMR (75 MHz, Acetone d_6 , TMS): δ (ppm) 155.7 (s, 1C, C=O), 150.5 (d, m, 1C, $^1J_{C-F} = 257$ Hz, C_{arom-F}), 150.1 (m, 1C, C_{arom}), 147.7 (d, m, 1C, $^1J_{C-F} = 134$ Hz, C_{arom-F}), 145.9 (d, m, 1C, $^1J_{C-F} = 120$ Hz, C_{arom-F}), 143.4 (s, 1C, C_{arom}), 132.4 (q, 2C, $^2J_{C-F} = 33$ Hz, C-CF₃), 124.5 (q, 2C, $^1J_{C-F} = 270$ Hz, -CF₃), 119.1 (m, 1C, C_{arom}), 115.1 (m, 2C, C_{arom}), 109.6 (t, 1C, $^1J_{C-N} = 4$ Hz, C≡N), 108.1 (d, 1C, $^1J_{C-N} = 4$ Hz, C≡N), 104.1 (m, 1C, C_{arom}), 99.9 (m, 1C, C_{arom}), 76.2 (s, 1C, -CH₂-), 40.8 (s, 1C, -CH₂-).

UV-Visible (Acetonitrile) λ_{max} (ϵ)= 210 nm (19250), 240 nm (19250 L.mol⁻¹.cm⁻¹), 300 nm (3900 L.mol⁻¹.cm⁻¹), 320 nm (4500 L.mol⁻¹.cm⁻¹).

Fluorescence (Acetonitrile) λ_{exc} = 325 nm, $\lambda_{em,max}$ = 375 nm.

HRMS (ESI⁺ - TOF) m/z [M+H]⁺: calculated for C₁₉H₁₀F₉N₄O₂ 496.0660, found 496.0655.

Melting point: 154 – 156 °C.

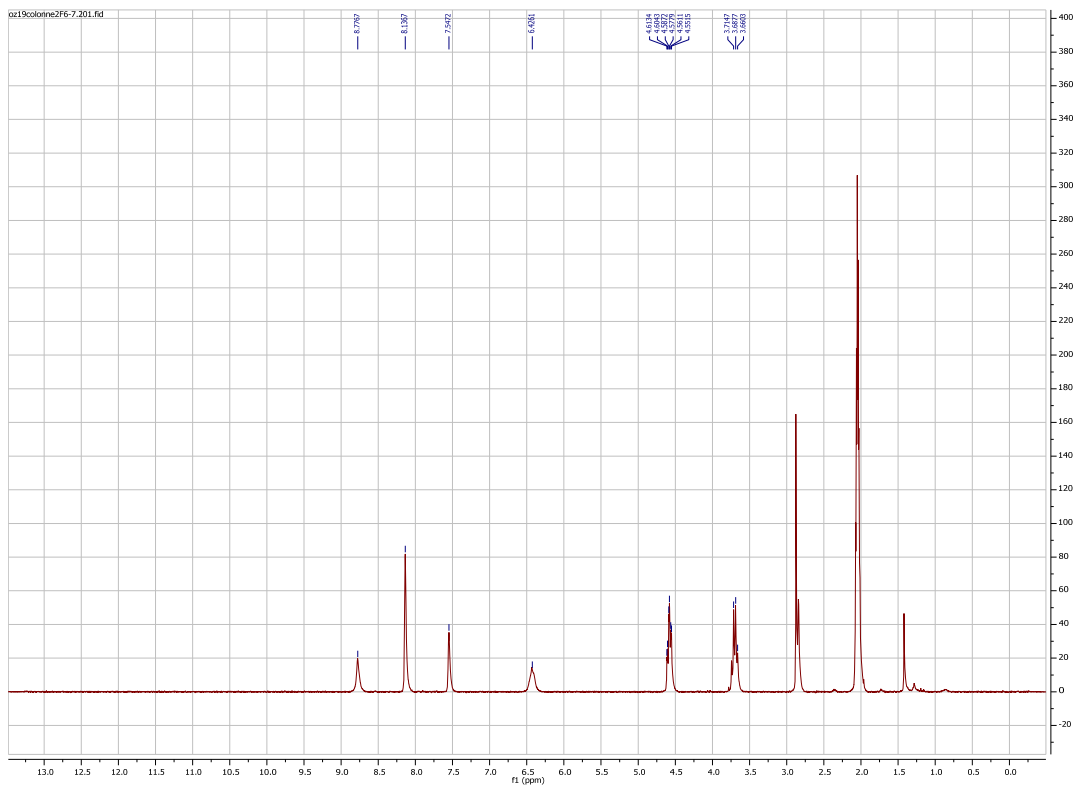


Figure S1 ¹H NMR spectrum of **2** (200MHz)

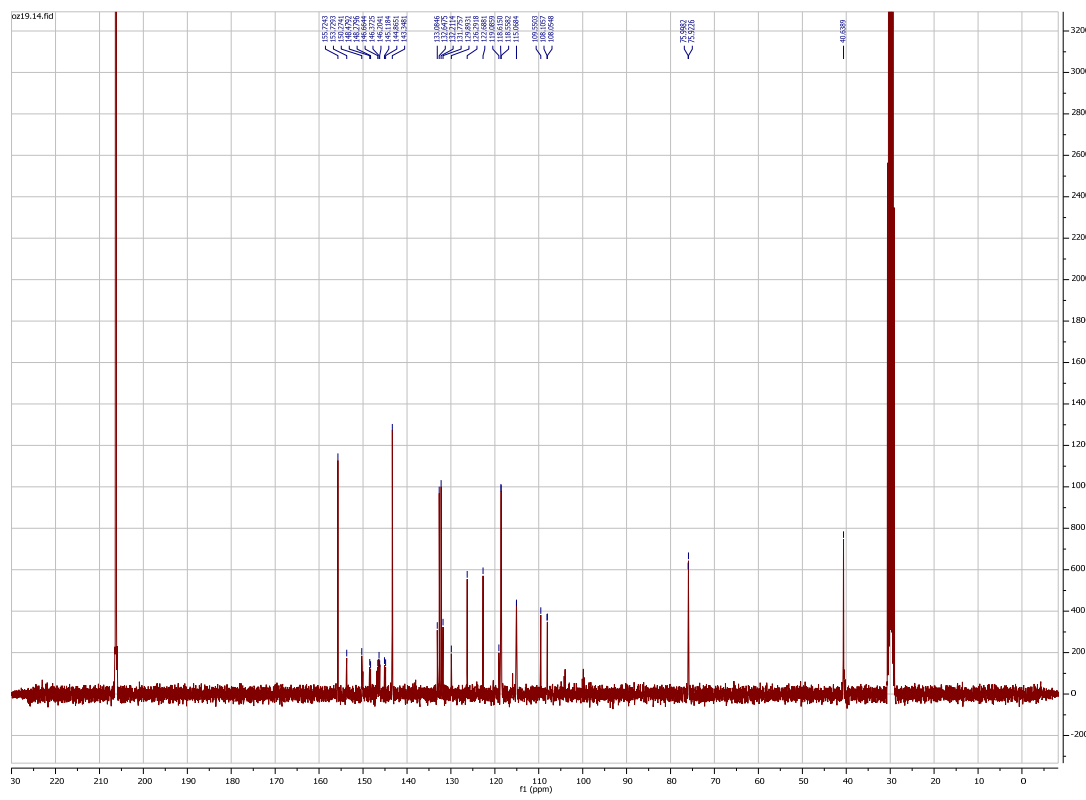


Figure S2 ¹³C NMR spectrum of **2** (75 MHz)

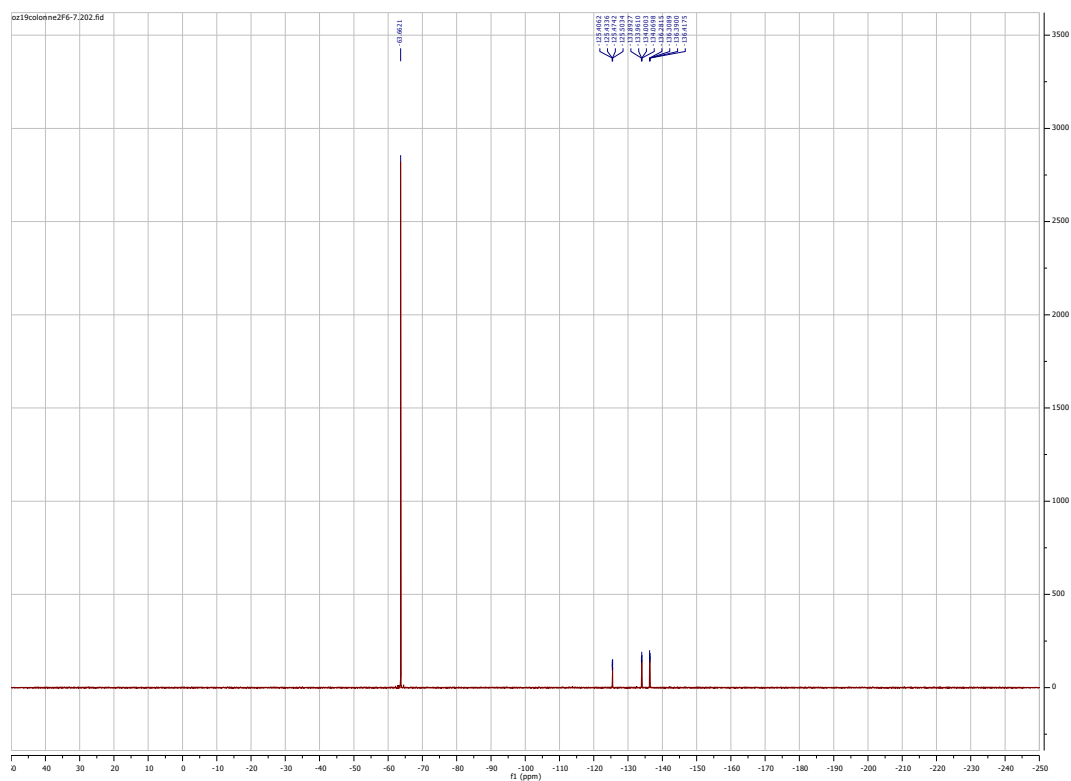


Figure S3 ^{19}F NMR spectrum of **2** (282 MHz)

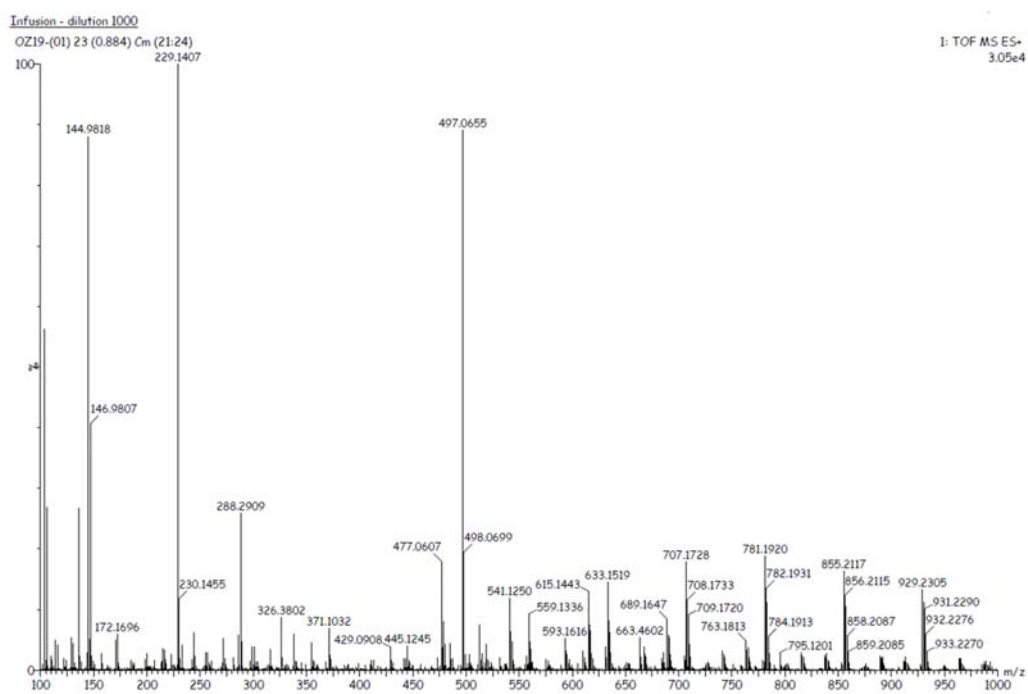
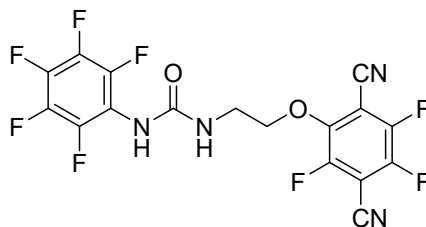


Figure S4 Mass spectrum of **2** (TOF MS ES+)

1-(2-(2,5-dicyano-3,4,6-trifluorophenoxy)ethyl)-3-(perfluorophenyl)urea



2,3,5,6-Tetrafluorophthalonitrile (100mg, 0.5mmol, 1eq), 1-(2-hydroxyethyl)-3-perfluorophenyl)urea (270mg, 0.5mmol, 1eq) and dry K_2CO_3 (69mg, 0.5mmol, 1eq) were added into a dry flask with a magnetic stirrer. 2.5mL of dry acetonitrile were added under argon atmosphere. The mixture was stirred at room temperature for 15 hours. After no more evolution of the reaction followed by thin layer chromatography, the mixture was diluted with ethyl acetate and quenched with water at 0°C. Aqueous layers were extracted with ethyl acetate. The organic layers were gathered, washed with brine and dried over $MgSO_4$. The crude product was purified by two subsequent column chromatographies on silica gel eluting with a gradient of solvents (eluent : Cyclohexane/ethyl acetate 70/30 then 60/40). Finally, the product was washed three times with pentane and diethylether, affording 25 mg of the desired 1-(2-(2,5-dicyano-3,4,6-trifluorophenoxy)ethyl)-3-(perfluorophenyl)urea **38** as a slightly pink powder. Yield : 25 mg, 12%.

1H NMR (300 MHz, Acetone d_6 , TMS): δ (ppm) 7.84 (s, 1H, -NH-), 6.55 (s, 1H, -NH-), 4.57 (td, 2H, $^3J_{H-H} = 9$ Hz, $^1J_{H-H} = 3$ Hz, -CH $_2$ -), 3.68 (q, 2H, $^3J_{H-H} = 9$ Hz, -CH $_2$ -).

^{19}F NMR (282 MHz, Acetone d_6 , $CFCl_3$): δ (ppm) -124.2 (dd, 1F, $^3J_{C-F} = 20$ Hz, $^3J_{C-F} = 6$ Hz, F_{arom}), -132.9 (dd, 1F, $^2J_{C-F} = 31$ Hz, $^3J_{C-F} = 20$ Hz, F_{arom}), -135.2 (dd, 1F, $^2J_{C-F} = 31$ Hz, $^3J_{C-F} = 8$ Hz, F_{arom}), -147.0 (dd, 2F, $^2J_{C-F} = 34$ Hz, $^3J_{C-F} = 8$ Hz, F_{arom}), -161.1 (t, 1F, $^2J_{C-F} = 31$ Hz, F_{arom}), -165.21 (t, m, 2F, $^2J_{C-F} = 34$ Hz, F_{arom}).

UV-Visible (Acetonitrile) λ_{max} (ϵ) = 210 nm (21000 L.mol $^{-1}$.cm $^{-1}$), 242 nm (15700 L.mol $^{-1}$.cm $^{-1}$), 250 nm (14750 L.mol $^{-1}$.cm $^{-1}$), 323 nm (3450 L.mol $^{-1}$.cm $^{-1}$).

Fluorescence (Acetonitrile) $\lambda_{exc} = 325$ nm, $\lambda_{em,max} = 375$ nm.

HRMS (ESI $^+$ - TOF) m/z [M+H] $^+$: calculated for $C_{17}H_7F_8N_4O_2$ 451.0441, found 451.0437.

Melting point: 132.2 – 132.8 °C.

4 NMR titrations

4.1 Practical analysis procedure

Prior to each analysis, anion salts were solubilized into acetone and precipitated by addition of diethylether to remove water. Salts were then dried to remove residual solvents and stored in the desiccator until use.

2mL of a solution containing the anion receptor was prepared (3.5mmol/L). 500 μ L were placed into a new NMR tube. 1mL of stock solution was taken and desired amount of anionic guest as the tetrabutylammonium (NBu₄⁺) salt was added.

NMR titrations were performed by adding aliquots of a solution containing the anionic guest (0.07M for NBu₄Cl, 0.28M for NBu₄Br, 0.81M for NBu₄I and 1.83M for NBu₄SCN) and the receptor (3.5mM) in MeCN-d₃ to the NMR tube. After each addition, a ¹H NMR spectrum was recorded.

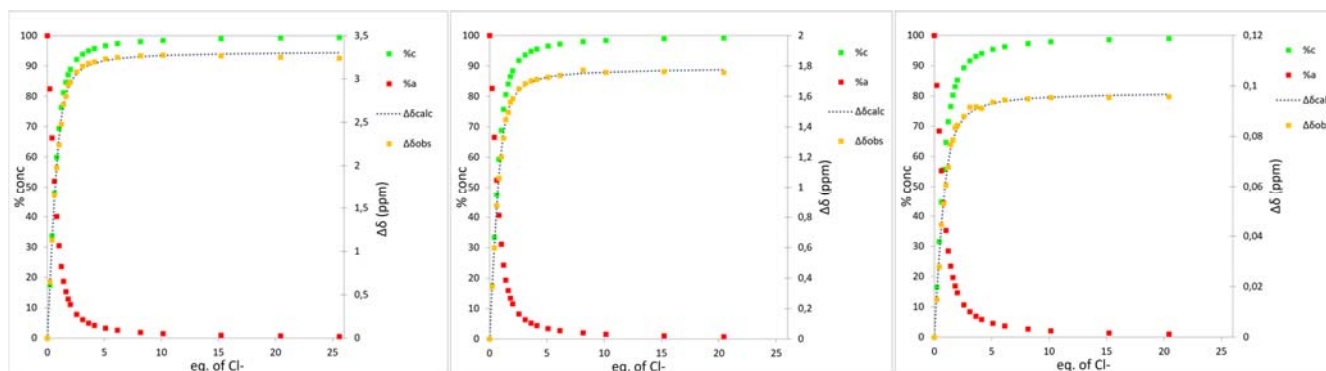
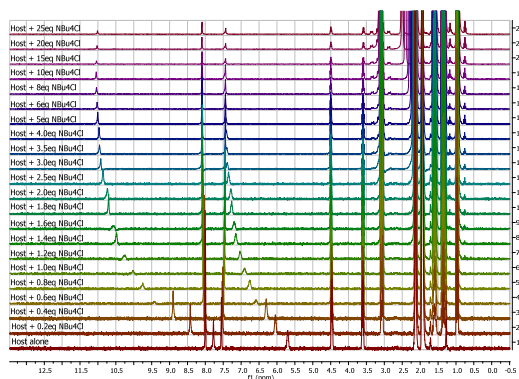
¹H NMR spectra were calibrated to the residual proton solvent peak in MeCN-d₃ (δ = 1.94ppm) at 300 K. Plot stackings were made using MestReNova Version 6.0. Non-linear least-square curve fitting of the titration data were double checked to be a 1:1 binding model using a reported procedure^[7] on Excel software and SPECFIT software.

determination of K_a

$$c = \frac{1}{2} a^{\circ} \left(1 + R + \frac{1}{a^{\circ} \times K} - \sqrt{\left(1 + R + \frac{1}{a^{\circ} \times K} \right)^2 - 4R} \right)$$

with c: concentration of complex, a^o : concentration of ligand during titration, R: number of equivalents of TBAX added

4.2 Titration of **2** with NBu₄Cl



H_a
 $K_a = 2060 \text{ L/mol}$
 $[\text{ligand}] = 0.0035 \text{ M}$
 $\delta_{c, \text{lim}} = 11.09 \text{ ppm}$

H_b
 $K_a = 1958 \text{ L/mol}$
 $[\text{ligand}] = 0.0035 \text{ M}$
 $\delta_{c, \text{lim}} = 7.48 \text{ ppm}$

H_c
 $K_a = 1439 \text{ L/mol}$
 $[\text{ligand}] = 0.0035 \text{ M}$
 $\delta_{c, \text{lim}} = 8.09 \text{ ppm}$

Figure S9 ¹H NMR titration of **2** with TBACl

[PROGRAM]
Name = SPECFIT
Version = 3.0

[FILE]
Name = OZ10+TBACL_RMN_FORMAT_SPECFIT.FAC
Path = C:\Users\Utilisateur\Desktop\
Date = 02-juin-21
Time = 18:07:37
Ncomp = 2
Nmeas = 22
Nwave = 6

[FACTOR ANALYSIS]
Tolerance = 1,000E-09
Max.Factors = 10
Num.Factors = 5
Significant = 3
Eigen Noise = 2,322E-03
Exp't Noise = 2,322E-03
Eigenvalue Square Sum Residual Prediction
1 1,126E+06 2,521E+01 4,387E-01 Data Vector
2 2,521E+01 4,141E-03 5,644E-03 Data Vector
3 3,446E-03 6,958E-04 2,322E-03 Data Vector
4 4,639E-04 2,319E-04 1,346E-03 Probably Noise
5 1,933E-04 3,856E-05 5,512E-04 Probably Noise

[MODEL]
Date = 02-juin-21
Time = 18:08:00
Model = 0
Index = 3
Function = 1
Species = 3
Params = 3

[SPECIES]	[COLORED]	[FIXED]	[SPECTRUM]
1 0 0	False	False	
0 1 0	True	False	
1 1 0	True	False	

[SPECIES]	[FIXED]	[PARAMETER]	[ERROR]
1 0 0	True	0,00000E+00 +/-	0,00000E+00
0 1 0	True	0,00000E+00 +/-	0,00000E+00
1 1 0	False	3,30094E+00 +/-	1,67661E-02

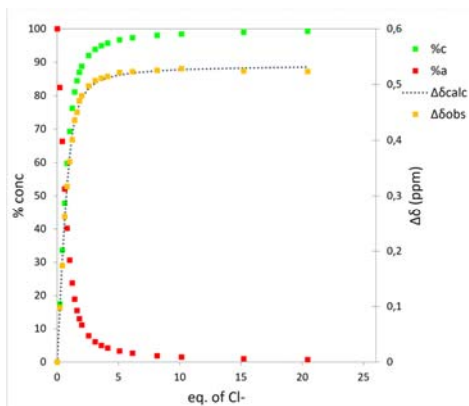
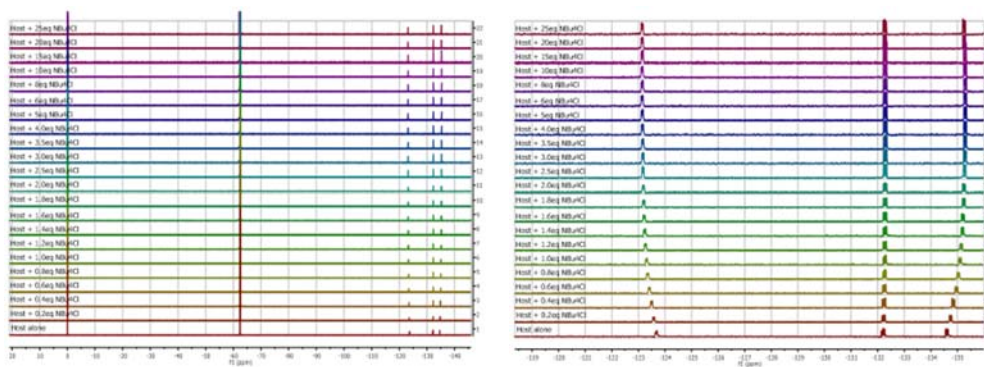
[CONVERGENCE]
Iterations = 11
Convergence Limit = 1,000E-03
Convergence Found = 4,443E-06
Marquardt Parameter = 0,0
Sum(Y-y)² Residuals = 4,01202E-02
Std. Deviation of Fit(Y) = 1,75003E-02

[STATISTICS]
Experimental Noise = 2,322E-03
Relative Error Of Fit = 0,0189%
Durbin-Watson Factor = 1,0260
Goodness Of Fit, Chi² = 5,678E+01
Durbin-Watson Factor (raw data) = None
Goodness Of Fit, Chi² (raw data) = None

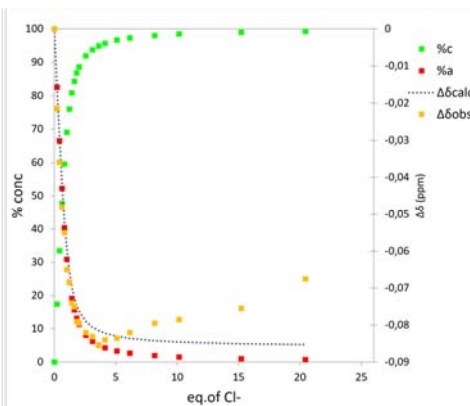
[COVARIANCE]
1,549E-03

[CORRELATION]
1,000E+00

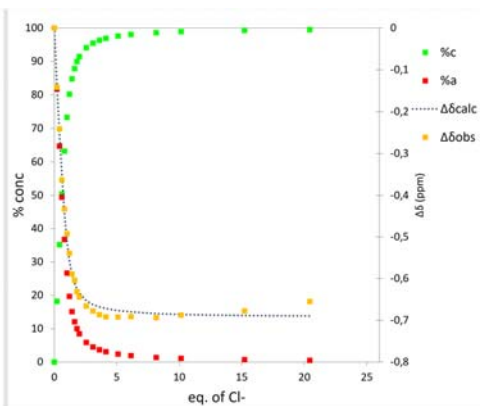
[END FILE]



F_a
 $K_a = 2035 \text{ L/mol}$
 $[\text{ligand}] = 0.0035 \text{ M}$
 $\delta_{c, \text{lim}} = -123.13 \text{ ppm}$



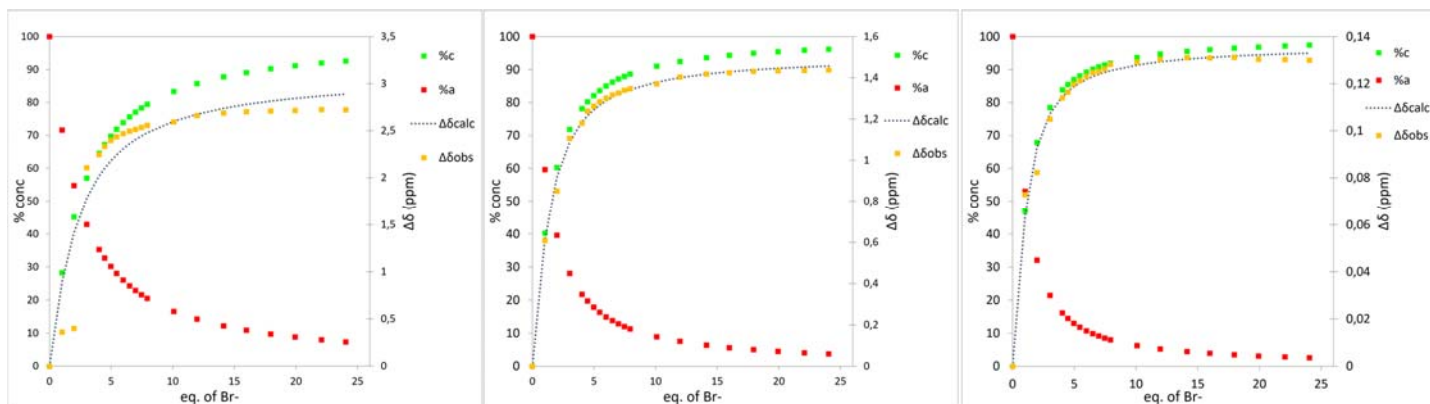
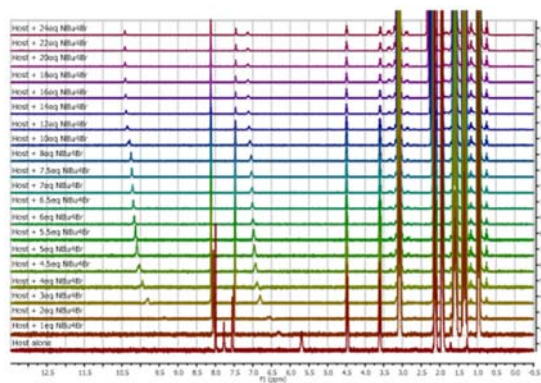
F_b
 $K_a = 2000 \text{ L/mol}$
 $[\text{ligand}] = 0.0035 \text{ M}$
 $\delta_{c, \text{lim}} = -132.28 \text{ ppm}$



F_c
 $K_a = 2831 \text{ L/mol}$
 $[\text{ligand}] = 0.0035 \text{ M}$
 $\delta_{c, \text{lim}} = -135.29 \text{ ppm}$

Figure S10 ^{19}F NMR titration of **2** with TBACl

4.3 Titration of **2** with NBu_4Br



H_a
 $K_a = 155 \text{ L/mol}$
 $[\text{ligand}] = 0.0035 \text{ M}$
 $\delta_{c, \text{lim}} = 10.81 \text{ ppm}$

H_b
 $K_a = 317 \text{ L/mol}$
 $[\text{ligand}] = 0.0035 \text{ M}$
 $\delta_{c, \text{lim}} = 7.21 \text{ ppm}$

H_c
 $K_a = 467 \text{ L/mol}$
 $[\text{ligand}] = 0.0035 \text{ M}$
 $\delta_{c, \text{lim}} = 8.13 \text{ ppm}$

Figure S11 ^1H NMR titration of **2** with TBABr

[PROGRAM]
Name = SPECFIT
Version = 3.0

[FILE]
Name = QZ19+TBABR_RMN_FORMAT_SPECFIT.FAC
Path = C:\Users\Utilisateur\Desktop\
Date = 02-juin-21
Time = 18:22:32
Ncomp = 2
Nmeas = 21
Nwave = 6

[FACTOR ANALYSIS]
Tolerance = 1,000E-09
Max.Factors = 10
Num.Factors = 6
Significant = 4
Eigen Noise = 1,379E-03
Exp't Noise = 1,379E-03
Eigenvalue Square Sum Residual Prediction
1 1,073E+06 1,699E+01 3,686E-01 Data Vector
2 1,670E+01 2,833E-01 4,780E-02 Data Vector
3 2,794E-01 3,887E-03 5,621E-03 Data Vector
4 3,656E-03 2,321E-04 1,379E-03 Data Vector
5 1,614E-04 7,070E-05 7,644E-04 Probably Noise
6 7,070E-05 6,802E-11 7,529E-07 Probably Noise

[MODEL]
Date = 02-juin-21
Time = 18:22:44
Model = 0
Index = 3
Function = 1
Species = 3
Params = 3

[SPECIES]	[COLORED]	[FIXED]	[SPECTRUM]
1 0 0	False	False	
0 1 0	True	False	
1 1 0	True	False	

[SPECIES]	[FIXED]	[PARAMETER]	[ERROR]
1 0 0	True	0,00000E+00 +/-	0,00000E+00
0 1 0	True	0,00000E+00 +/-	0,00000E+00
1 1 0	False	2,31201E+00 +/-	8,01622E-02

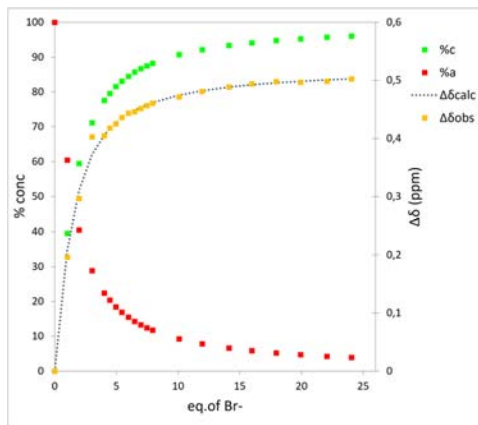
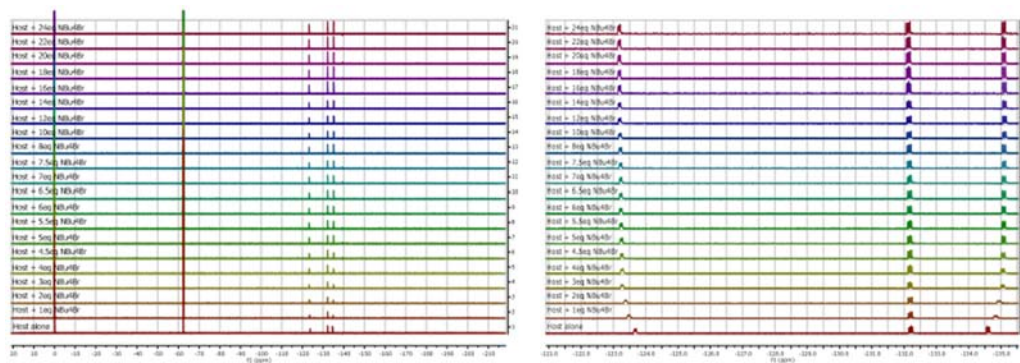
[CONVERGENCE]
Iterations = 8
Convergence Limit = 1,000E-03
Convergence Found = 6,661E-04
Marquardt Parameter = 0,0
Sum(Y-y)² Residuals = 1,68932E+00
Std. Deviation of Fit(Y) = 1,16252E-01

[STATISTICS]
Experimental Noise = 1,379E-03
Relative Error Of Fit = 0,1255%
Durbin-Watson Factor = 1,5819
Goodness Of Fit, Chi² = 7,103E+03
Durbin-Watson Factor (raw data) = None
Goodness Of Fit, Chi² (raw data) = None

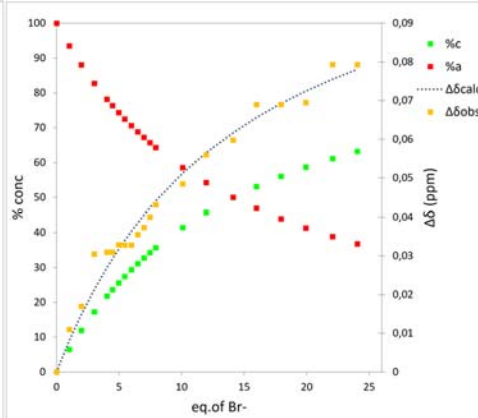
[COVARIANCE]
4,109E-02

[CORRELATION]
1,000E+00

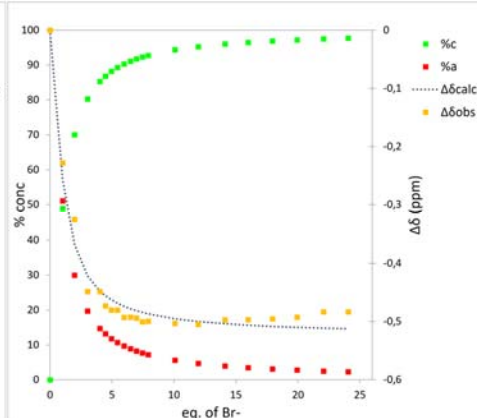
[END FILE]



F_a
 $K_a = 305 \text{ L/mol}$
 $[\text{ligand}] = 0.0035 \text{ M}$
 $\delta_{c, \text{lim}} = -123.15 \text{ ppm}$



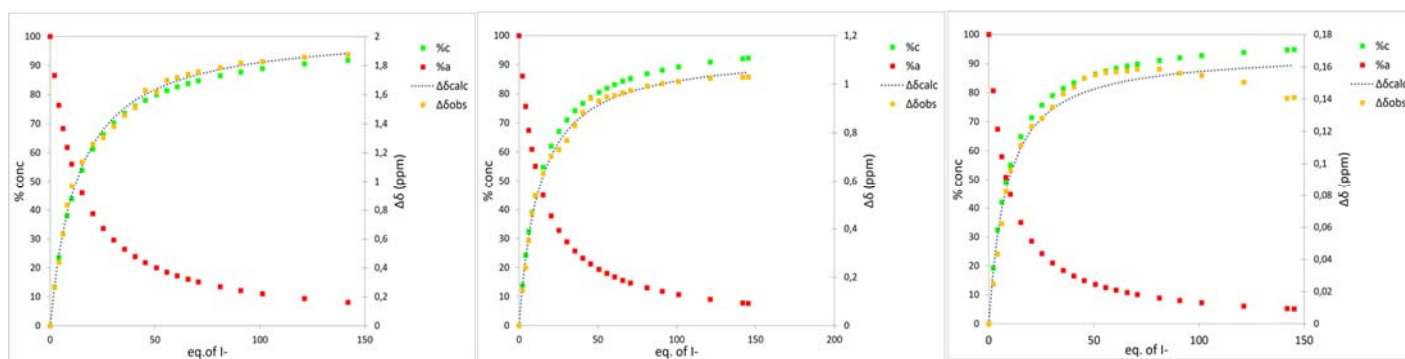
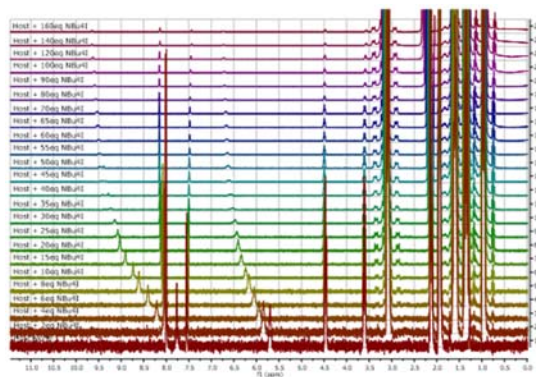
F_b
 $K_a = 21 \text{ L/mol}$
 $[\text{ligand}] = 0.0035 \text{ M}$
 $\delta_{c, \text{lim}} = -132.08 \text{ ppm}$



F_c
 $K_a = 523 \text{ L/mol}$
 $[\text{ligand}] = 0.0035 \text{ M}$
 $\delta_{c, \text{lim}} = -135.13 \text{ ppm}$

Figure S12 ¹⁹F NMR titration of **2** with TBABr

4.4 Titration of **2** with NBu_4I



H_a
 $K_a = 23 \text{ L/mol}$
 $[\text{ligand}] = 0.0035 \text{ M}$
 $\delta_{c, \text{lim}} = 9.82 \text{ ppm}$

H_b
 $K_a = 24 \text{ L/mol}$
 $[\text{ligand}] = 0.0035 \text{ M}$
 $\delta_{c, \text{lim}} = 6.84 \text{ ppm}$

H_c
 $K_a = 36 \text{ L/mol}$
 $[\text{ligand}] = 0.0035 \text{ M}$
 $\delta_{c, \text{lim}} = 8.17 \text{ ppm}$

Figure S13 ^1H NMR titration of **2** with TBAI

[PROGRAM]

Name = SPECFIT
Version = 3.0

[FILE]

Name = OZ19+TBAI_RMN_FORMAT_SPECFIT.FAC
Path = C:\Users\Utilisateur\Desktop\
Date = 02-juin-21
Time = 18:38:11
Ncomp = 2
Nmeas = 24
Nwave = 6

[FACTOR ANALYSIS]

Tolerance = 1,000E-09
Max.Factors = 10
Num.Factors = 5
Significant = 5
Eigen Noise = 4,332E-04
Exp't Noise = 4,332E-04

#	Eigenvalue	Square Sum	Residual	Prediction
1	1,224E+06	9,782E+00	2,615E-01	Data Vector
2	9,748E+00	3,462E-02	1,561E-02	Data Vector
3	3,232E-02	2,302E-03	4,041E-03	Data Vector
4	2,100E-03	2,023E-04	1,202E-03	Data Vector
5	1,763E-04	2,608E-05	4,332E-04	Data Vector

[MODEL]

Date = 02-juin-21
Time = 18:38:23
Model = 0
Index = 3
Function = 1
Species = 3
Params = 3

[SPECIES]	[COLORED]	[FIXED]	[SPECTRUM]
1 0 0	False	False	
0 1 0	True	False	
1 1 0	True	False	

[SPECIES]	[FIXED]	[PARAMETER]	[ERROR]
1 0 0	True	0,00000E+00 +/-	0,00000E+00
0 1 0	True	0,00000E+00 +/-	0,00000E+00
1 1 0	False	1,35919E+00 +/-	3,52774E-02

[CONVERGENCE]

Iterations = 8
Convergence Limit = 1,000E-03
Convergence Found = 2,792E-05
Marquardt Parameter = 0,0
Sum(Y-y)² Residuals = 1,78863E-01
Std. Deviation of Fit(Y) = 3,53665E-02

[STATISTICS]

Experimental Noise = 4,332E-04
Relative Error Of Fit = 0,0382%
Durbin-Watson Factor = 0,3057
Goodness Of Fit, Chi² = 6,666E+03
Durbin-Watson Factor (raw data) = None
Goodness Of Fit, Chi² (raw data) = None

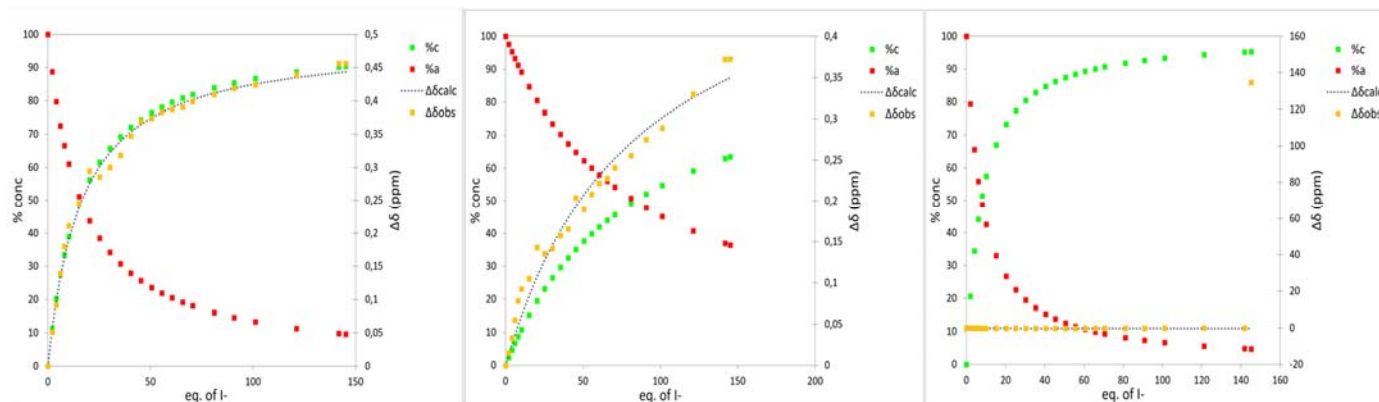
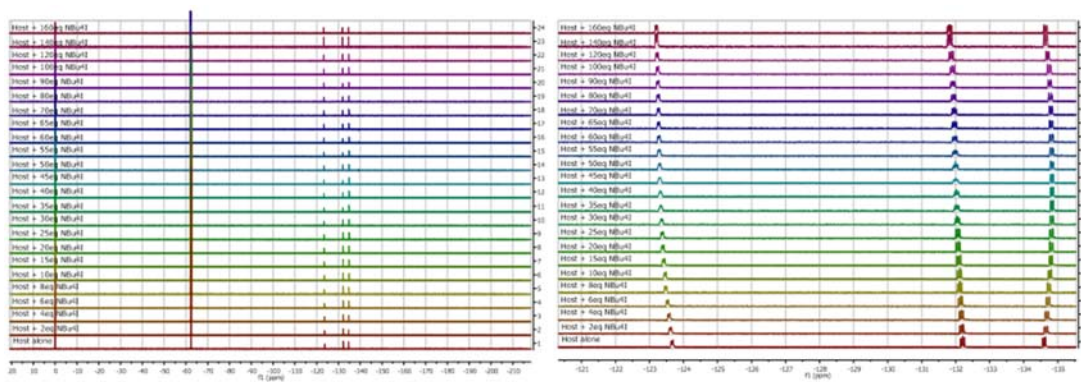
[COVARIANCE]

7,160E-03

[CORRELATION]

1,000E+00

[END FILE]



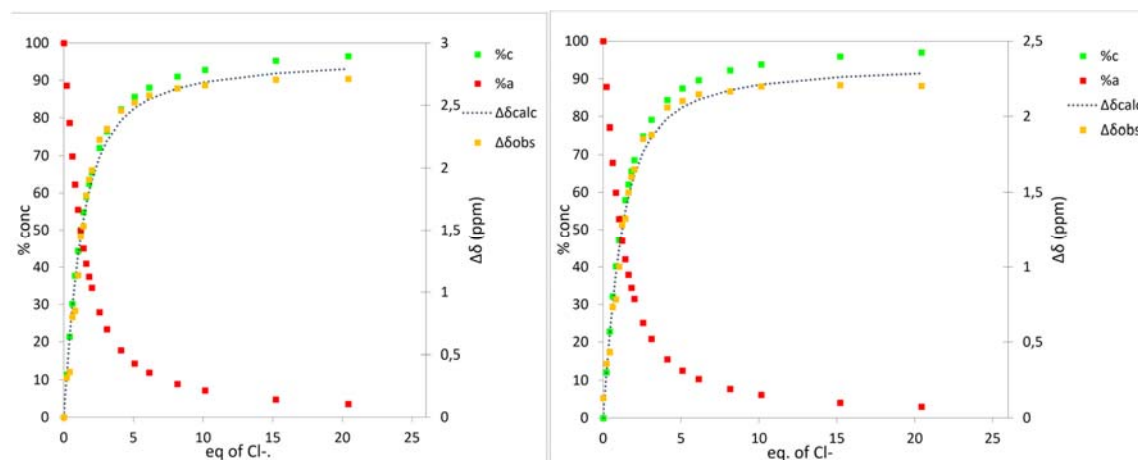
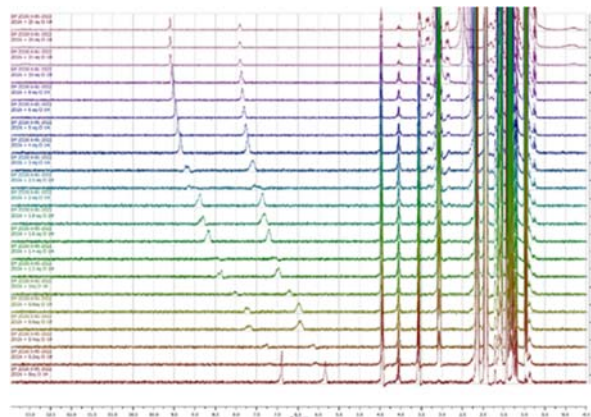
F_a
 $K_a = 19 \text{ L/mol}$
 $[\text{ligand}] = 0.0035 \text{ M}$
 $\delta_{c, \text{lim}} = -123.17 \text{ ppm}$

F_b
 $K_a = 3 \text{ L/mol}$
 $[\text{ligand}] = 0.0035 \text{ M}$
 $\delta_{c, \text{lim}} = -131.64 \text{ ppm}$

F_c
 $K_a = 40 \text{ L/mol}$
 $[\text{ligand}] = 0.0035 \text{ M}$
 $\delta_{c, \text{lim}} = -134.88 \text{ ppm}$

Figure S14 ¹⁹F NMR titration of 2 with TBAI

4.5 Titration of **3** with NBu₄Cl



H_a
 $K_a = 403 \text{ L/mol}$
 $[\text{ligand}] = 0.0035 \text{ M}$
 $\delta_{c, \text{lim}} = 9.78 \text{ ppm}$

H_b
 $K_a = 472 \text{ L/mol}$
 $[\text{ligand}] = 0.0035 \text{ M}$
 $\delta_{c, \text{lim}} = 8.05 \text{ ppm}$

Figure S15 ¹⁵H NMR titration of **3** with TBACl

```

[PROGRAM]
Name = SPECTIT
Version = 3.0

[FILE]
Name = FICHER SPECTIT 2026-CL.FAC
Path = C:\Users\Utilisateur\Desktop\
Date = 11-janv-23
Time = 10:59:20
Ncomp = 2
Nmeas = 20
Nwave = 8

[FACTOR ANALYSIS]
Tolerance = 1,000E-09
Max.Factors = 10
Num.Factors = 4
Significant = 2
Eigen Noise = 2,098E-02
Exp't Noise = 2,098E-02
# Eigenvalue Square Sum Residual Prediction
1 2,519E+06 3,063E+01 4,388E-01 Data Vector
2 3,056E+01 6,952E-02 2,098E-02 Data Vector
3 4,737E-02 2,215E-02 1,188E-02 Possibly Data
4 8,348E-03 1,380E-02 9,405E-03 Probably Noise

[MODEL]
Date = 11-janv-23
Time = 10:59:54
Model = 0
Index = 3
Function = 1
Species = 3
Params = 3

[SPECIES] [COLORED] [FIXED] [SPECTRUM]
1 0 0 False False
0 1 0 True False
1 1 0 True False

[SPECIES] [FIXED] [PARAMETER] [ERROR]
1 0 0 True 0,00000E+00 +/- 0,00000E+00
0 1 0 True 0,00000E+00 +/- 0,00000E+00
1 1 0 False 2,69290E+00 +/- 3,53109E-02

[CONVERGENCE]
Iterations = 10
Convergence Limit = 1,000E-03
Convergence Found = 2,966E-05
Marquardt Parameter = 0,0
Sum(Y-y)^2 Residuals = 4,00041E-01
Std. Deviation of Fit(Y) = 5,01595E-02

[STATISTICS]

```

```

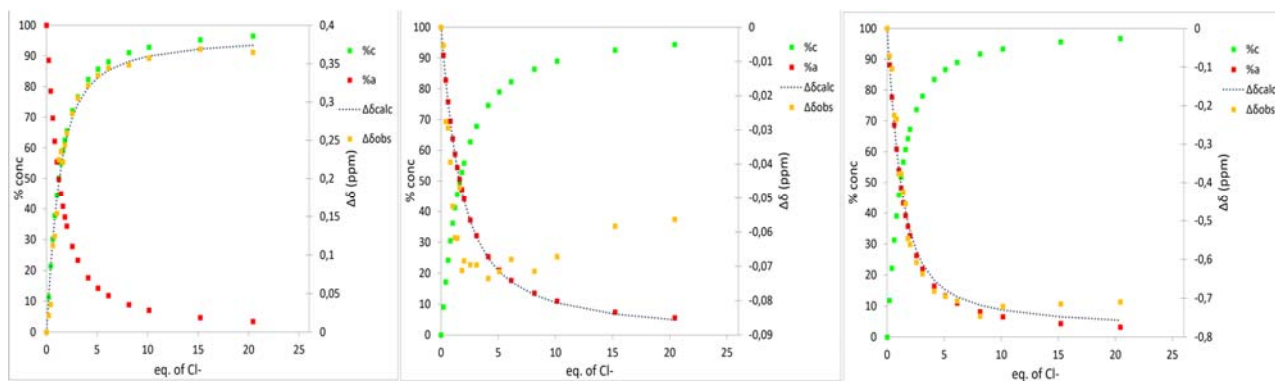
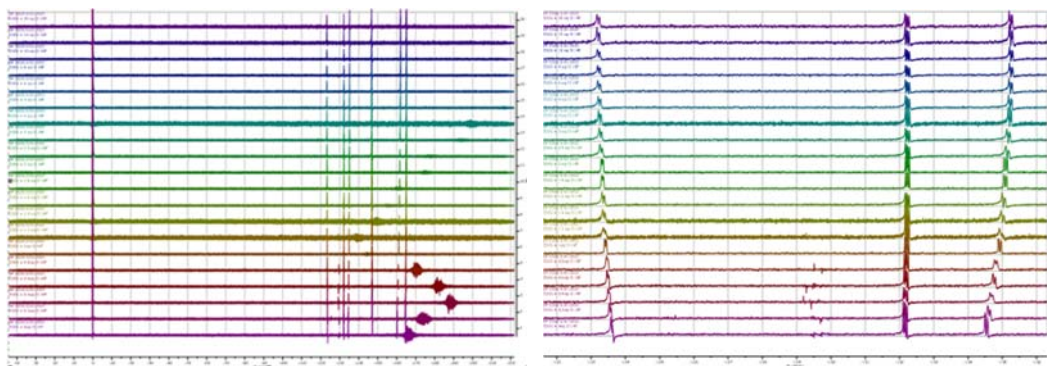
Experimental Noise = 2,098E-02
Relative Error Of Fit = 0,0399%
Durbin-Watson Factor = 1,0398
Goodness Of Fit, Chi^2 = 5,718E+00
Durbin-Watson Factor (raw data) = None
Goodness Of Fit, Chi^2 (raw data) = None

[COVARIANCE]
7,175E-03

[CORRELATION]
1,000E+00

[END FILE]

```



F_a
 $K_a = 405 \text{ L/mol}$
 $[\text{ligand}] = 0.0035 \text{ M}$
 $\delta_{c, \text{lim}} = -123.19 \text{ ppm}$

H_b
 $K_a = \text{L/mol}$
 $[\text{ligand}] = 0.0035 \text{ M}$
 $\delta_{c, \text{lim}} = -132.25 \text{ ppm}$

H_c
 $K_a = 441 \text{ L/mol}$
 $[\text{ligand}] = 0.0035 \text{ M}$
 $\delta_{c, \text{lim}} = -135.32 \text{ ppm}$

Figure S16 ¹⁹F NMR titration of **3** with TBACl

4.6 Titration of **3** with NBu₄Br

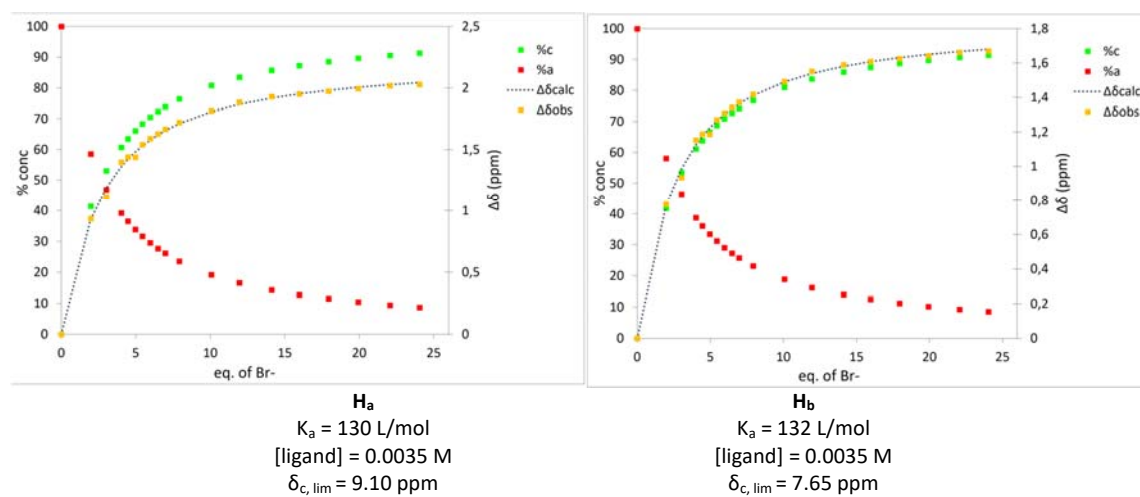
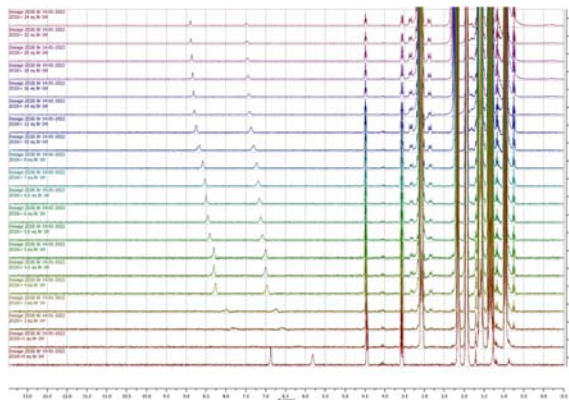


Figure S17 ¹H NMR titration of **3** with TBABr

[PROGRAM]
Name = SPECFIT
Version = 3.0

[FILE]
Name = FICHER SPECFIT 2026-BR.DAT
Path = C:\Users\Utilisateur\Desktop\
Date = 11-janv-23
Time = 10:55:22
Ncomp = 2
Nmeas = 19
Nwave = 8

[MODEL]
Date = 11-janv-23
Time = 10:55:48
Model = 0
Index = 3
Function = 1
Species = 3
Params = 3

[SPECIES]	[COLORED]	[FIXED]	[SPECTRUM]
1 0 0		False	False
0 1 0		True	False
1 1 0		True	False

[SPECIES]	[FIXED]	[PARAMETER]	[ERROR]
1 0 0		True	0,00000E+00 +/-
0 1 0		True	0,00000E+00 +/-
1 1 0		False	2,14452E+00 +/-
			1,78198E-02

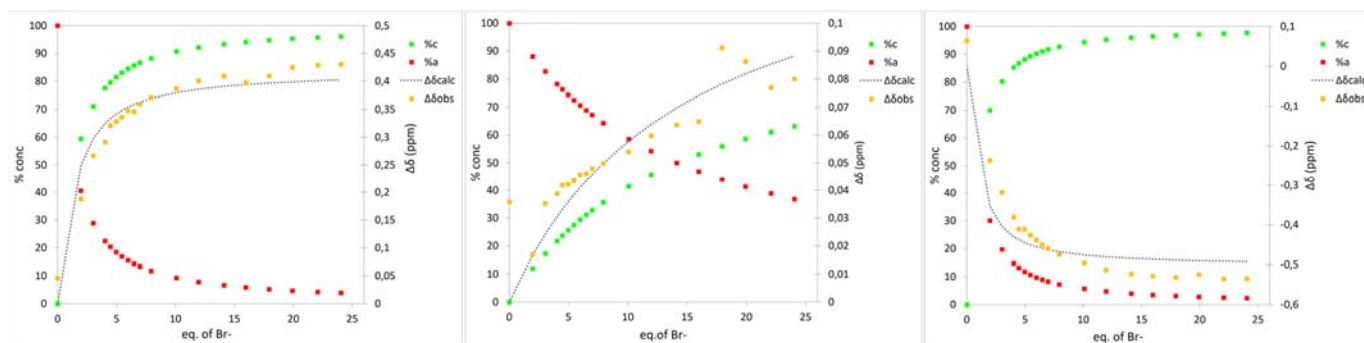
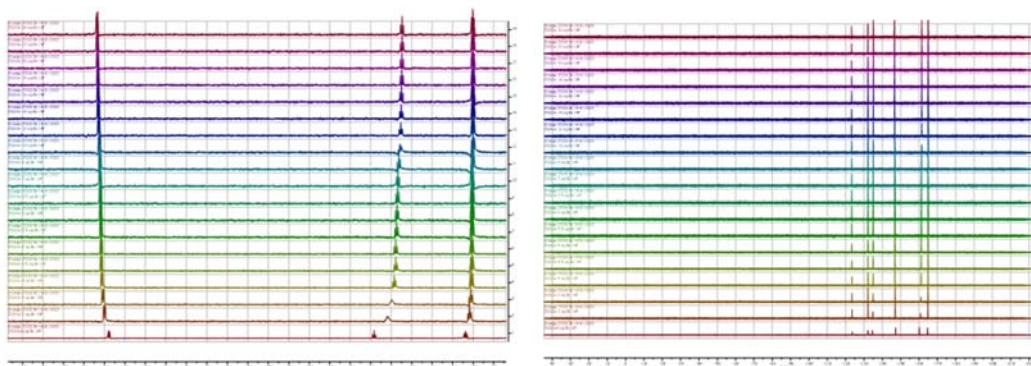
[CONVERGENCE]
Iterations = 5
Convergence Limit = 1,000E-03
Convergence Found = 6,161E-05
Marquardt Parameter = 0,0
Sum(Y-y)² Residuals = 5,43707E-02
Std. Deviation of Fit(Y) = 1,89755E-02

[STATISTICS]
Experimental Noise = 6,941E-03
Relative Error Of Fit = 0,0151%
Durbin-Watson Factor = 1,4358
Goodness Of Fit, Chi² = 7,474E+00
Durbin-Watson Factor (raw data) = 1,4385
Goodness Of Fit, Chi² (raw data) = None

[COVARIANCE]
1,754E-03

[CORRELATION]
1,000E+00

[END FILE]



F_a
 $K_a = 305 \text{ L/mol}$
 $[\text{ligand}] = 0.0035 \text{ M}$
 $\delta_{c, \text{lim}} = -123.25 \text{ ppm}$

F_b
 $K_a = 21 \text{ L/mol}$
 $[\text{ligand}] = 0.0035 \text{ M}$
 $\delta_{c, \text{lim}} = -132.06 \text{ ppm}$

F_c
 $K_a = 523 \text{ L/mol}$
 $[\text{ligand}] = 0.0035 \text{ M}$
 $\delta_{c, \text{lim}} = -135.11 \text{ ppm}$

Figure S18 ¹⁹F NMR titration of **3** with TBABr

4.7 Titration of **3** with NBu_4I

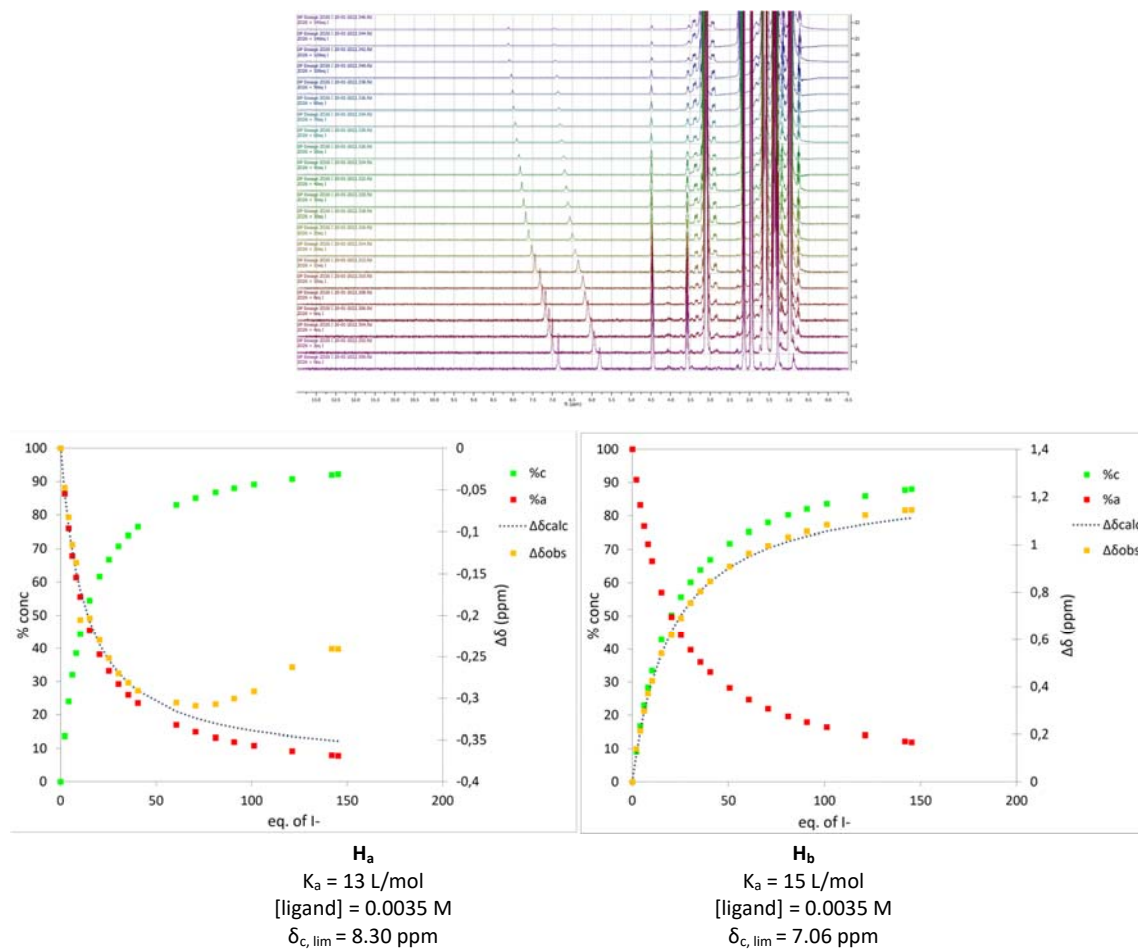


Figure S19 ^1H NMR titration of **3** with TBAI


```

[PROGRAM]
Name = SPECFIT
Version = 3.0

[FILE]
Name = FICHER SPECFIT 2026-CL2.FAC
Path = C:\Users\Utilisateur\Desktop\
Date = 11-janv-23
Time = 11:01:06
Ncomp = 2
Nmeas = 21
Nwave = 8

[FACTOR ANALYSIS]
Tolerance = 1,000E-09
Max.Factors = 10
Num.Factors = 6
Significant = 4
Eigen Noise = 4,375E-03
Exp't Noise = 4,375E-03
# Eigenvalue Square Sum Residual Prediction
1 2,633E+06 8,939E+00 2,314E-01 Data Vector
2 8,771E+00 1,681E-01 3,182E-02 Data Vector
3 1,064E-01 6,169E-02 1,934E-02 Data Vector
4 5,855E-02 3,139E-03 4,375E-03 Data Vector
5 2,176E-03 9,631E-04 2,431E-03 Probably Noise
6 7,349E-04 2,282E-04 1,187E-03 Probably Noise

[MODEL]
Date = 11-janv-23
Time = 11:01:29
Model = 0
Index = 3
Function = 1
Species = 3
Params = 3

[SPECIES] [COLORED] [FIXED] [SPECTRUM]
1 0 0 False False
0 1 0 True False
1 1 0 True False

[SPECIES] [FIXED] [PARAMETER] [ERROR]
1 0 0 True 0,00000E+00 +/- 0,00000E+00
0 1 0 True 0,00000E+00 +/- 0,00000E+00
1 1 0 False 1,09549E+00 +/- 6,01820E-02

[CONVERGENCE]
Iterations = 20
Convergence Limit = 1,000E-03
Convergence Found = 3,524E-04
Marquardt Parameter = 0,0
Sum(Y-y)^2 Residuals = 3,80636E-01
Std. Deviation of Fit(Y) = 4,77416E-02

```

```

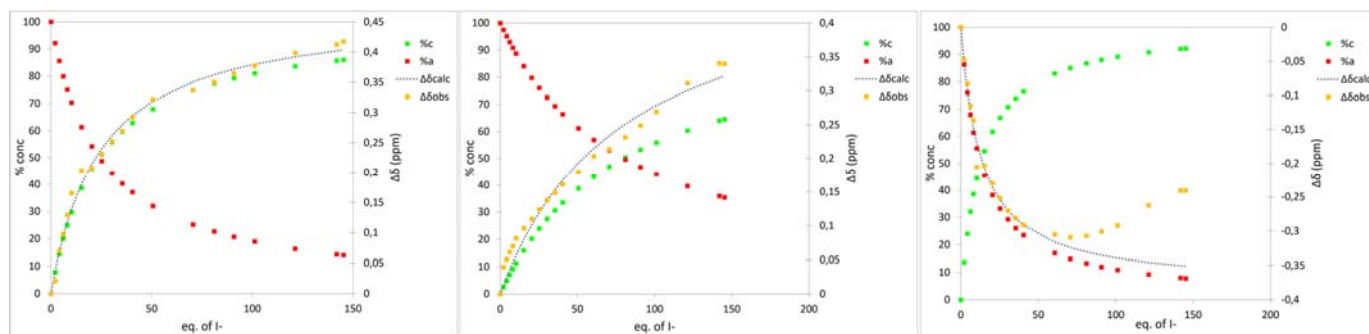
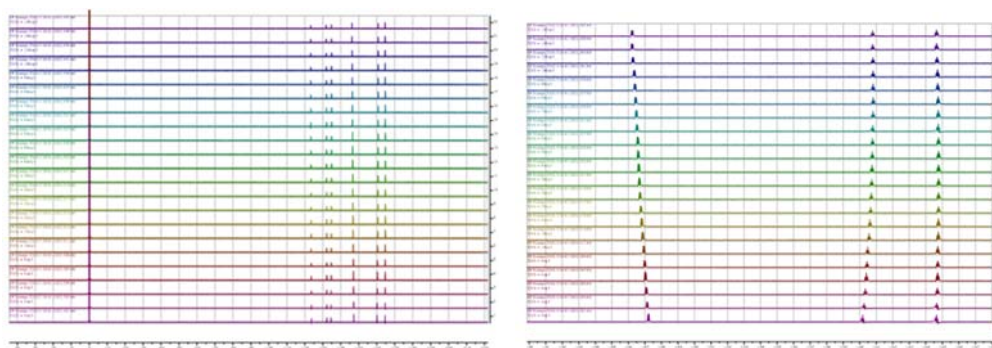
[STATISTICS]
Experimental Noise = 4,375E-03
Relative Error Of Fit = 0,0380%
Durbin-Watson Factor = 1,3399
Goodness Of Fit, Chi^2 = 1,191E+02
Durbin-Watson Factor (raw data) = None
Goodness Of Fit, Chi^2 (raw data) = None

[COVARIANCE]
2,209E-02

[CORRELATION]
1,000E+00

[END FILE]

```



F_a
 $K_a = 12 \text{ L/mol}$
 $[\text{ligand}] = 0.0035 \text{ M}$
 $\delta_{c, \text{lim}} = -123.22 \text{ ppm}$

F_b
 $K_a = 4 \text{ L/mol}$
 $[\text{ligand}] = 0.0035 \text{ M}$
 $\delta_{c, \text{lim}} = -131.71 \text{ ppm}$

F_c
 $K_a = 23 \text{ L/mol}$
 $[\text{ligand}] = 0.0035 \text{ M}$
 $\delta_{c, \text{lim}} = -134.93 \text{ ppm}$

Figure S20 ¹⁹F NMR titration of **3** with TBAI

5. Photophysical analysis and procedures

5.1. General practical analysis procedure

Previously to each analysis, anion salts were solubilized into acetone and precipitated by addition of diethylether to remove water. Salts were then dried to remove residual solvents and stored in the dessicator until use.

10mL of a stock solution of the anion receptor were prepared (10^{-3} mol/L) in acetonitrile. 2mL of this solution was taken and diluted at $2 \cdot 10^{-5}$ mol/L. 2mL of this solution at $2 \cdot 10^{-4}$ mol/L were introduced into a quartz cuvette. 2mL of the stock solution was taken, desired amount of salt was added (55mg for Bu_4NI , 330mg for Bu_4NBr , 600mg for Bu_4NI and 600mg for Bu_4NSCN) and diluted at $2 \cdot 10^{-5}$ mol/L.

2.5mL of solution were added to a 1cm quartz glass cuvette. Aliquots of the solution containing the anion and the receptor are subsequently added to the sample cuvette for each measurement.

After blank subtraction, absorbance spectra were measured from 200 to 700nm. From the absorbance spectra were determined the absorbance maximum (325nm), that corresponds to the excitation wavelength for the emission spectra.

Emission spectra were measured from 335 nm ($\lambda_{\text{abs,max}}+10$) to 700nm using the wavelength determined before as excitation wavelength. Slites were calibrated at 2.1nm. All experiments were proceeded in temperature-controlled room at 300K.

Fluorescence decay data were analyzed using the Globals software package developed at the Laboratory for Fluorescence Dynamics at the University of Illinois at Urbana-Champaign, which includes reconvolution analysis and global non-linear least-squares minimization method.

Experimental measurements were plotted using Excel software. Determination of binding constants was done using a method developed by Valeur *et al.*^[8] using non-linear least-squares minimization method.

$$Y = Y_0 + \frac{Y_{\text{lim}} - Y_0}{2} \left\{ 1 + \frac{c_M}{c_L} + \frac{1}{K_s c_L} - \left[\left(1 + \frac{c_M}{c_L} + \frac{1}{K_s c_L} \right)^2 - 4 \frac{c_M}{c_L} \right]^{1/2} \right\}$$

Where :

Y : Measured intensity at fluorescence maximum

Y_0 : Measured intensity when no salt was added

Y_{lim} : Calculated intensity when an infinity of equivalents of salts are added

c_M : Anion concentration

c_L : Receptor concentration

K_s : Association constant of receptor/anion complex

Binding constants were also determined using SPECFIT/32™ Global Analysis System software.^[9,10] This software allows global analysis of equilibrium and kinetic systems with Expanded SVD and nonlinear regression modeling by the Levenberg-Marquardt method.

5.2. Determination of quantum yields of **2** and **3**

Emission spectra of reference and compounds **2** or **3** were recorded using the maximum absorption wavelength of the reference, Quinine, as excitation wavelength. The fluorescence quantum yield Φ_F was determined using Quinine as reference ($\Phi_F = \text{Acetonitrile}$).^[11]

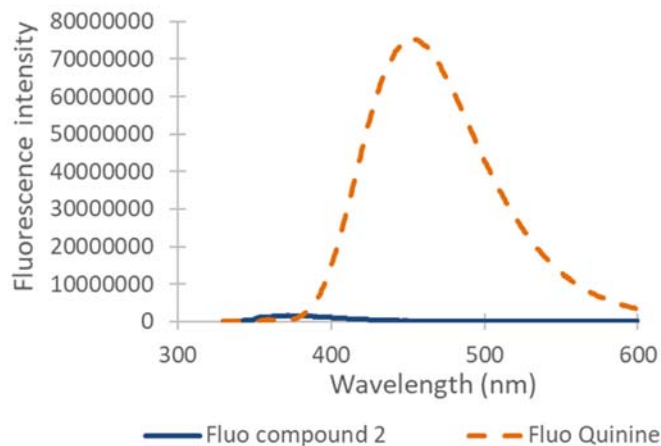


Figure S21 Emission curves of 2 and Quinine in Quinine conditions

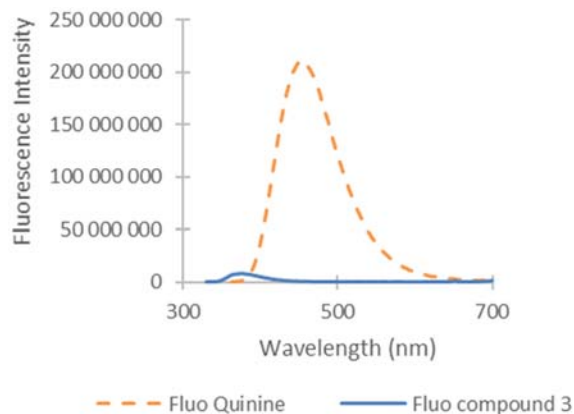


Figure S22 Emission curves of 3 and Quinine in Quinine conditions

From these spectra was determined the quantum yield using the definition described by Brouwer *et al.*^[12]:

$$\Phi_f^i = \frac{F^i f_s n_i^2}{F^s f_i n_s^2} \Phi_f^s$$

Where :

Φ_f^i and Φ_f^s are fluorescence quantum yields of sample and standard reference

F^i and F^s are integrated areas of sample and standard fluorescence curves

f_i and f_s are absorption factors of sample and standard reference, calculated from the formula $f_x = 1 - 10^{-A_x}$, where A_x is the absorbance of species x

n_i and n_s correspond to refraction indexes of sample and standard reference

5.3. Time dependent DFT analysis of compounds **2** and **3**

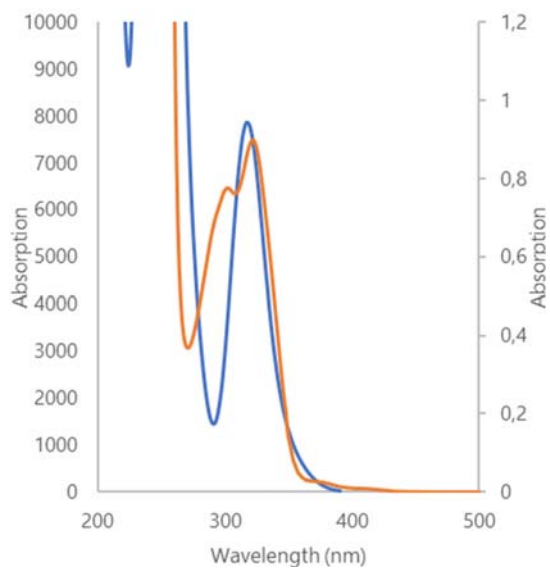


Figure S23 Experimental (orange) and calculated (blue) absorption spectra of **2** (from 200 to 50 nm)

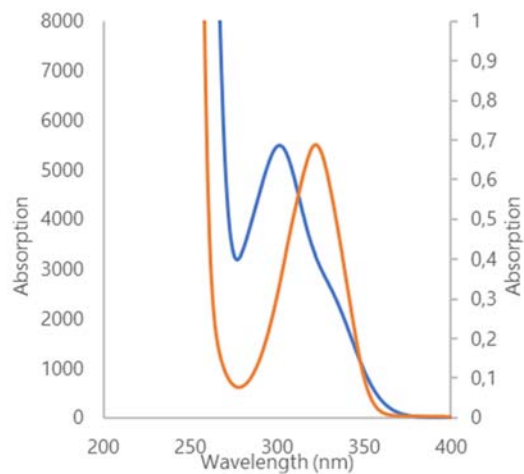


Figure S24 Experimental (orange) and calculated (blue) absorption spectra of **3**

5.4. Titration of **2** with Nbu₄Cl

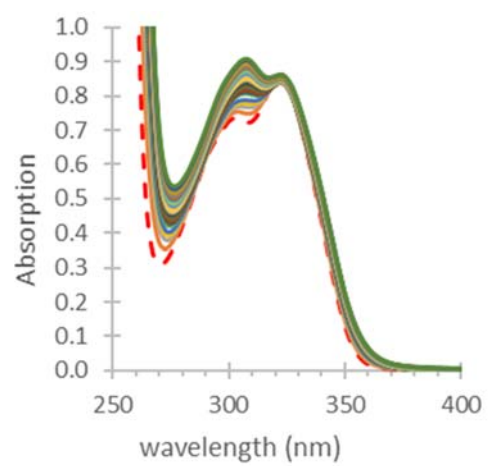


Figure S25 UV-visible titration of **2** with TBACl (from 0 to 70 equivalents) in ACN, ($[2] = 2 \cdot 10^{-4} M$)

[PROGRAM]

Name = SPECFIT
Version = 3.0

[FILE]

Name = OZ19+TBACL_ABS_FORMAT_SPECFIT.FAC
Path = C:\Users\Utilisateur\Desktop\
Date = 02-juin-21
Time = 17:56:36
Ncomp = 2
Nmeas = 24
Nwave = 240

[FACTOR ANALYSIS]

Tolerance = 1,000E-09
Max.Factors = 10
Num.Factors = 10
Significant = 5
Eigen Noise = 1,198E-04
Exp't Noise = 1,198E-04

#	Eigenvalue	Square Sum	Residual	Prediction
1	1,376E+03	1,231E+01	4,623E-02	Data Vector
2	1,227E+01	3,632E-02	2,511E-03	Data Vector
3	3,591E-02	4,081E-04	2,663E-04	Data Vector
4	2,477E-04	1,604E-04	1,668E-04	Data Vector
5	7,814E-05	8,227E-05	1,198E-04	Data Vector
6	3,098E-05	5,129E-05	9,442E-05	Possibly Data
7	1,504E-05	3,626E-05	7,939E-05	Probably Noise
8	8,798E-06	2,746E-05	6,909E-05	Probably Noise
9	4,516E-06	2,294E-05	6,316E-05	Probably Noise
10	3,170E-06	1,977E-05	5,864E-05	Probably Noise

[MODEL]

Date = 02-juin-21
Time = 17:57:24
Model = 0
Index = 3
Function = 1
Species = 3
Params = 3

[SPECIES]	[COLORED]	[FIXED]	[SPECTRUM]
1 0 0	False	False	
0 1 0	True	False	
1 1 0	True	False	

[SPECIES]	[FIXED]	[PARAMETER]	[ERROR]
1 0 0	True	0,00000E+00 +/-	0,00000E+00
0 1 0	True	0,00000E+00 +/-	0,00000E+00
1 1 0	False	3,04556E+00 +/-	1,73449E-02

[CONVERGENCE]

Iterations = 10
Convergence Limit = 1,000E-03
Convergence Found = 2,179E-05
Marquardt Parameter = 0,0
Sum(Y-y)² Residuals = 1,51194E-01
Std. Deviation of Fit(Y) = 5,12382E-03

[STATISTICS]

Experimental Noise = 1,198E-04
Relative Error Of Fit = 1,0437%
Durbin-Watson Factor = 0,4403
Goodness Of Fit, Chi² = 1,837E+03
Durbin-Watson Factor (raw data) = None
Goodness Of Fit, Chi² (raw data) = None

[COVARIANCE]

1,660E-03

[CORRELATION]

1,000E+00

[END FILE]

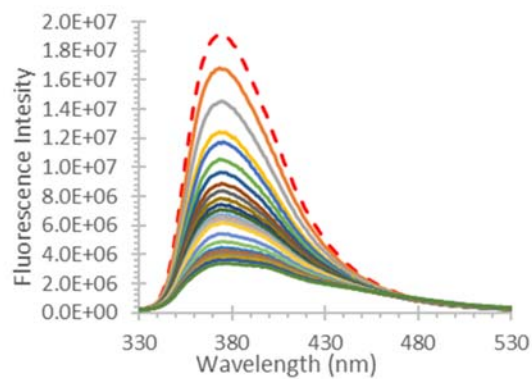
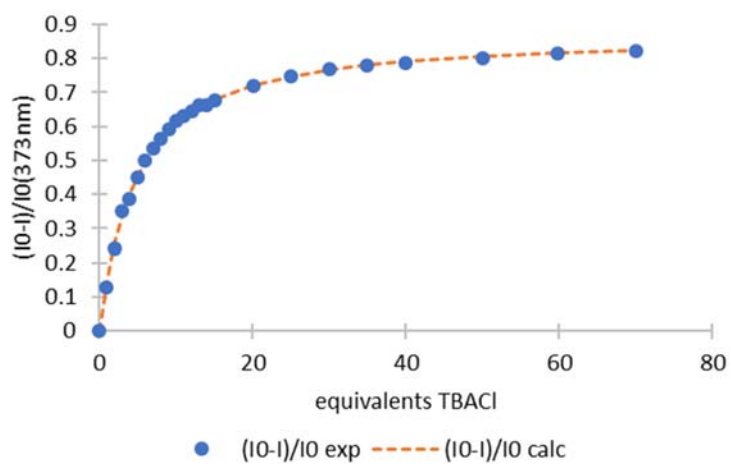


Figure S26 Fluorescence titration of **2** with TBACl (from 0 to 70 equivalents) in ACN, ($[2] = 2.10^{-4} M$)

$\lambda_{exc} = 325 \text{ nm}$



$$K_a = 1222 \text{ M}^{-1}$$

$$[\text{Ligand}] = 0.0002 \text{ M}$$

$$I_{\text{fluo,lim}} = 2426773 \text{ A.U}$$

Figure S27 Mathematical fit of fluorescence titration of **2** with TBACl (from 0 to 70 equivalents) in ACN, ($[2] = 2.10^{-4} M$) $\lambda_{exc} = 325 \text{ nm}$

[PROGRAM]
Name = SPECFIT
Version = 3.0

[FILE]
Name = OZ19+TBACL_FLUO_FORMAT_SPECFIT.FAC
Path = C:\Users\Utilisateur\Desktop\
Date = 02-juin-21
Time = 18:02:27
Ncomp = 2
Nmeas = 24
Nwave = 271

[FACTOR ANALYSIS]
Tolerance = 1,000E-09
Max.Factors = 10
Num.Factors = 6
Significant = 3
Eigen Noise = 1,724E+04
Expt Noise = 1,724E+04

#	Eigenvalue	Square Sum	Residual	Prediction
1	9,263E+16	5,918E+14	3,017E+05	Data Vector
2	5,844E+14	7,360E+12	3,364E+04	Data Vector
3	5,427E+12	1,932E+12	1,724E+04	Data Vector
4	4,748E+11	1,458E+12	1,497E+04	Probably Noise
5	1,900E+11	1,268E+12	1,397E+04	Probably Noise
6	1,516E+11	1,116E+12	1,311E+04	Probably Noise

[MODEL]
Date = 02-juin-21
Time = 18:02:42
Model = 0
Index = 3
Function = 1
Species = 3
Params = 3

[SPECIES]	[COLORED]	[FIXED]	[SPECTRUM]
1 0 0	False	False	
0 1 0	True	False	
1 1 0	True	False	

[SPECIES]	[FIXED]	[PARAMETER]	[ERROR]
1 0 0	True	0,00000E+00 +/-	0,00000E+00
0 1 0	True	0,00000E+00 +/-	0,00000E+00
1 1 0	False	3,10125E+00 +/-	7,58765E-03

[CONVERGENCE]
Iterations = 8
Convergence Limit = 1,000E-03
Convergence Found = 4,620E-08
Marquand Parameter = 0,0
Sum(Y-y)^2 Residuals = 1,72267E+13
Std. Deviation of Fit(Y) = 5,14688E+04

[STATISTICS]
Experimental Noise = 1,724E+04
Relative Error Of Fit = 1,3598%
Durbin-Watson Factor = 1,5370
Goodness Of Fit, Chi^2 = 8,912E+00
Durbin-Watson Factor (raw data) = None
Goodness Of Fit, Chi^2 (raw data) = None

[COVARIANCE]
3,106E-04

[CORRELATION]
1,000E+00

[END FILE]

5.5. Titration of **2** with NBu₄Br

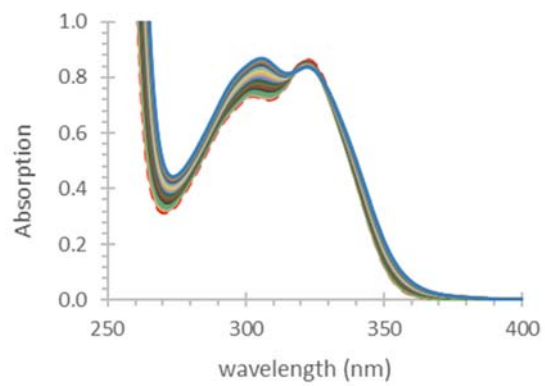


Figure S28 UV-visible titration of **2** with TBABr (from 0 to 160 equivalents) in ACN, ($[2] = 2 \cdot 10^{-4} M$)

[PROGRAM]
Name = SPECFIT
Version = 3.0

[FILE]
Name = OZ19+TBABR_ABS_FORMAT_SPECFIT.FAC
Path = C:\Users\Utilisateur\Desktop\
Date = 02-juin-21
Time = 18:13:53
Ncomp = 2
Nmeas = 23
Nwave = 240

[FACTOR ANALYSIS]
Tolerance = 1,000E-09
Max.Factors = 10
Num.Factors = 10
Significant = 5
Eigen Noise = 8,785E-05
Exp't Noise = 8,785E-05

#	Eigenvalue	Square Sum	Residual	Prediction
1	9,951E+02	9,132E+00	4,088E-02	Data Vector
2	9,129E+00	2,582E-03	8,940E-04	Data Vector
3	2,103E-03	4,785E-04	2,945E-04	Data Vector
4	3,593E-04	1,192E-04	1,470E-04	Data Vector
5	7,660E-05	4,257E-05	8,785E-05	Data Vector
6	1,273E-05	2,983E-05	7,355E-05	Possibly Data
7	5,048E-06	2,478E-05	6,705E-05	Probably Noise
8	3,833E-06	2,095E-05	6,165E-05	Probably Noise
9	3,102E-06	1,785E-05	5,691E-05	Probably Noise
10	2,365E-06	1,548E-05	5,301E-05	Probably Noise

[MODEL]
Date = 02-juin-21
Time = 18:14:26
Model = 0
Index = 3
Function = 1
Species = 3
Params = 3

[SPECIES]	[COLORED]	[FIXED]	[SPECTRUM]
1 0 0	False	False	
0 1 0	True	False	
1 1 0	True	False	

[SPECIES]	[FIXED]	[PARAMETER]	[ERROR]
1 0 0	True	0,00000E+00 +/-	0,00000E+00
0 1 0	True	0,00000E+00 +/-	0,00000E+00
1 1 0	False	2,51438E+00 +/-	7,13976E-03

[CONVERGENCE]
Iterations = 10
Convergence Limit = 1,000E-03
Convergence Found = 2,772E-08
Marquardt Parameter = 0,0
Sum(Y-y)² Residuals = 9,54464E-03
Std. Deviation of Fit(Y) = 1,31507E-03

[STATISTICS]
Experimental Noise = 8,785E-05
Relative Error Of Fit = 0,3083%
Durbin-Watson Factor = 0,7795
Goodness Of Fit, Chi² = 2,241E+02
Durbin-Watson Factor (raw data) = None
Goodness Of Fit, Chi² (raw data) = None

[COVARIANCE]
2,748E-04

[CORRELATION]
1,000E+00

[END FILE]

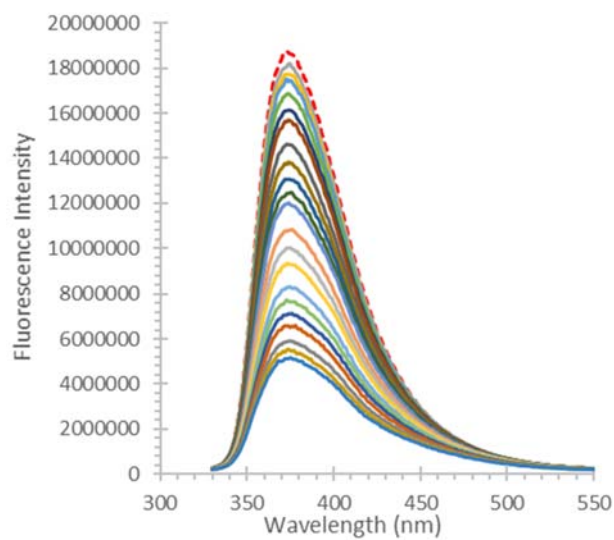


Figure S29 Fluorescence titration of **2** with TBABr (from 0 to 160 equivalents) in ACN, ($[2] = 2 \cdot 10^{-4} M$ $\lambda_{exc} = 325 \text{ nm}$)

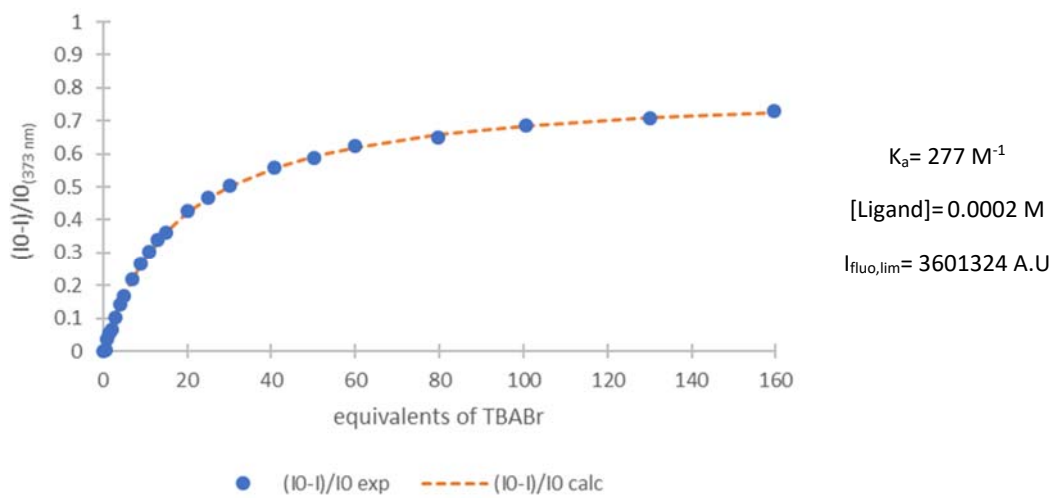


Figure S30 Mathematical fit of fluorescence titration of **2** with TBABr (from 0 to 160 equivalents) in ACN, ($[2] = 2 \cdot 10^{-4} M$ $\lambda_{exc} = 325 \text{ nm}$)

[PROGRAM]
Name = SPECFIT
Version = 3.0

[FILE]
Name = OZ19+TBABR_FLUO_FORMAT_SPECFIT.FAC
Path = C:\Users\Utilisateur\Desktop\
Date = 02-juin-21
Time = 18:18:32
Ncomp = 2
Nmeas = 23
Nwave = 271

[FACTOR ANALYSIS]
Tolerance = 1,000E-09
Max.Factors = 10
Num.Factors = 5
Significant = 3
Eigen Noise = 2,022E+04
Exp't Noise = 2,022E+04
Eigenvalue Square Sum Residual Prediction
1 1,820E+17 1,948E+14 1,768E+05 Data Vector
2 1,891E+14 5,688E+12 3,021E+04 Data Vector
3 3,141E+12 2,547E+12 2,022E+04 Data Vector
4 2,915E+11 2,255E+12 1,903E+04 Probably Noise
5 2,493E+11 2,006E+12 1,795E+04 Probably Noise

[MODEL]
Date = 02-juin-21
Time = 18:19:03
Model = 0
Index = 3
Function = 1
Species = 3
Params = 3

[SPECIES]	[COLORED]	[FIXED]	[SPECTRUM]
1 0 0	False	False	
0 1 0	True	False	
1 1 0	True	False	

[SPECIES]	[FIXED]	[PARAMETER]	[ERROR]
1 0 0	True	0,00000E+00 +/-	0,00000E+00
0 1 0	True	0,00000E+00 +/-	0,00000E+00
1 1 0	False	2,43972E+00 +/-	1,04362E-02

[CONVERGENCE]
Iterations = 8
Convergence Limit = 1,000E-03
Convergence Found = 1,331E-06
Marquardt Parameter = 0,0
Sum(Y-y)² Residuals = 2,68307E+13
Std. Deviation of Fit(Y) = 6,56149E+04

[STATISTICS]
Experimental Noise = 2,022E+04
Relative Error Of Fit = 1,2137%
Durbin-Watson Factor = 0,7189
Goodness Of Fit, Chi² = 1,053E+01
Durbin-Watson Factor (raw data) = None
Goodness Of Fit, Chi² (raw data) = None

[COVARIANCE]
5,915E-04

[CORRELATION]
1,000E+00

[END FILE]

5.6. Titration of **2** with NBu₄I

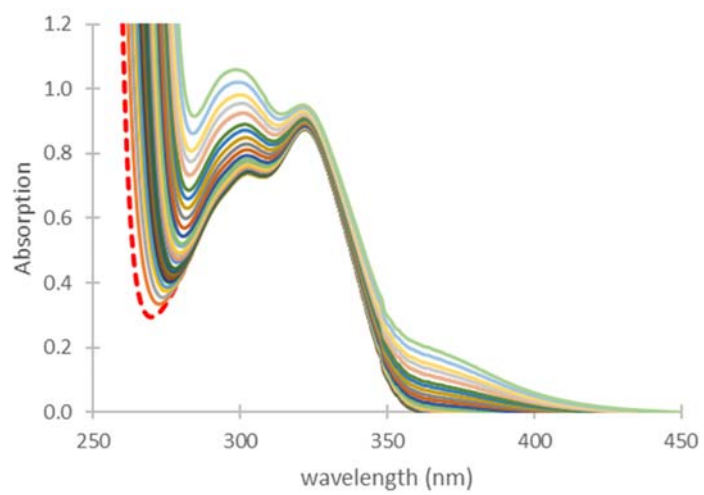


Figure S31 UV-visible titration of **2** with TBAI (from 0 to 200 equivalents) in ACN, ($[2] = 2 \cdot 10^{-4} M$, $\lambda_{exc} = 325 \text{ nm}$)

[PROGRAM]

Name = SPECFIT
Version = 3.0

[FILE]

Name = OZ19+TBAI_ABS_FORMAT_SPECFIT.FAC
Path = C:\Users\Utilisateur\Desktop\
Date = 02-juin-21
Time = 18:28:48
Ncomp = 2
Nmeas = 30
Nwave = 250

[FACTOR ANALYSIS]

Tolerance = 1,000E-09
Max.Factors = 10
Num.Factors = 10
Significant = 7
Eigen Noise = 5,372E-03
Exp't Noise = 5,372E-03

#	Eigenvalue	Square Sum	Residual	Prediction
1	8,050E+03	3,137E+02	2,045E-01	Data Vector
2	2,580E+02	5,775E+01	8,776E-02	Data Vector
3	4,505E+01	1,270E+01	4,117E-02	Data Vector
4	8,683E+00	4,022E+00	2,318E-02	Data Vector
5	2,719E+00	1,303E+00	1,318E-02	Data Vector
6	7,793E-01	5,238E-01	8,358E-03	Data Vector
7	3,073E-01	2,163E-01	5,372E-03	Data Vector
8	1,155E-01	1,007E-01	3,667E-03	Possibly Data
9	4,529E-02	5,544E-02	2,720E-03	Probably Noise
10	1,519E-02	4,024E-02	2,318E-03	Probably Noise

[MODEL]

Date = 02-juin-21
Time = 18:28:55
Model = 0
Index = 3
Function = 1
Species = 3
Params = 3

[SPECIES]	[COLORED]	[FIXED]	[SPECTRUM]
1 0 0	True	False	
0 1 0	True	False	
1 1 0	True	False	

[SPECIES]	[FIXED]	[PARAMETER]	[ERROR]
1 0 0	True	0,00000E+00 +/-	0,00000E+00
0 1 0	True	0,00000E+00 +/-	0,00000E+00
1 1 0	False	2,69389E+00 +/-	6,39340E-02

[CONVERGENCE]

Iterations = 9
Convergence Limit = 1,000E-03
Convergence Found = 8,207E-04
Marquardt Parameter = 0,0
Sum(Y-y)² Residuals = 2,58784E+01
Std. Deviation of Fit(Y) = 5,87444E-02

[STATISTICS]

Experimental Noise = 5,372E-03
Relative Error Of Fit = 5,5710%
Durbin-Watson Factor = 0,2949
Goodness Of Fit, Chi² = 1,196E+02
Durbin-Watson Factor (raw data) = None
Goodness Of Fit, Chi² (raw data) = None

[COVARIANCE]

2,515E-02

[CORRELATION]

1,000E+00

[END FILE]

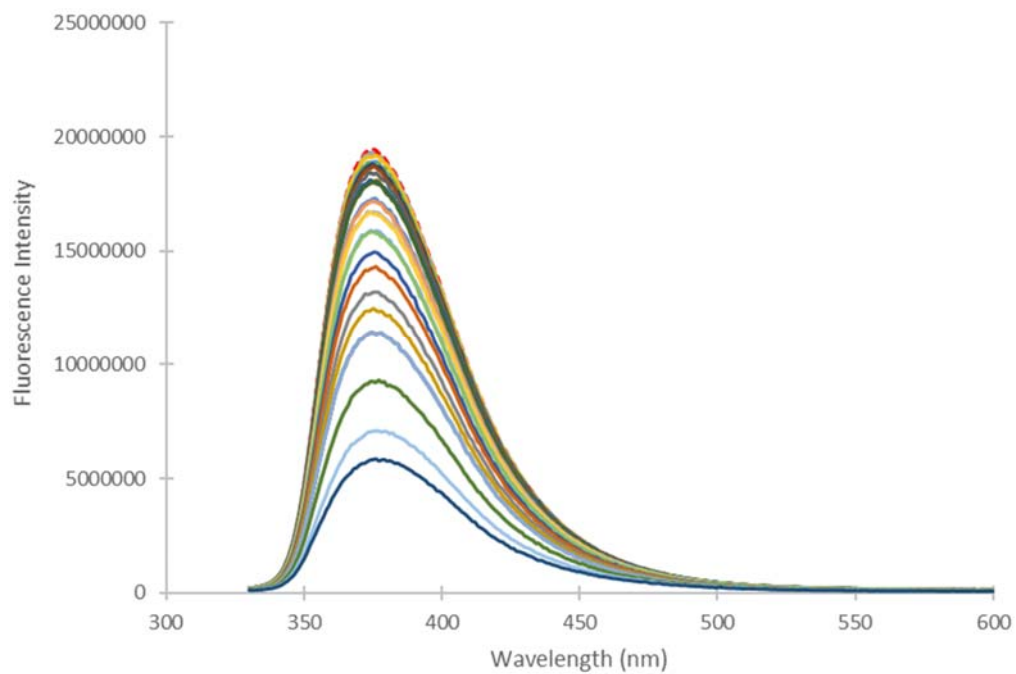


Figure S32 Fluorescence titration of **2** with TBAI (from 0 to 200 equivalents) in ACN, ($[2] = 2 \cdot 10^{-4} M$, $\lambda_{exc} = 325 \text{ nm}$)

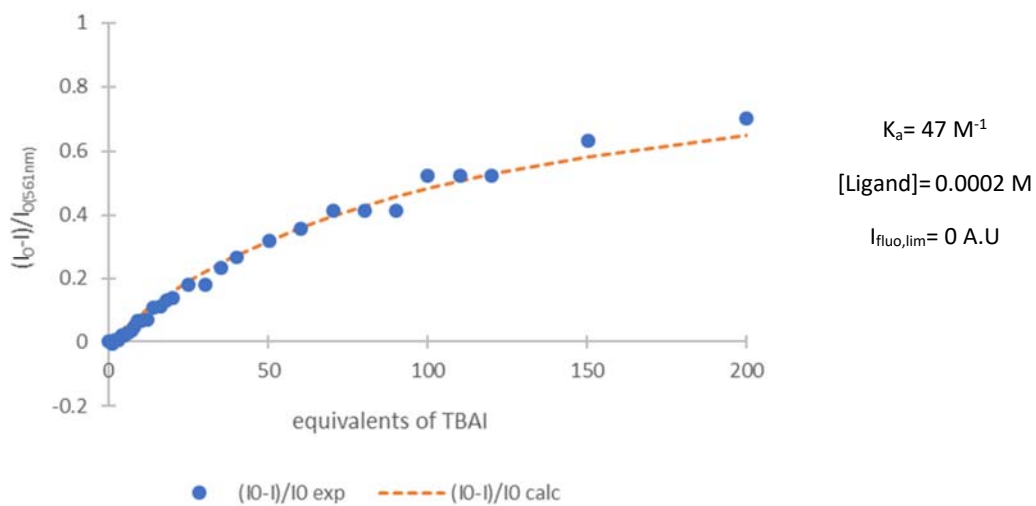


Figure S33 Mathematical fit of fluorescence titration of **2** with TBAI (from 0 to 200 equivalents) in ACN, ($[2] = 2 \cdot 10^{-4} M$, $\lambda_{exc} = 325 \text{ nm}$).

[PROGRAM]
Name = SPECFIT
Version = 3.0

[FILE]
Name = OZ19+TBAI_FLUO_FORMAT_SPECFIT.FAC
Path = C:\Users\Utilisateur\Desktop\
Date = 02-juin-21
Time = 18:33:14
Ncomp = 2
Nmeas = 30
Nwave = 271

[FACTOR ANALYSIS]
Tolerance = 1,000E-09
Max.Factors = 10
Num.Factors = 3
Significant = 2
Eigen Noise = 2,282E+04
Exp't Noise = 2,282E+04
Eigenvalue Square Sum Residual Prediction
1 3,109E+17 3,838E+13 6,871E+04 Data Vector
2 3,415E+13 4,233E+12 2,282E+04 Data Vector
3 4,336E+11 3,799E+12 2,162E+04 Probably Noise

[MODEL]
Date = 02-juin-21
Time = 18:35:10
Model = 0
Index = 3
Function = 1
Species = 3
Params = 3

[SPECIES]	[COLORED]	[FIXED]	[SPECTRUM]
1 0 0	False	False	
0 1 0	True	False	
1 1 0	False	False	

[SPECIES]	[FIXED]	[PARAMETER]	[ERROR]
1 0 0	True	0,00000E+00 +/-	0,00000E+00
0 1 0	True	0,00000E+00 +/-	0,00000E+00
1 1 0	False	1,68583E+00 +/-	1,34358E-02

[CONVERGENCE]
Iterations = 5
Convergence Limit = 1,000E-03
Convergence Found = 5,597E-06
Marquadt Parameter = 0,0
Sum(Y-y)² Residuals = 1,84696E+14
Std. Deviation of Fit(Y) = 1,50734E+05

[STATISTICS]
Experimental Noise = 2,282E+04
Relative Error Of Fit = 2,4380%
Durbin-Watson Factor = 1,3265
Goodness Of Fit, Chi² = 4,363E+01
Durbin-Watson Factor (raw data) = None
Goodness Of Fit, Chi² (raw data) = None

[COVARIANCE]
9,873E-04

[CORRELATION]
1,000E+00

[END FILE]

5.7. Titration of **3** with NBu₄Cl

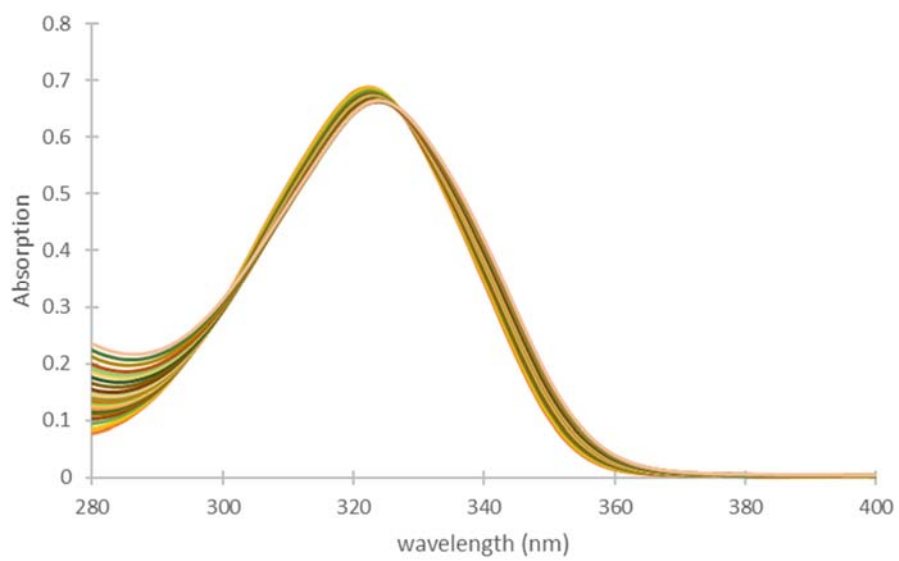


Figure S34 UV-visible titration of **3** with TBACl (from 0 to 70 equivalents) in ACN, ([**3**] = $2 \cdot 10^{-4} M$).

[PROGRAM]
Name = SPECFIT
Version = 3.0

[FILE]
Name = OZ35+TBACL_ABS_FORMAT_SPECFIT.FAC
Path = C:\Users\Utilisateur\Desktop\
Date = 04-juin-21
Time = 19:22:12
Ncomp = 2
Nmeas = 24
Nwave = 480

[FACTOR ANALYSIS]
Tolerance = 1,000E-09
Max.Factors = 10
Num.Factors = 9
Significant = 4
Eigen Noise = 4,547E-04
Expt Noise = 4,547E-04

#	Eigenvalue	Square Sum	Residual	Prediction
1	8,638E+03	6,127E+00	2,306E-02	Data Vector
2	5,964E+00	1,632E-01	3,764E-03	Data Vector
3	1,550E-01	8,166E-03	8,422E-04	Data Vector
4	5,788E-03	2,381E-03	4,547E-04	Data Vector
5	5,497E-04	1,831E-03	3,988E-04	Probably Noise
6	3,762E-04	1,455E-03	3,555E-04	Probably Noise
7	2,681E-04	1,187E-03	3,211E-04	Probably Noise
8	2,083E-04	9,788E-04	2,916E-04	Probably Noise
9	1,407E-04	8,380E-04	2,698E-04	Probably Noise

[MODEL]
Date = 04-juin-21
Time = 19:22:25
Model = 0
Index = 3
Function = 1
Species = 3
Params = 3

[SPECIES]	[COLORED]	[FIXED]	[SPECTRUM]
1 0 0	False	False	
0 1 0	True	False	
1 1 0	True	False	

[SPECIES]	[FIXED]	[PARAMETER]	[ERROR]
1 0 0	True	0,00000E+00 +/-	0,00000E+00
0 1 0	True	0,00000E+00 +/-	0,00000E+00
1 1 0	False	2,58988E+00 +/-	3,05112E-02

[CONVERGENCE]
Iterations = 9
Convergence Limit = 1,000E-03
Convergence Found = 6,236E-04
Marquardt Parameter = 0,0
Sum(Y-y)² Residuals = 2,10578E-01
Std. Deviation of Fit(Y) = 4,27562E-03

[STATISTICS]
Experimental Noise = 4,547E-04
Relative Error Of Fit = 0,4936%
Durbin-Watson Factor = 0,2802
Goodness Of Fit, Chi² = 8,841E+01
Durbin-Watson Factor (raw data) = None
Goodness Of Fit, Chi² (raw data) = None

[COVARIANCE]
5,297E-03

[CORRELATION]
1,000E+00

[END FILE]

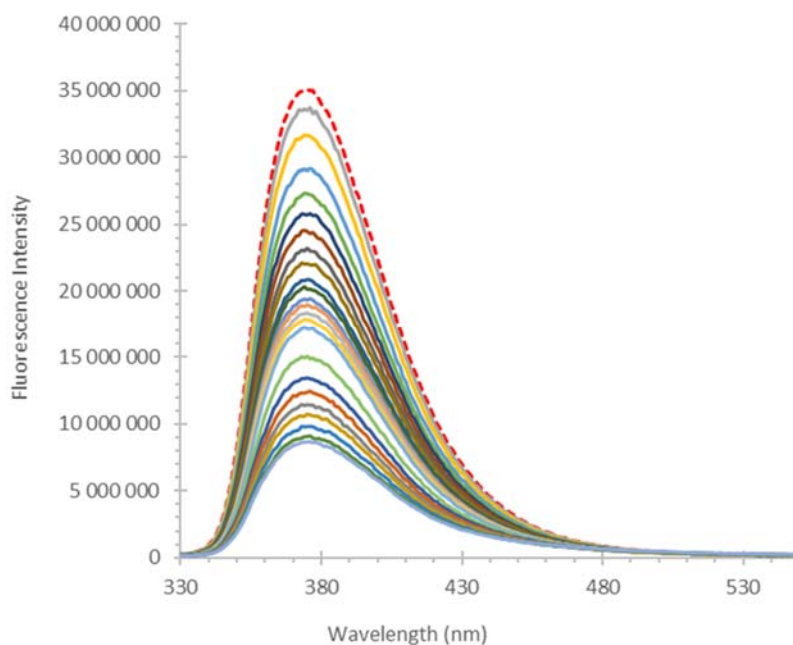


Figure S35 Fluorescence titration of **3** with TBACl (from 0 to 70 equivalents) in ACN, ($[3] = 2.10^{-4} M$, $\lambda_{exc} = 325$ nm).

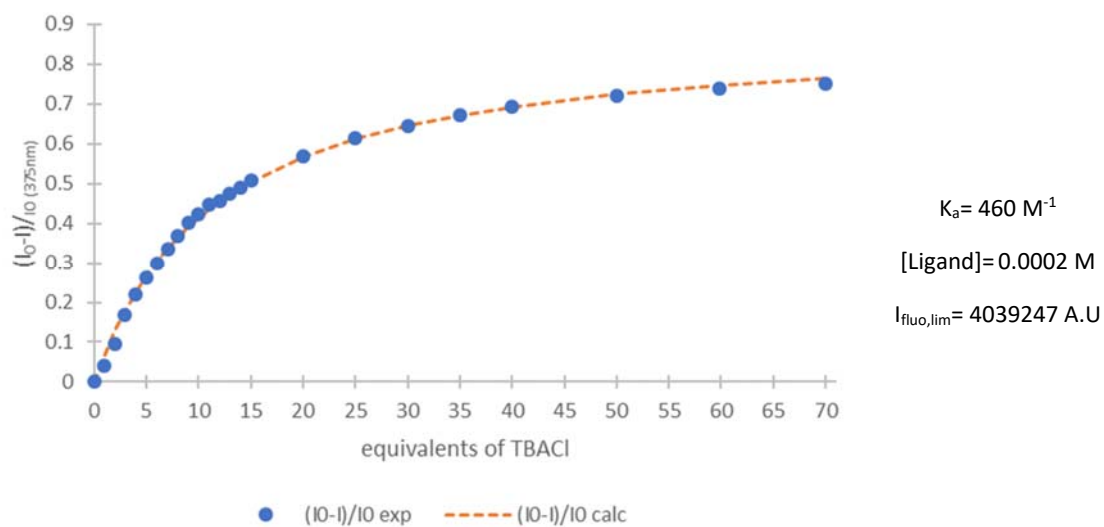


Figure S36 Mathematical fit of fluorescence titration of **3** with TBACl (from 0 to 70 equivalents) in ACN, ($[3] = 2.10^{-4} M$, $\lambda_{exc} = 325$ nm).

[PROGRAM]
Name = SPECFIT
Version = 3.0

[FILE]
Name = OZ35+TBACL_FLUO_FORMAT_SPECFIT.FAC
Path = C:\Users\Utilisateur\Desktop\
Date = 04-juin-21
Time = 19:28:28
Ncomp = 2
Nmeas = 24
Nwave = 271

[FACTOR ANALYSIS]
Tolerance = 1,000E-09
Max.Factors = 10
Num.Factors = 6
Significant = 2
Eigen Noise = 3,693E+04
Expt Noise = 3,693E+04
Eigenvalue Square Sum Residual Prediction
1 4,279E+17 1,101E+14 1,301E+05 Data Vector
2 1,012E+14 8,868E+12 3,693E+04 Data Vector
3 3,243E+12 5,623E+12 2,941E+04 Possibly Data
4 7,197E+11 4,903E+12 2,748E+04 Probably Noise
5 5,898E+11 4,313E+12 2,578E+04 Probably Noise
6 4,343E+11 3,879E+12 2,443E+04 Probably Noise

[MODEL]
Date = 04-juin-21
Time = 19:36:13
Model = 0
Index = 3
Function = 1
Species = 3
Params = 3

[SPECIES]	[COLORED]	[FIXED]	[SPECTRUM]
1 0 0	False	False	
0 1 0	True	False	
1 1 0	True	False	

[SPECIES]	[FIXED]	[PARAMETER]	[ERROR]
1 0 0	True	0,00000E+00 +/-	0,00000E+00
0 1 0	True	0,00000E+00 +/-	0,00000E+00
1 1 0	False	2,71604E+00 +/-	9,43317E-03

[CONVERGENCE]
Iterations = 3
Convergence Limit = 1,000E-03
Convergence Found = 4,120E-07
Marquardt Parameter = 0,0
Sum(Y-y)² Residuals = 7,61971E+13
Std. Deviation of Fit(Y) = 1,08246E+05

[STATISTICS]
Experimental Noise = 3,693E+04
Relative Error Of Fit = 1,3345%
Durbin-Watson Factor = 1,2620
Goodness Of Fit, Chi² = 8,593E+00
Durbin-Watson Factor (raw data) = None
Goodness Of Fit, Chi² (raw data) = None

[COVARIANCE]
4,822E-04

[CORRELATION]
1,000E+00

[END FILE]

5.8. Titration of **3** with NBu₄Br

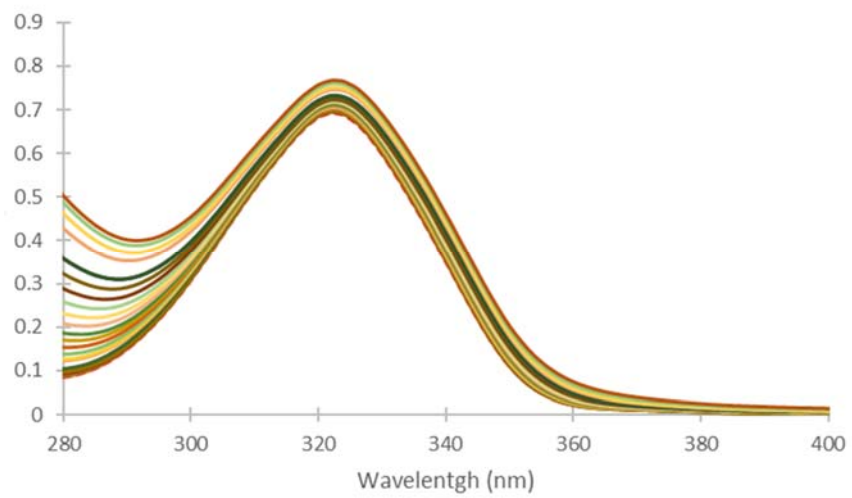


Figure S37 UV-visible titration of **3** with TBABr (from 0 to 160 equivalents) in ACN, ($[3] = 2.10^{-4}$).

[PROGRAM]
Name = SPECFIT
Version = 3.0

[FILE]
Name = OZ35+TBABR_ABS_FORMAT_SPECFIT.FAC
Path = C:\Users\Utilisateur\Desktop\
Date = 04-juin-21
Time = 19:45:37
Ncomp = 2
Nmeas = 23
Nwave = 460

[FACTOR ANALYSIS]
Tolerance = 1,000E-09
Max.Factors = 10
Num.Factors = 10
Significant = 6
Eigen Noise = 3,924E-04
Exp't Noise = 3,924E-04

#	Eigenvalue	Square Sum	Residual	Prediction
1	3,997E+03	1,617E+01	3,909E-02	Data Vector
2	1,610E+01	7,081E-02	2,587E-03	Data Vector
3	5,795E-02	1,287E-02	1,103E-03	Data Vector
4	6,697E-03	6,170E-03	7,638E-04	Data Vector
5	2,754E-03	3,417E-03	5,684E-04	Data Vector
6	1,789E-03	1,628E-03	3,924E-04	Data Vector
7	5,256E-04	1,102E-03	3,229E-04	Probably Noise
8	3,969E-04	7,054E-04	2,583E-04	Probably Noise
9	1,866E-04	5,189E-04	2,215E-04	Probably Noise
10	1,178E-04	4,010E-04	1,948E-04	Probably Noise

[MODEL]
Date = 04-juin-21
Time = 19:45:52
Model = 0
Index = 3
Function = 1
Species = 3
Params = 3

[SPECIES]	[COLORED]	[FIXED]	[SPECTRUM]
1 0 0	False	False	
0 1 0	True	False	
1 1 0	True	False	

[SPECIES]	[FIXED]	[PARAMETER]	[ERROR]
1 0 0	True	0,00000E+00 +/-	0,00000E+00
0 1 0	True	0,00000E+00 +/-	0,00000E+00
1 1 0	False	1,99439E+00 +/-	3,01563E-02

[CONVERGENCE]
Iterations = 8
Convergence Limit = 1,000E-03
Convergence Found = 7,006E-06
Marquardt Parameter = 0,0
Sum(Y-y)² Residuals = 2,78505E-01
Std. Deviation of Fit(Y) = 5,13091E-03

[STATISTICS]
Experimental Noise = 3,924E-04
Relative Error Of Fit = 0,8330%
Durbin-Watson Factor = 1,0463
Goodness Of Fit, Chi² = 1,710E+02
Durbin-Watson Factor (raw data) = None
Goodness Of Fit, Chi² (raw data) = None

[COVARIANCE]
5,170E-03

[CORRELATION]
1,000E+00

[END FILE]

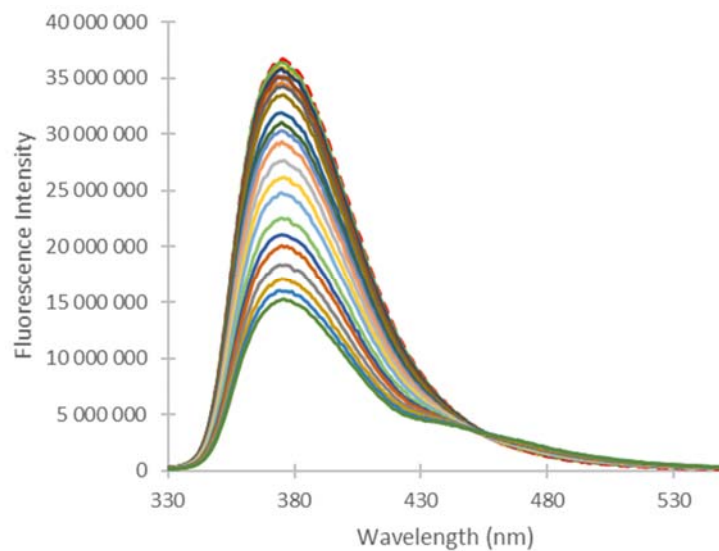


Figure S38 Fluorescence titration of **3** with TBABr (from 0 to 160 equivalents) in ACN, ($[3] = 2.10^{-4} M$ $\lambda_{exc} = 325$ nm).

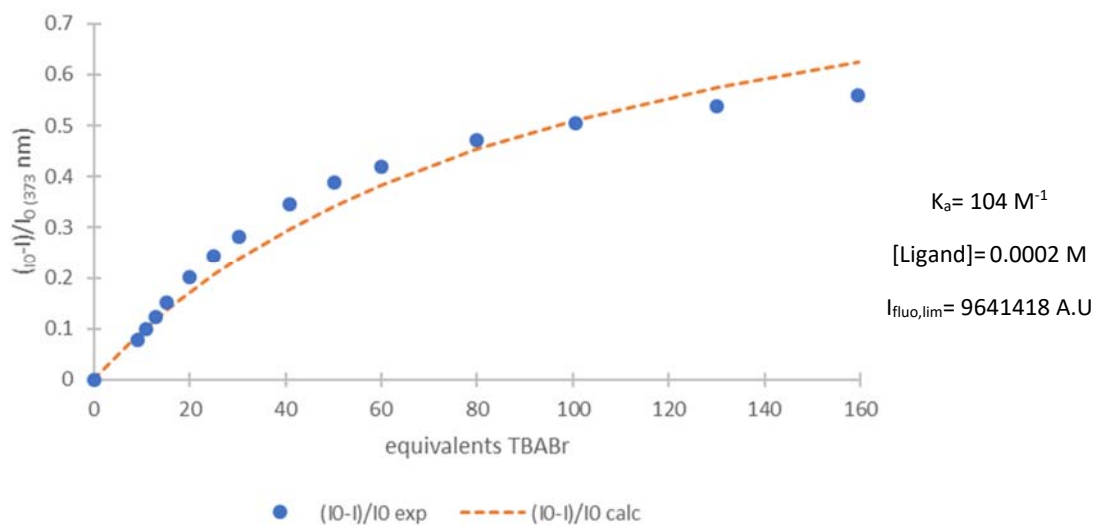


Figure S39 Mathematical fit of fluorescence titration of **3** with TBABr (from 0 to 160 equivalents) in ACN, ($[3] = 2.10^{-4} M$ $\lambda_{exc} = 325$ nm).

[PROGRAM]
Name = SPECFIT
Version = 3.0

[FILE]
Name = OZ35+TBABR_FLUO_FORMAT_SPECFIT.FAC
Path = C:\Users\Utilisateur\Desktop\
Date = 04-juin-21
Time = 19:50:49
Ncomp = 2
Nmeas = 23
Nwave = 270

[FACTOR ANALYSIS]
Tolerance = 1,000E-09
Max.Factors = 10
Num.Factors = 5
Significant = 2
Eigen Noise = 4,834E+04
Exp't Noise = 4,834E+04
Eigenvalue Square Sum Residual Prediction
1 8,008E+17 8,292E+14 3,654E+05 Data Vector
2 8,147E+14 1,451E+13 4,834E+04 Data Vector
3 4,492E+12 1,002E+13 4,017E+04 Possibly Data
4 2,124E+12 7,893E+12 3,568E+04 Probably Noise
5 8,681E+11 7,024E+12 3,365E+04 Probably Noise

[MODEL]
Date = 04-juin-21
Time = 19:52:19
Model = 0
Index = 3
Function = 1
Species = 3
Params = 3

[SPECIES]	[COLORED]	[FIXED]	[SPECTRUM]
1 0 0	False	False	
0 1 0	True	False	
1 1 0	True	False	

[SPECIES]	[FIXED]	[PARAMETER]	[ERROR]
1 0 0	True	0,00000E+00 +/-	0,00000E+00
0 1 0	True	0,00000E+00 +/-	0,00000E+00
1 1 0	False	2,09520E+00 +/-	3,16728E-02

[CONVERGENCE]
Iterations = 3
Convergence Limit = 1,000E-03
Convergence Found = 4,758E-10
Marquardt Parameter = 0,0
Sum(Y-y)² Residuals = 4,87164E+14
Std. Deviation of Fit(Y) = 2,80109E+05

[STATISTICS]
Experimental Noise = 4,834E+04
Relative Error Of Fit = 2,4659%
Durbin-Watson Factor = 0,3661
Goodness Of Fit, Chi² = 3,357E+01
Durbin-Watson Factor (raw data) = None
Goodness Of Fit, Chi² (raw data) = None

[COVARIANCE]
5,724E-03

[CORRELATION]
1,000E+00

[END FILE]

5.9. Titration of **3** with NBu₄I

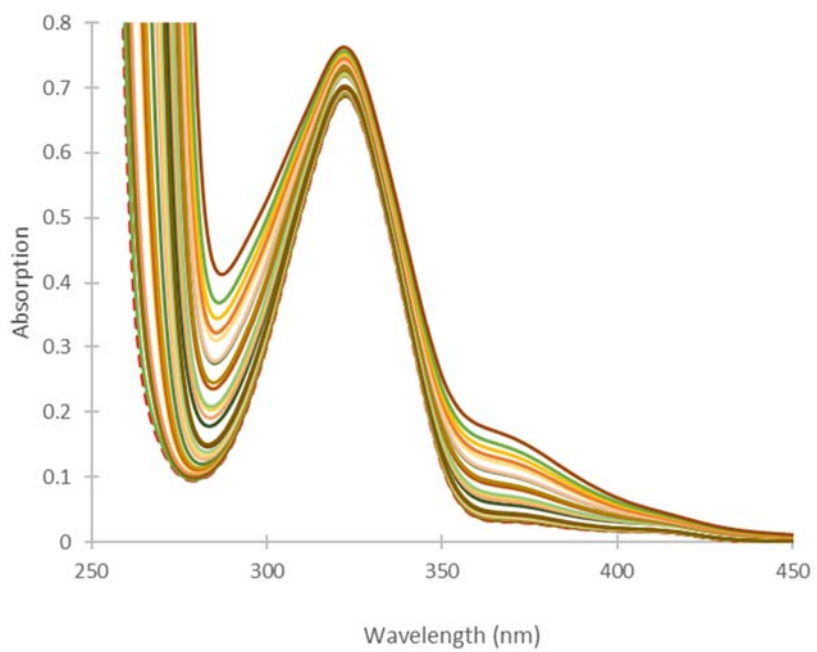


Figure S40 UV-visible titration of **3** with TBAI (from 0 to 200 equivalents) in ACN, ($[3] = 2.10^{-4}M$).

[PROGRAM]
Name = SPECFIT
Version = 3.0

[FILE]
Name = OZ35+TBAI_ABS_FORMAT_SPECFIT.FAC
Path = C:\Users\Utilisateur\Desktop\
Date = 04-juin-21
Time = 20:40:31
Ncomp = 2
Nmeas = 30
Nwave = 430

[FACTOR ANALYSIS]
Tolerance = 1,000E-09
Max. Factors = 10
Num. Factors = 10
Significant = 7
Eigen Noise = 1,207E-04
Exp't Noise = 1,207E-04
Eigenvalue Square Sum Residual Prediction
1 7,263E+02 9,469E+01 8,568E-02 Data Vector
2 9,424E+01 4,467E-01 5,885E-03 Data Vector
3 3,655E-01 8,121E-02 2,509E-03 Data Vector
4 7,219E-02 9,021E-03 8,364E-04 Data Vector
5 7,048E-03 1,973E-03 3,912E-04 Data Vector
6 1,265E-03 7,075E-04 2,342E-04 Data Vector
7 5,195E-04 1,880E-04 1,207E-04 Data Vector
8 8,626E-05 1,017E-04 8,882E-05 Possibly Data
9 4,214E-05 5,957E-05 6,798E-05 Probably Noise
10 1,334E-05 4,623E-05 5,989E-05 Probably Noise

[MODEL]
Date = 04-juin-21
Time = 20:41:03
Model = 0
Index = 3
Function = 1
Species = 3
Params = 3

[SPECIES]	[COLORED]	[FIXED]	[SPECTRUM]
1 0 0	True	False	
0 1 0	True	False	
1 1 0	True	False	

[SPECIES]	[FIXED]	[PARAMETER]	[ERROR]
1 0 0	True	0,00000E+00 +/-	0,00000E+00
0 1 0	True	0,00000E+00 +/-	0,00000E+00
1 1 0	False	8,30314E-01 +/-	2,74208E-01

[CONVERGENCE]
Iterations = 4
Convergence Limit = 1,000E-03
Convergence Found = 2,111E-05
Marquardt Parameter = 0,0
Sum(Y-y)² Residuals = 5,13078E-01
Std. Deviation of Fit(Y) = 6,30687E-03

[STATISTICS]
Experimental Noise = 1,207E-04
Relative Error Of Fit = 2,5008%
Durbin-Watson Factor = 1,6694
Goodness Of Fit, Chi² = 2,728E+03
Durbin-Watson Factor (raw data) = None
Goodness Of Fit, Chi² (raw data) = None

[COVARIANCE]
7,748E-01

[CORRELATION]
1,000E+00

[END FILE]

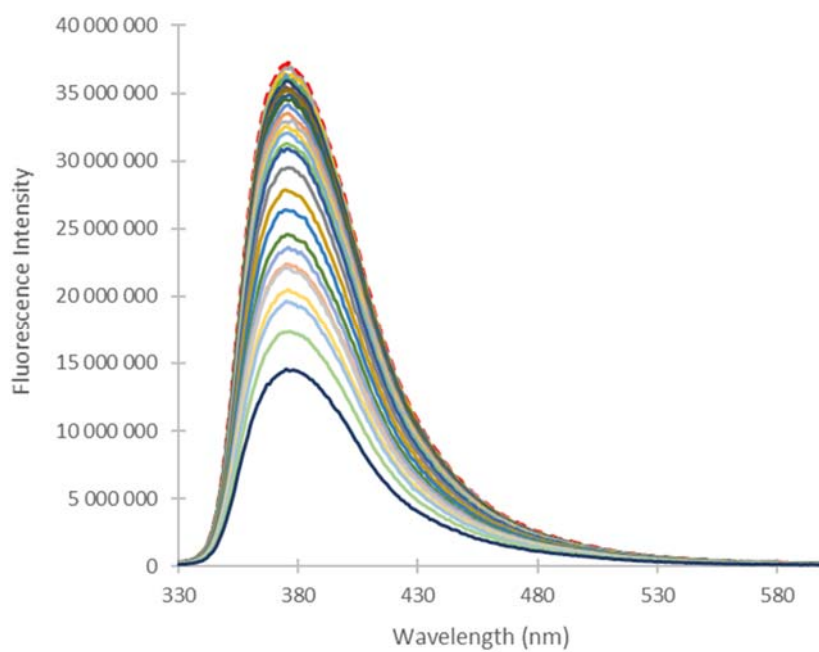


Figure S41 Fluorescence titration of **3** with TBAI (from 0 to 200 equivalents) in ACN, ($[3] = 2.10^{-4} M$, $\lambda_{exc} = 325 \text{ nm}$).

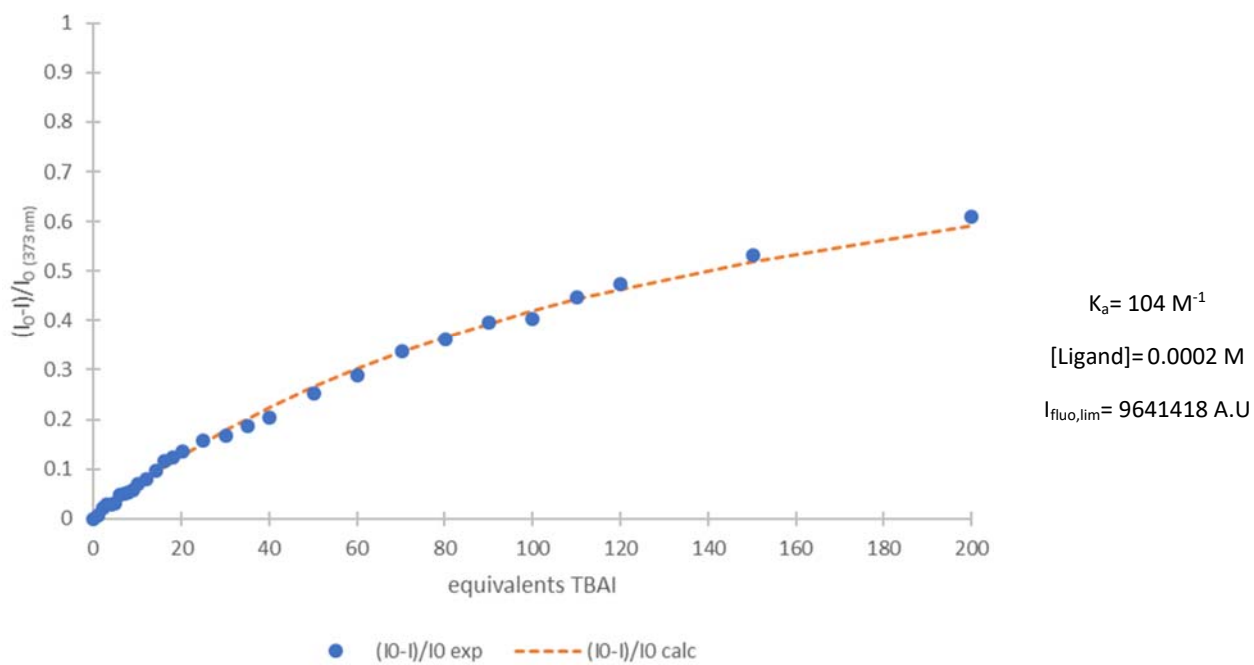


Figure S42 Mathematical fit of fluorescence of **3** with TBAI (from 0 to 200 equivalents) in ACN, ($[3] = 2.10^{-4} M$, $\lambda_{exc} = 325 \text{ nm}$).

[PROGRAM]
Name = SPECFIT
Version = 3.0

[FILE]
Name = OZ35+TBAJ_FLUO_FORMAT_SPECFIT.FAC
Path = C:\Users\Utilisateur\Desktop\
Date = 04-juin-21
Time = 20:44:43
Ncomp = 2
Nmeas = 30
Nwave = 271

[FACTOR ANALYSIS]
Tolerance = 1,000E-09
Max.Factors = 10
Num.Factors = 6
Significant = 2
Eigen Noise = 4,830E+04
Exp't Noise = 4,830E+04
Eigenvalue Square Sum Residual Prediction
1 1,244E+18 3,872E+13 6,902E+04 Data Vector
2 1,976E+13 1,896E+13 4,830E+04 Data Vector
3 3,326E+12 1,564E+13 4,387E+04 Probably Noise
4 2,096E+12 1,354E+13 4,082E+04 Probably Noise
5 1,296E+12 1,225E+13 3,882E+04 Probably Noise
6 1,068E+12 1,118E+13 3,709E+04 Probably Noise

[MODEL]
Date = 04-juin-21
Time = 20:46:36
Model = 0
Index = 3
Function = 1
Species = 3
Params = 3

[SPECIES]	[COLORED]	[FIXED]	[SPECTRUM]
1 0 0	False	False	
0 1 0	True	False	
1 1 0	False	False	

[SPECIES]	[FIXED]	[PARAMETER]	[ERROR]
1 0 0	True	0,00000E+00 +/-	0,00000E+00
0 1 0	True	0,00000E+00 +/-	0,00000E+00
1 1 0	False	1,56268E+00 +/-	6,77681E-03

[CONVERGENCE]
Iterations = 3
Convergence Limit = 1,000E-03
Convergence Found = 5,717E-08
Marquardt Parameter = 0,0
Sum(Y-y)² Residuals = 1,54506E+14
Std. Deviation of Fit(Y) = 1,37865E+05

[STATISTICS]
Experimental Noise = 4,830E+04
Relative Error Of Fit = 1,1146%
Durbin-Watson Factor = 0,8383
Goodness Of Fit, Chi² = 8,147E+00
Durbin-Watson Factor (raw data) = None
Goodness Of Fit, Chi² (raw data) = None

[COVARIANCE]
2,473E-04

[CORRELATION]
1,000E+00

[END FILE]

6. Mass spectrometry experiments

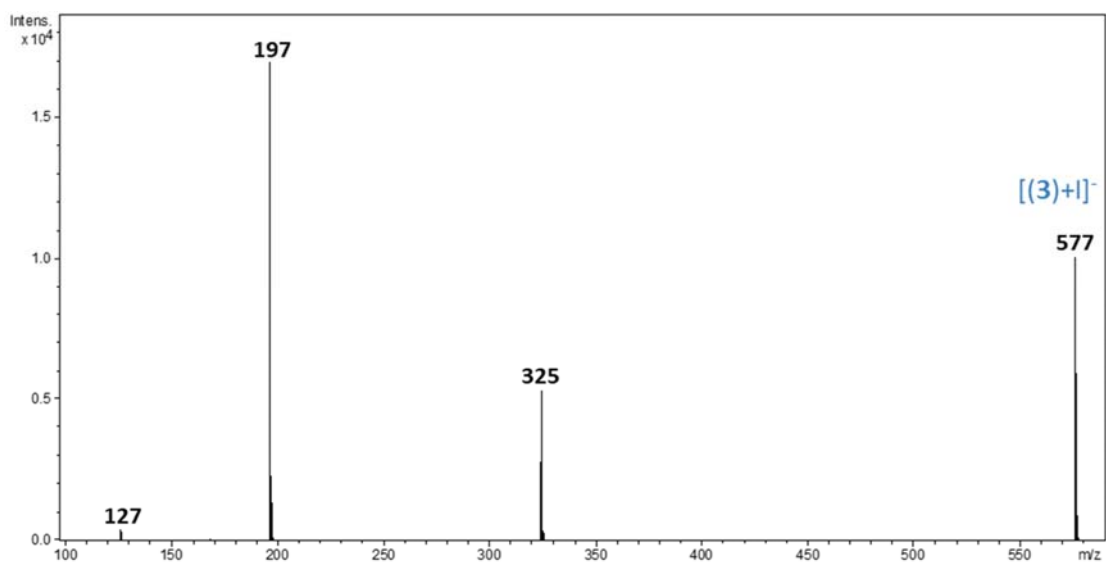


Figure S43 MS CID spectrum of the [(3) + 1]⁻ ion (m/z 577) after reduction of the low mass cutoff at m/z 100.

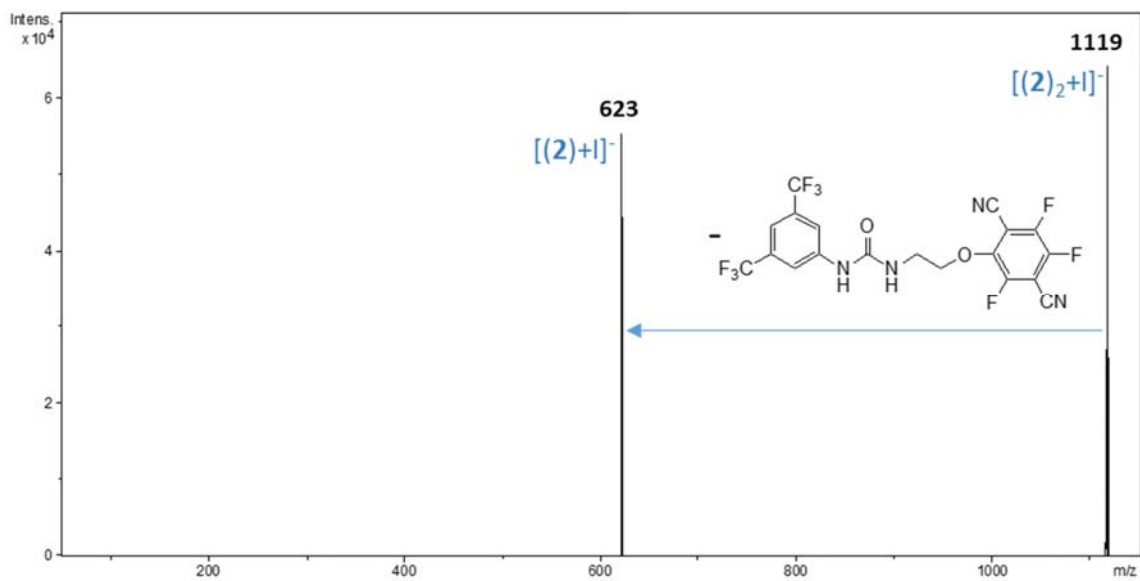


Figure S44 CID spectrum of the [(2)₂ + 1]⁻ dimeric ion (m/z 1119). The only product ion observed is associated with the elimination of the intact receptor

7. Bibliography

- [1] H. E. Gottlieb, V. Kotlyar, A. Nudelman, *Journal of Organic Chemistry* **1997**, *62*, 7512–7515.
- [2] J. Contreras-García, E. R. Johnson, S. Keinan, R. Chaudret, J.-P. Piquemal, D. N. Beratan, W. Yang, *J. Chem. Theory Comput.* **2011**, *7*, 625–632.
- [3] Henry S. Rzepa, “Script for creating an NCI surface as a Jvxl compressed file from a (Gaussian) cube of total electron density,” can be found under <https://www.ch.ic.ac.uk/rzepa/cub2nci/>, **2013**.
- [4] E. F. Pettersen, T. D. Goddard, C. C. Huang, G. S. Couch, D. M. Greenblatt, E. C. Meng, T. E. Ferrin, *J. Comput. Chem.* **2004**, *25*, 1605–1612.
- [5] R. Plais, G. Gouarin, A. Gaucher, V. Haldys, A. Brosseau, G. Clavier, J. Salpin, D. Prim, *ChemPhysChem* **2020**, *21*, 1249–1257.
- [6] R. Plais, G. Gouarin, A. Bournier, O. Zayene, V. Mussard, F. Bourdreux, J. Marrot, A. Brosseau, A. Gaucher, G. Clavier, J.-Y. Salpin, D. Prim, *ChemPhysChem* **2023**, *24*, e202200524.
- [7] G. Tardajos, G. González-Gaitano, *J. Chem. Educ.* **2004**, *81*, 270.
- [8] B. Valeur, M. N. Berberan-Santos, *Molecular Fluorescence: Principles and Applications, Second Edition*, **2012**.
- [9] H. Gampp, M. Maeder, C. J. Meyer, A. D. Zuberbühler, *Talanta* **1985**, *32*, 95–101.
- [10] H. Gampp, M. Maeder, C. J. Meyer, A. D. Zuberbühler, *Talanta* **1985**, *32*, 257–264.
- [11] C. Würth, M. Grabolle, J. Pauli, M. Spieles, U. Resch-Genger, *Nat Protoc* **2013**, *8*, 1535–1550.
- [12] A. M. Brouwer, *Pure and Applied Chemistry* **2011**, *83*, 2213–2228.